

SUPERVISORS

Dr. Franz Riemelmoser

Engineering & IT

Fachhochschule Kärnten

Dr. Gregory Mocko

Mechanical Engineering

Clemson University

**MECHANICAL PROPERTIES OF ADDITIVE
MANUFACTURED HONEYCOMB STRUCTURES**

Master's Thesis | B. Eng. Sebastian Barner | 1210686009 | 2015

MECHANICAL PROPERTIES OF ADDITIVE MANUFACTURED HONEYCOMB STRUCTURES

Thesis to achieve the title 'Master of Science in Mechanical Engineering'

Submitted March 12, 2015

Fachhochschule Kärnten, Villach, Österreich

Studienbereich Engineering & IT

Masterstudiengang Maschinenbau-Leichtbau

The research which underlies this thesis was conducted at

Clemson University, South Carolina, USA

Department of Mechanical Engineering

Clemson Engineering Design Applications and Research (CEDAR)

Supervisors

Dr. Franz Riemelmoser

Studienbereich Engineering & IT

Fachhochschule Kärnten

Dr. Gregory M. Mocko

Department of Mechanical Engineering

Clemson University

Eidesstattliche Erklärung

Ich erkläre hiermit:

Dass ich die vorliegende Masterarbeit selbstständig und ohne fremde Hilfe verfasst und noch nicht anderweitig zu Prüfungszwecken vorgelegt habe.

Dass ich keine anderen als die angegebenen Hilfsmittel benutzt, die den verwendeten Quellen wörtlich oder inhaltlich entnommenen Stellen als solche kenntlich gemacht und mich auch sonst keiner unerlaubten Hilfe bedient habe.

Dass die elektronisch abgegebene Arbeit mit einer eingereichten Hardcopy übereinstimmt.

Dass ich einwillige, dass ein Belegexemplar der von mir erstellten Masterarbeit in den Bestand der Fachhochschulbibliothek aufgenommen und benutzbar gemacht wird (= Veröffentlichung gem. § 8 UrhG).

Lenningen, den 10. März 2015

Sebastian Barner

Danksagung

Bedanken möchte ich mich zunächst bei Herrn Dr. Gregory Mocko, der mir es ermöglicht hat an die Clemson University zu kommen und unter seiner Betreuung die Forschung zu vorliegender Masterarbeit durchzuführen. Die wöchentlichen Diskussionen haben mir viel Freude bereitet.

Dankeschön an alle CEDAR Mitgliedern, vor allem denjenigen, die mit mir ein Labor geteilt haben, für Ihre offene und freundliche Art. Sie waren stets hilfsbereit und haben mir damit den Einstieg an der Clemson University leicht gemacht.

Danke auch an James Lowe und Nakul Ravikumar für die Bereitstellung der Zugprüfmaschinen und an Tim Pruett für den tollen Einsatz bei der Fertigung meiner Proben.

Vielen Dank an Herrn Dr. Franz Riemelmoser für die Ermöglichung des Studiums in Villach, für seine interessanten und lehrreichen Vorlesungen an der Fachhochschule Kärnten und der Betreuung meiner Masterarbeit.

Ein Dankeschön gilt auch dem International Office der Fachhochschule Kärnten für die Unterstützung der Organisation meiner Auslandssemester in Dänemark und den USA.

Für die finanzielle Unterstützung meiner Masterarbeit möchte ich mich herzlich bei der Marshallplan-Jubiläumsstiftung bedanken.

Ein ganz besonderer Dank gilt meinem Leidensgenossen, Mitstudenten und Freund Patrick Senger, mit dem ich ein super Team (auch bekannt als „Deutsches Eck“) während unserer Studienzeit gebildet habe. Zusammen wurden alle Aufgabenstellungen und Probleme toll gemeistert.

Vielen lieben Dank an meine Familie und Freunde, die trotz der Distanz während meiner Studienzeit in Villach, Aarhus und Clemson immer für mich da waren.

Kurzfassung

Die vorliegende Masterarbeit behandelt das Thema der mechanischen Materialeigenschaften von additiv gefertigten Kunststoff-Wabenstrukturen. Es wird untersucht welche Auswirkungen der Schichtaufbau durch additive Fertigungsverfahren auf die Strukturen hat. Diskutiert wird, ob ein Aufbau entlang der Zellstege oder gar ein schichtenloser Aufbau Vorteile gegenüber dem aktuell herkömmlichen schichtweisen Aufbau mit sich bringt. Dazu wird zunächst der aktuelle Stand der Technik analysiert, eine neue Zielsetzung definiert und daraus eine Forschungsidee abgeleitet. Die Forschungsarbeit beinhaltet die Entwicklung, Fertigung und Testung von Zugproben mit zugrundeliegender Wabenstruktur. Abschließend werden die Testergebnisse dem anfangs erarbeiteten Wissen gegenübergestellt, Schlussfolgerungen gezogen und Ausblicke gegeben.

Acknowledgment

First, I would like thank Dr. Gregory Mocko, for giving me the opportunity doing research under his supervision at the Department of Mechanical Engineering at Clemson University. The weekly discussions were always exciting.

Thanks to all CEDAR members, especially to the ones who shared the lab with me, for their open and kind manner. They made it easy for me to start at Clemson University.

A thank-you to James Lowe and Nakul Ravikumar for making tensile testing available, and to Tim Pruett for his great efforts in producing my specimens.

Thanks a lot to Dr. Franz Riemelmoser for enabling the master studies in Villach to me, for his interesting and instructive lessons at Fachhochschule Kärnten and for supervising my master's thesis.

A thank-you as well goes to the International Office of FH Kärnten for supporting the organization of my semesters abroad in Denmark and the USA.

For the financial support of my master's thesis, I would like to thank the Austrian Marshall Plan Foundation.

Special thanks go to my fellow student and friend Patrick Senger, with whom I formed a fantastic team (also known as the "German Corner") during our study time. Greatly we solved all exercises and problems together.

Lovely thanks to my family and friends. Despite the far distances, they were always there for me during my studies in Villach, Aarhus and Clemson.

Abstract

The research presented in this thesis is focused on the mechanical properties of additive manufactured honeycomb structures out of plastic. The influences of the layered buildup of additive manufacturing methods on cellular structures are investigated. A buildup along the primary axis of the cell walls and an entire layerless buildup is discussed to figure out if there are any advantages compared to the conventional layered buildup. Therefore, the current state of the art is analyzed, problems and new goals defined and a research idea derived. The research work contains the development, manufacturing and testing of tensile specimens with honeycomb structure. Finally, the test results are compared to the initial knowledge and conclusion and perspectives are made.

The main goal of this research was to explore the existence of advantages in generating the material along the primary axis of the cell walls instead of a layered buildup. For that, three different kind of tensile specimens out of polycarbonate with a hexagonal honeycomb structure were developed: The first one representing the full material generation along the primary axis of the cell walls, simulated by a milled honeycomb structure; the second one representing an layered material generation along the primary axis of the cell walls, using the additive manufacturing method Fused Deposition Modeling; and the third one representing cell walls with a layered buildup perpendicular/under a certain angle to their primary axis, as well using Fused Deposition Modeling.

Test results support the hypothesis of cell walls generated along their primary axis having superior mechanical properties; But only for this special case, using Fused Deposition Modeling and the same material (polycarbonate) for all three types of honeycombs.

The other additive manufacturing methods regarded in this research as well display that buildup direction and accordingly layer orientation has an impact on material properties. When developing cellular structures and cellular materials, this has to be taken into consideration.

Further, the influences of layer thicknesses and wall thicknesses on material properties have to be investigated. Concomitant circumstances are the influences of voids and cracks, as they can have fatal consequences for cellular structures and materials. The smallest scale feature must be considered in using additive manufacturing machines.

All additive manufacturing methods have their individualities. These have to be examined in more detail to receive information about process influences on material behavior. A standard should be created to provide a basis in view of design to functionality, which is fundamental in lightweight engineering.

Contents

1 Introduction	2
1.1 Motivation	2
1.2 Background	2
1.3 Research Hypothesis	3
2 Literature Review	5
2.1 Cellular Structures and Materials.....	5
2.1.1 Man-Made Cellular Materials.....	6
2.1.2 Auxetic Structures	9
2.2 Additive Manufacturing	11
2.2.1 Methods and Characteristics of Additive Manufacturing	14
2.2.2 Additive Manufacturing of Designed Cellular Materials	19
2.2.3 Material Properties depending on Part Orientation.....	20
2.2.4 Layer-less Additive Manufacturing	25
3 Problem Definition and Objectives	28
4 Research Approach	30
5 Accomplishment	35
5.1 Design and Development of Tensile Specimens.....	35
5.1.1 Honeycomb Specimen	36
5.1.2 Solid Specimen.....	38
5.2 Mechanical Behavior of Honeycombs.....	39
5.3 Manufacturing of Specimens.....	40

5.3.1 Fused Deposition Modeling (FDM).....	41
5.3.2 Milling	46
5.3.3 Poly-Jet Modeling (PJM).....	47
5.3.4 Selective Laser Sintering (SLS).....	49
5.4 Tensile Testing	51
5.4.1 Accomplishment of Tensile Tests.....	52
5.4.2 Fracture Behavior.....	54
5.4.3 Test Results and Comparison	58
I Fused Deposition Modeling.....	58
II Milling.....	62
III Poly-Jet Modeling	65
IV Selective Laser Sintering.....	69
V Comparison	73
6 Conclusion and Perspective	77
References	83
Notation	87
Abbreviation	88
Units.....	89
Figures.....	90
Tables	93
Appendix.....	XI

Chapter 1 : INTRODUCTION

1.1 Motivation

Today, in a time where resource constraints dictate the market and ecological awareness is one of the greatest challenges, people and especially engineers are forced to think about new ways to develop and design the products of tomorrow.

Lightweight engineering is trying to find new solutions to make products lighter, but not weaker, at its best even stronger. Solutions can be on the one hand to use new techniques to design products in a different way to use less material; on the other hand to use lighter materials or to find new materials with improved characteristics. Next to this, lightweight engineering can also reduce the amount of the manufacturing costs, which is not necessarily, but certainly reduce the operation expenses of the end product. Well-known examples are car bodies out of aluminum or airplane frameworks out of composite materials.

1.2 Background

One solution for lighter products is the usage of cellular structures and materials, which include honeycombs (two-dimensional), foams or designed lattice structures (both three-dimensional). The hollow spaces reduce weight, but still ensure the required strength, provided that they were designed correctly. A particular form of designed cellular materials are auxetic materials, belonging to the group of mechanical meta-materials¹. Next to light weight, auxetic materials have big potentials in protective or energy absorbing constructions for aerospace, automotive and medical engineering, because of their unusual properties in the elastic regime of deformation: The transversal extension becomes bigger when

¹ Meta-material = designed material with properties (nearly) not found in nature

they are elongated longitudinally or smaller when they are compressed due to a negative Poisson's ratio².

While there are several ways to produce these cellular materials, the focus of this research is on additive manufacturing (AM). The background is the efficient buildup of parts and the possibility to create complex profiles and structures, which are not feasible with conventional manufacturing methods. Neither tools, nor position or orientation changes of the parts are necessary.

Additive manufacturing can be realized through photo-solidification, successive bonding or thermal energy, generating parts layer by layer. This procedure allows objects with hollow spaces, undercuts and filigree structures. Furthermore, complete assemblies can be produced with this method. Mostly, the fabricated objects are used as illustrative models and for functional tests. However, more and more additive manufacturing is used to fabricate end-products, because of good material properties and the stated facts.

1.3 Research Hypothesis

Manufacturing cellular structures and materials with layer based additive manufacturing methods will lead to a layered structure throughout the cell walls. As an alternative, the cell walls can probably be manufactured along their primary axis. The abolition of the layered structure could mean better mechanical properties. This will require the mechanical behavior of layered parts to be analyzed and transferred to cellular structures.

In addition, the additive manufacturing methods have to be analyzed how far they are suited to produce cellular structures or if there have to be explored new ways to build up the structures more efficient, with better mechanical properties and shape characteristics.

² Poisson's ratio = negative quotient of transverse strain and longitudinal strain

Chapter 2 : LITERATURE REVIEW

Literature Review

The following describes the background to this thesis, imparts basic knowledge and the current state in the areas of cellular materials and additive manufacturing.

2.1 Cellular Structures and Materials

Gibson and Ashby describe cellular materials as “an assembly of cells with solid edges and/or faces, packed together so that they fill space” [GA97]. Such materials in nature are for example wood, cork, sponge, coral or bee honeycombs. Further a cellular material is defined by the relative density

$$\bar{\rho} = \frac{\rho_{\#}}{\rho_s} \quad \text{[GA97] [DFA01]} \quad (2.1)$$

where the density of the cellular material $\rho_{\#}$ is divided by the density of the cell wall material ρ_s . If this term gets greater than 0.3 the cellular material turns into a solid material with pores [GA97] (Figure 1). Moreover, the characteristic length of a cell provides information about the type of structure. For example Nguyen et al speak about meso-structured materials which have a cell length in the range of 0.1 and ten millimeters [NPR12]. There are many different scale in literature that define cellular structures and meso-materials. In this research, the following nomenclature is established.

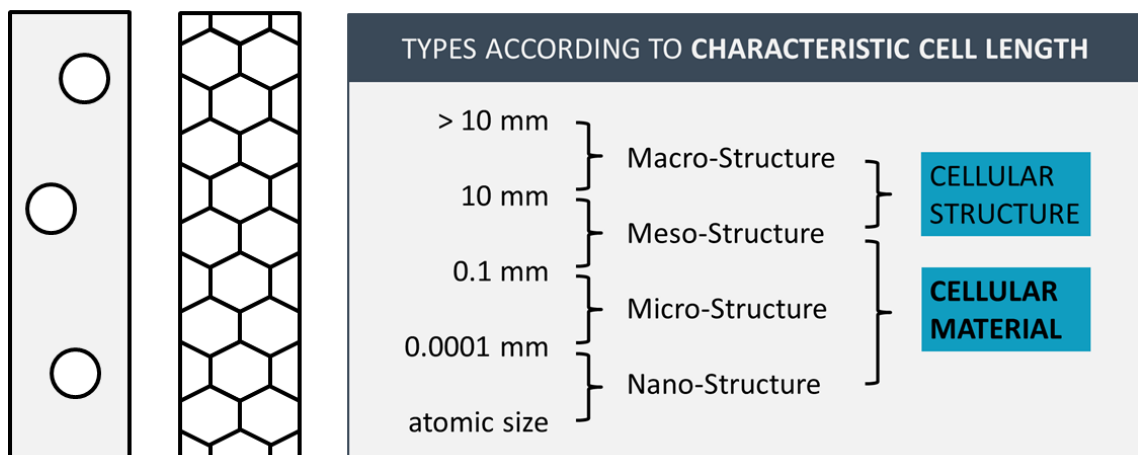


Figure 1: Porous material | cellular material | characteristic cell length and types of structures

2.1.1 Man-Made Cellular Materials

Like in many other cases, humans learned from nature, recognized the potentials of cellular structures having excellent properties at a relatively low mass and tried to copy them with their own means. For a better understanding man-made cellular materials should be divided into stochastic structures and designed periodic structures, as well as in two-dimensional and three-dimensional shapes [GA97][NPR12]:

- **Honeycombs (2D, stochastic, periodic)**
- **Foams (3D, stochastic)**
- **Designed Lattice Structures (3D, periodic)**

Furthermore, foams are existing as open-celled, so only cell walls, or closed-celled, which means each cell is closed by faces [GA97].

Designed two-dimensional cell shapes which fill a plane are triangles, quadrilaterals or hexagons with a center of symmetry; packaging of designed three-dimensional cells like in Figure 2 fill space [GA97].

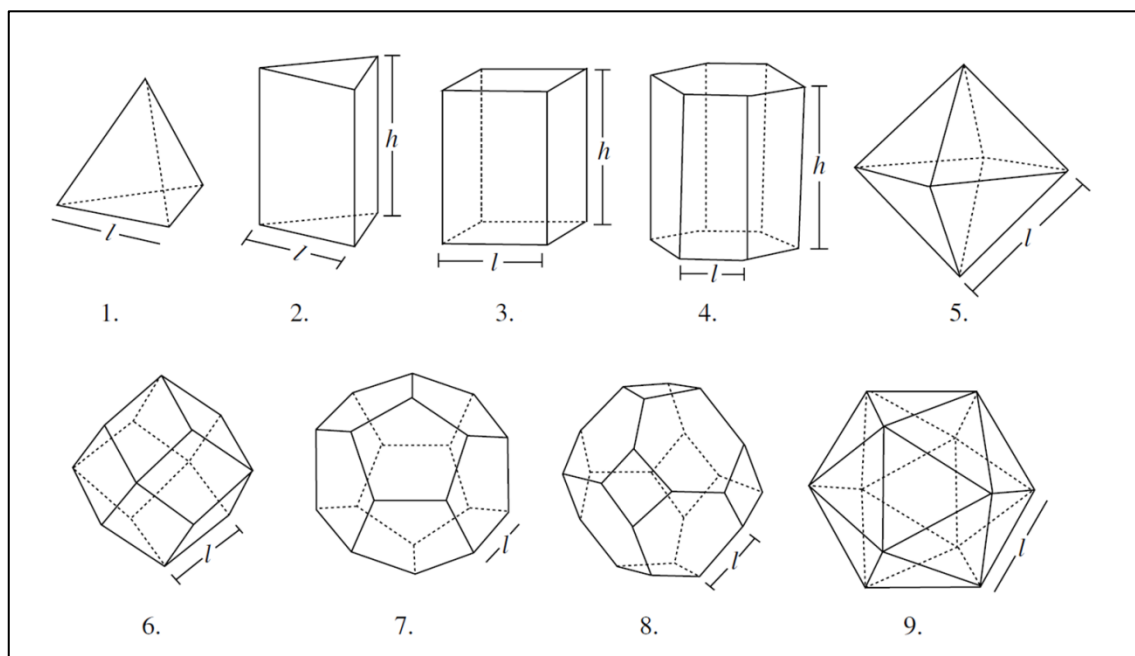


Figure 2: Types of three-dimensional cells: 1. Tetrahedron, 2. Triangular prism, 3. Rectangular prism, 4. Hexagonal prism, 5. Octahedron, 6. Rhombic dodecahedron, 7. Pentagonal dodecahedron, 8. Tetrakaidecahedron, 9. Icosahedron [GA97]

One advantage of cellular materials over solid materials can be (depending on the design of the structure and its resultant behavior) that in load case, the structure first absorbs energy before the actual material of the cell walls gets deformed. In impact loading, this scenario becomes apparent: A solid material gets directly damaged, whereas many cellular materials stretch or compress initially until the maximum of the cell structure deformation is reached. Those energy absorbing cellular materials have struts (cell walls) with a bending-dominated deformation (Figure 4 – D) under stress conditions, which means large strains, but low stiffness and strength [Ash06]. The stiffness degrades with the reduction of the density [ZLW14].

To increase the stiffness and strength at low density (Figure 3), cellular materials have to be designed in a different way, where the struts have a stretch-dominated deformation (Figure 4– A) under stress conditions [Ash06]. A nearly isotropic and favored design is the octet-truss lattice material, with unit cells formed out of one octahedral cell and four tetrahedral cells. Its strength scales the relative density $\bar{\rho}$, whereas foams scale only $\bar{\rho}^{1.5}$ [DFA01].

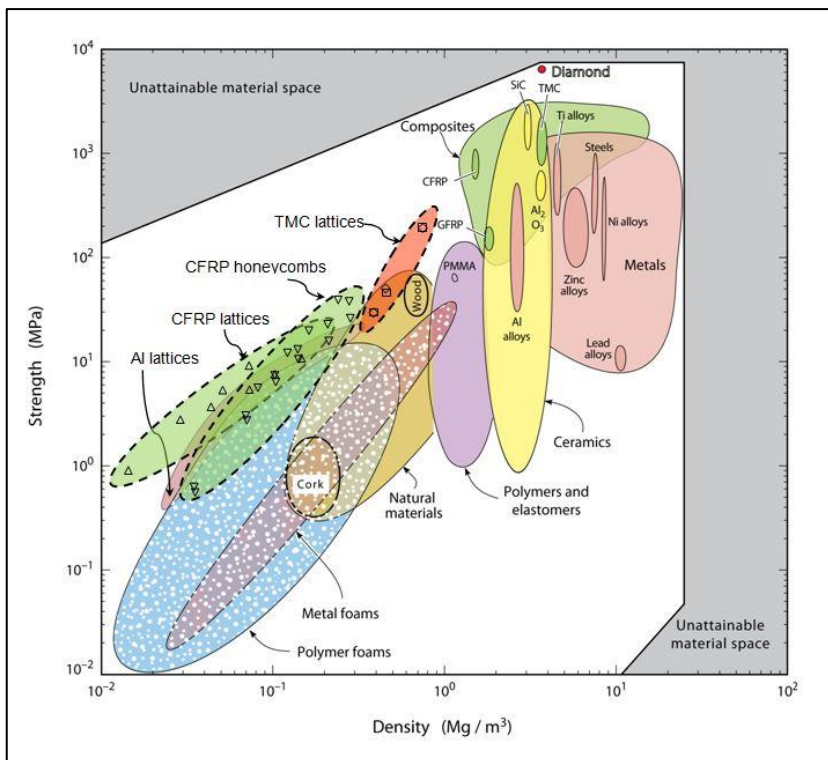


Figure 3: Density over strength of solid and cellular materials [vir]

Newer applications of octet-truss structured nano-materials (Figure 4 – A-C) show nearly constant stiffness with variation of the relative density. Moreover, the compressive strength scales the relative density between 1.1 and 2.7, depending on the type of the struts (solid or hollow-tube) [ZLW14].

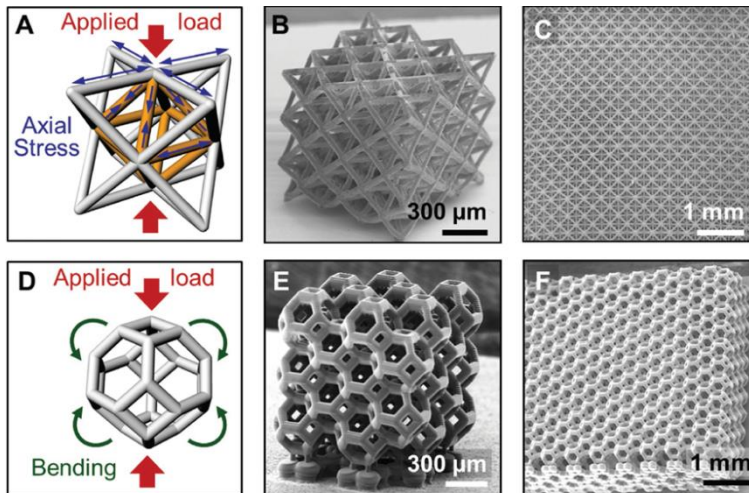


Figure 4: A Octet-truss unit cell, B and C Octet-truss lattice material, D Kelvin Foam unit cell, E and F Kelvin Foam [ZLW14]

Another example is a fully triangular and also nearly isotropic designed micro-truss structure (Figure 5). With unit cell lengths of ten micrometers, Bauer et al. managed to produce a structure which reaches compressive strengths up to 280 megapascals [BTS14]. The cellular material exceeds the strength-to-weight ratio of all designed materials with densities below 1,000 kilogram per cubic meter, as the lightest solid materials have a density around this number [BTS14].

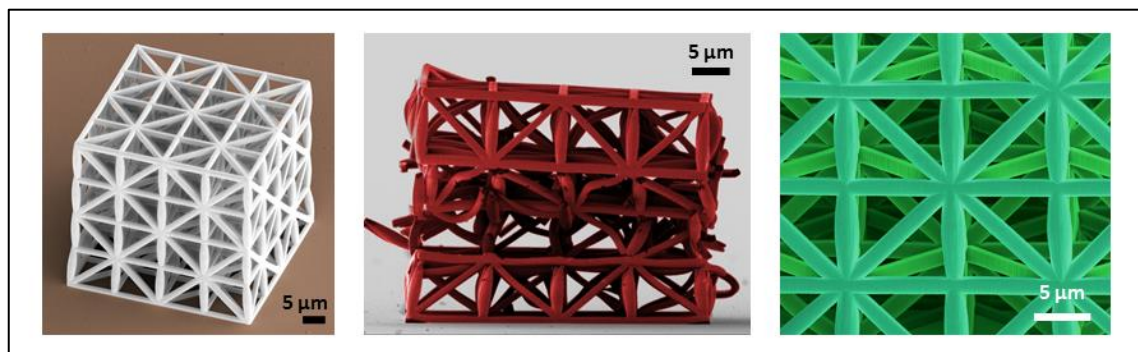


Figure 5: Left: fully triangular micro-truss structure – the cube edge length is about 40 micrometers | middle: deformed structure after uniaxial compression | right: close-up view [kit]

2.1.2 Auxetic Structures

The term *auxetic* was coined by K. E. Evans [Eva91] and describes mostly a special subgroup of designed cellular materials, as they are barely found in nature. Only a few molecular exhibit auxetic structures like iron pyrites or single crystal materials, and biomaterial auxetics like cow teat skin or cat skin are known so far [EA00].

Elongation in one direction of materials with isotropic, linear-elastic behavior leads to a compression in the other two spatial directions; compression in one direction leads to an expansion in the other two. Both linear-elastic deformations act without a change in volume [ORW11] (Figure 7).

In contrast, auxetic materials change their volume due to deformation and expand transversal under a longitudinal elongation and the other way around (Figure 7). The reason for this lays in the cell structure, in the arrangement of the cell walls. One of the most widely-used two-dimensional auxetic structure consists of hexagon cells with two pitched-in corners [ORW11] (Figure 6).

The auxetic behavior is expressed through a negative Poisson's ratio ν , because transversal and longitudinal strains are both positive or both negative.

$$\nu = -\frac{\varepsilon_{trans}}{\varepsilon_{long}} \quad [ORW11] \quad (2.2)$$

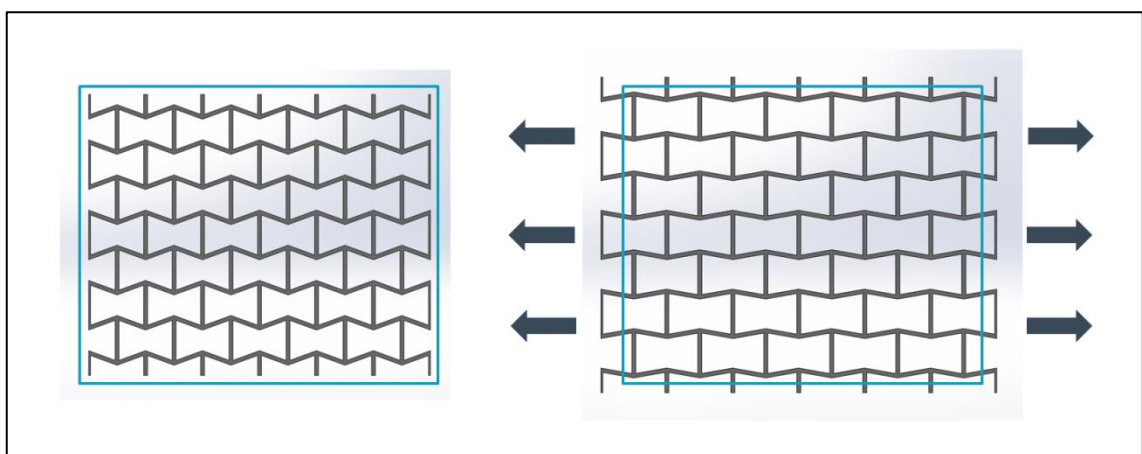


Figure 6: Auxetic honeycomb structure

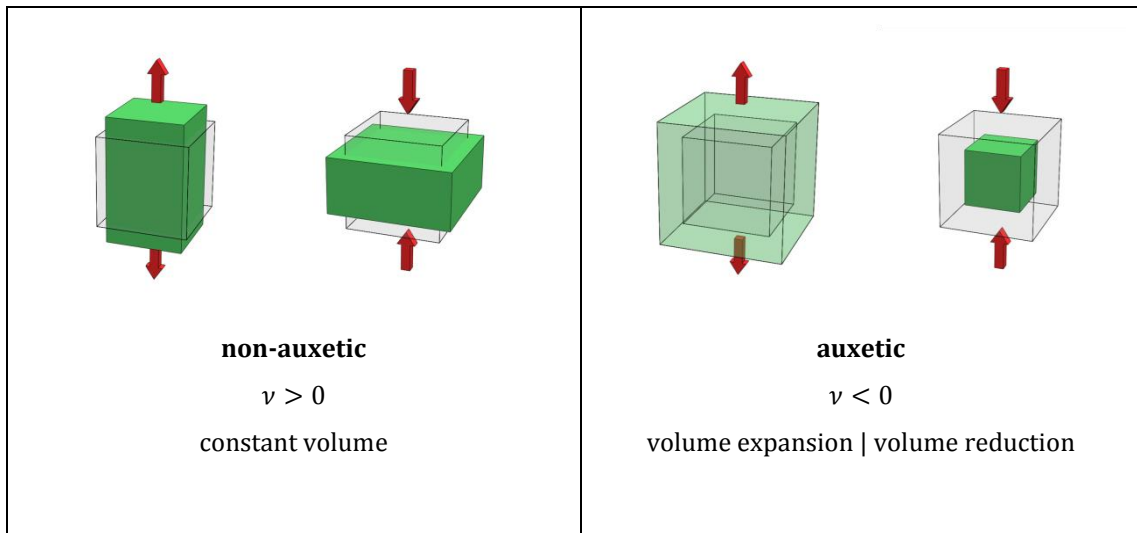


Figure 7: Non-auxetic and auxetic behavior [ORW11]

2.2 Additive Manufacturing

There are many ways to manufacture parts and entire products. Within this thesis, the focus is on additive manufacturing (AM) methods. The term additive manufacturing stands for all those manufacturing methods which create a product by adding material to form a three-dimensional object. In most cases layer by layer (layer based manufacturing, LBM) following a buildup code, directly derived from a three-dimensional model, similar to modern CNC³ manufacturing. With the difference that material is not removed, but plotted and no tool is needed. Hence, objects with hollow spaces, undercuts or complete assemblies are feasible.

Gladly also often is spoken about generative manufacturing, layer based manufacturing or rapid prototyping. A term often used to describe additive manufacturing is rapid prototyping (RP). However, because the additive manufacturing methods are not only used to produce prototypes, this is becoming less common. Meanwhile there are manufactured full-fledged parts or entire end-products with these methods. Moreover, the term rapid prototyping is also used for non-additive buildup of prototypes with methods like *high speed cutting* or *spark eroding*.

Next to rapid prototyping there are existing the terms of rapid tooling and rapid manufacturing. Rapid tooling means the additive manufacturing of a tool, which is used to produce a part or series of parts [AdF13]. For example an additive manufactured injection mold. Rapid Manufacturing describes the tool-less series production of end-products [AdF13] with AM-machines.

Additive manufacturing can be realized through photo-solidification, successive bonding or thermal energy; normally, as aforementioned, layer by layer using a two and a half dimensional-technique (2½D) [AdF13]: Generation of a pattern or shape in the x-y-plane, with a subsequent movement of the buildup platform in z-direction to create a second layer upon the first. A real three-dimensional (3D) buildup would mean a layer-less buildup, which will be discussed in chapter 2.2.3.

³ CNC = computerized numerical control

The process steps of additive manufacturing are stated in the following diagram (Figure 8). Generally first, a CAD-Model is imported to a pre-processing software program, where the part to be produced is placed, aligned and divided into layers. Depending on the process, several other parameters like speed, infill, support material, etc. are also defined. Subsequently, the part is manufactured and possibly machine finished.

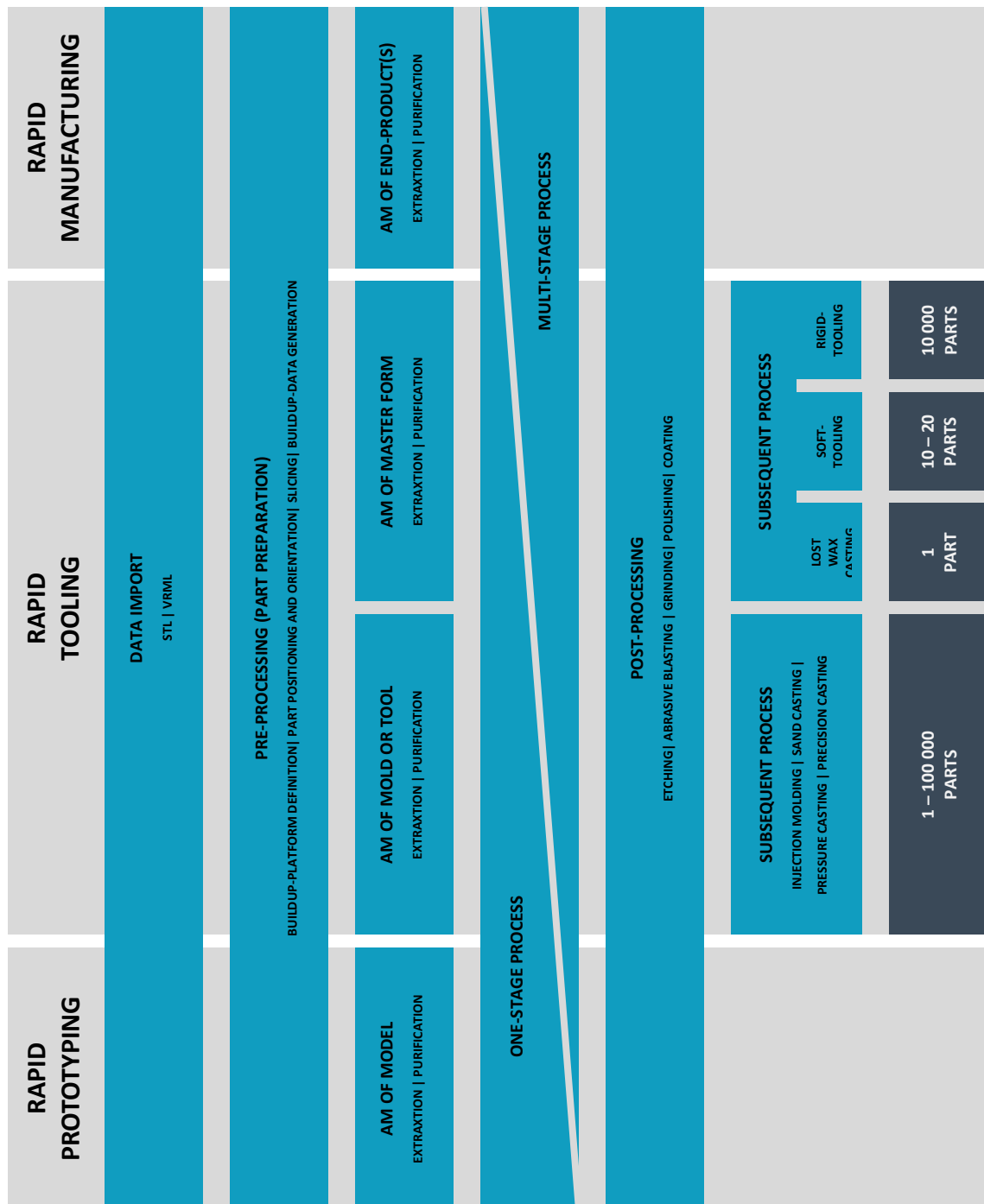


Figure 8: Process steps of additive manufacturing (according to figures of [AdF13])

Application areas for additive manufacturing are to be found nearly everywhere; currently particularly in the areas of architecture, fashion, molding tools, bio and medical engineering [AdF13]. With the exploration of new materials and techniques, which provide better material properties, additive manufacturing will play a big role in all kind of products in future. Especially for weight reduction there are large potentials (Figure 9).

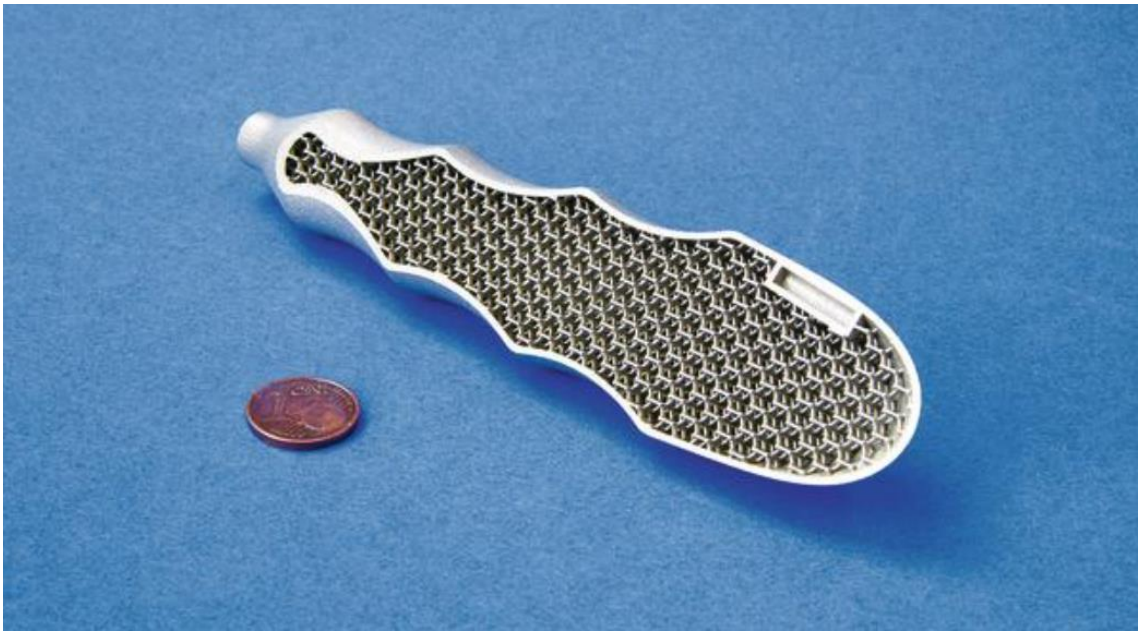


Figure 9: Weight reduction through cellular structure – handle bar for a medical instrument [mut]

2.2.1 Methods and Characteristics of Additive Manufacturing

Berger, Hartmann and Schmid [AdF13] classify the additive manufacturing methods into the initial states of the buildup material: solid, liquid and gaseous. Last-mentioned is used to generate really thin layers through a chemical reaction or physical solidification and finds its application mostly in the thin-film technology (electronics).

[AdF13] The layered buildup from an **initial liquid state** occurs in two and a half dimensions-technique in an indirect or direct form (Figure 10). A third, three-dimensional procedure is described in Chapter 2.2.3. Indirect means a planar areal application of the material and a selective solidification, direct a selective application and areal solidification. Special plastic materials consolidate through polymerization caused by exposure (UV-cure)⁴ or thermal energy.

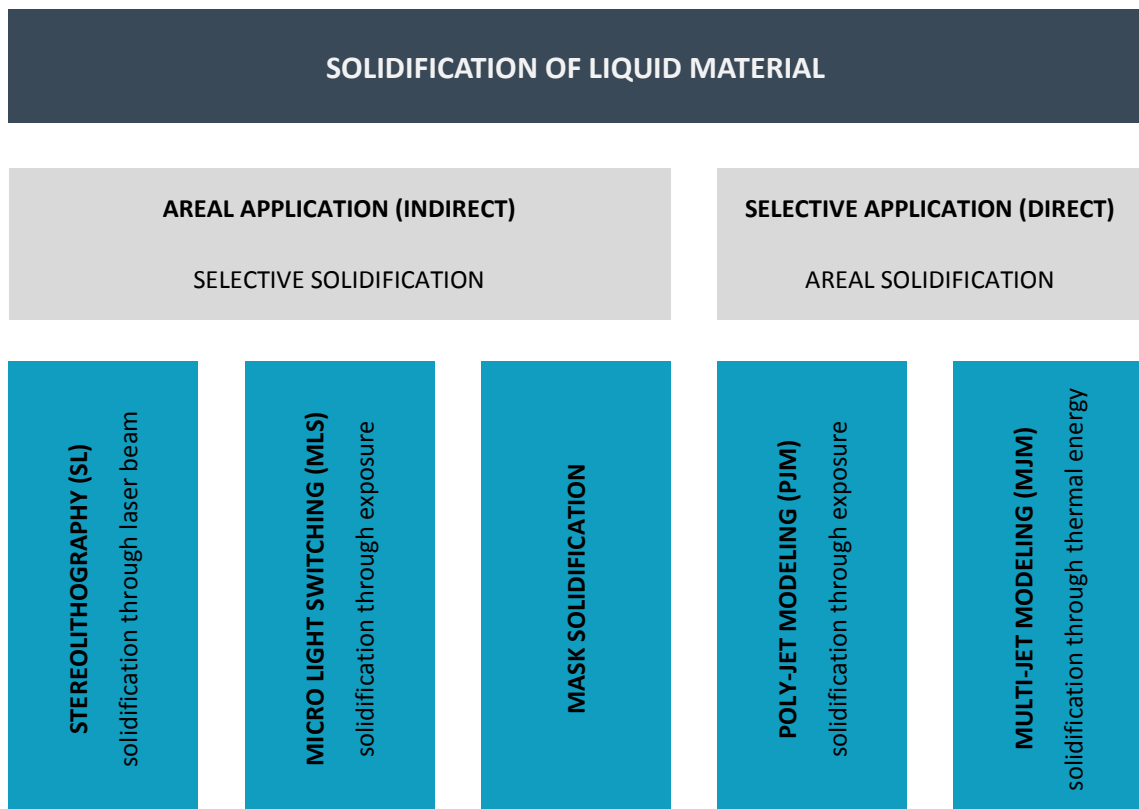


Figure 10: Types of AM-solidification of liquid buildup material (according to [AdF13])

⁴ UV = ultraviolet

The first fully functional machine was invented by Charles W. Hull in 1986 and named *Stereolithography* (SL). Nowadays often used is the method *Poly-Jet Modeling* (PJM), which plays its part within this thesis and will be discussed in detail later.

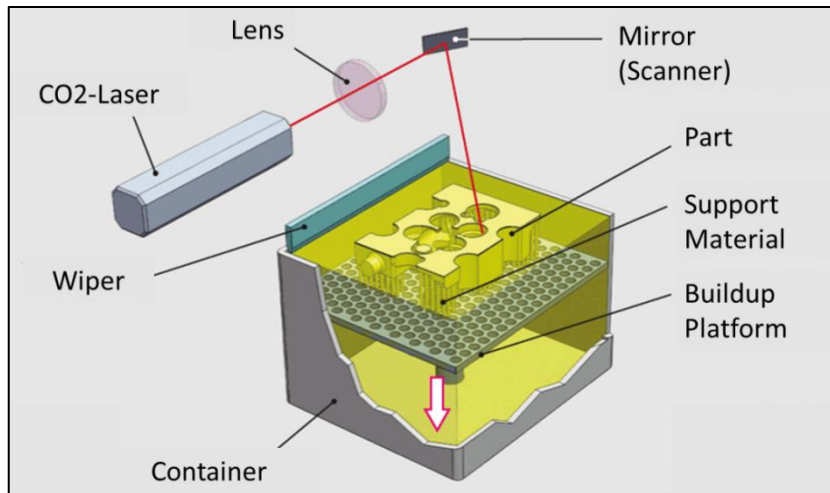


Figure 11: Stereolithography (SL) [AdF13]

[AdF13] The third category describes the buildup of materials with an **initial solid state** (Figure 11). These processes can also be carried out direct or indirect, but the subdivision is made into the second initial state of the buildup material: Commonly used are metals, minerals, plastics and composites in the form of powder, laminate or filament. Powders either are melted, baked or glued together with a laser, an electron beam or a mask. One of the methods is *Selective Laser Sintering* (SLS) which will be discussed later. Laminates are glued, bolted or welded together. Filaments out of metal are welded as well, whereas plastic filaments are extruded. Latter manufacturing method is called *Fused Layer* or *Deposition Modeling* (FLM / FDM) and will be described later as well. At the moment, it is probably the most popular procedure and comes into operation in most of the *Personal-3D-Printers*. A snowballing community works on or with such personal printers. For example *RepRap*, a printer which can be assembled only out of additive manufactured parts. Hence, this printer can reproduce itself [rep]. The price for personal printers is around 200 – 5000 Euro, whereas a professional printer can easily cost an amount of a six-figure sum.

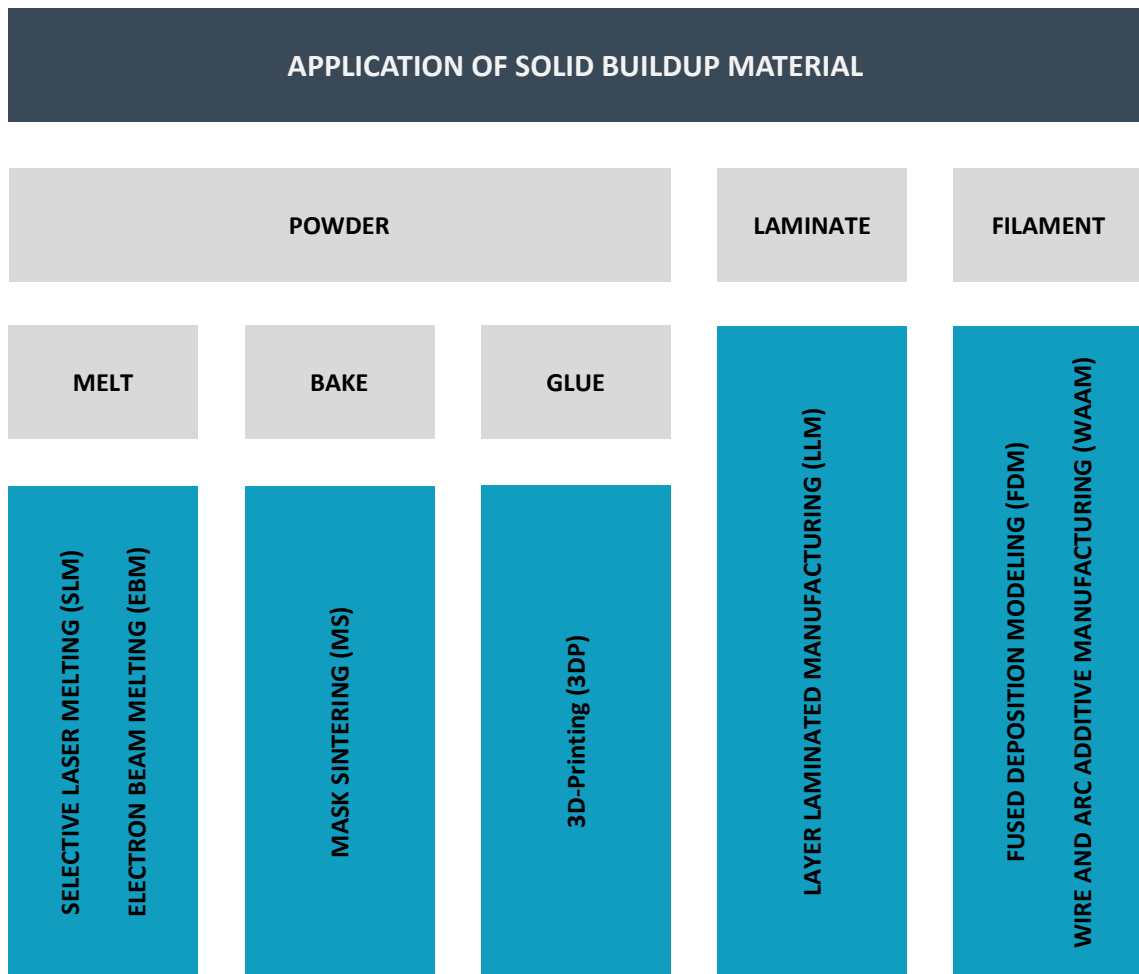


Figure 12: Types of AM-methods with initially solid buildup material (according to [AdF13])

Any kind of thinkable form or structure is of course not realizable without some help. This is why support material comes into operation (Figure 12). In the aforementioned indirect procedure, the buildup material is also the support material [AdF13], because it is distributed over the full available area and selectively solidified. This means the non-solidified residual material encases the part. However, sometimes a support structure is necessary, as the part could sink into the surrounding material due to its weight.

The direct operating procedures generate the support material next to the buildup material. The materials should be different as they will be bonded together during the process and are easier to detach from each other afterwards [AdF13].

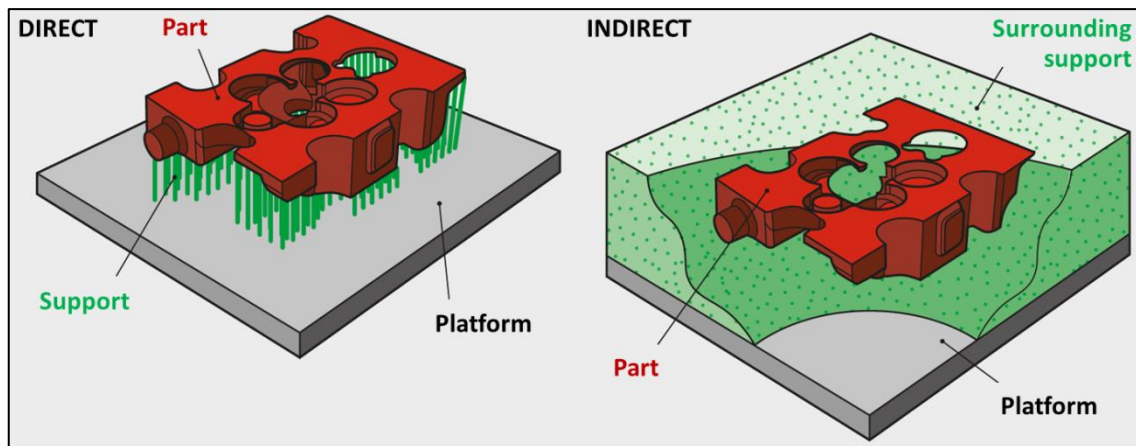


Figure 13: Support material – direct and indirect version (according to [AdF13])

A well-known characteristic of additive manufacturing is that surfaces of parts which are not parallel or perpendicular to the buildup-platform will have a step contour triggered by the layered buildup. The smaller the angle between platform and surface the greater the steps are (Figure 14– 2 & 3). But, the thinner the layers, the less the steps are visible (Figure 14– 3 & 4). With conventional additive manufacturing methods, there are minimal layer thicknesses of 0.014 – 0.05 millimeter reachable [AdF13], which is not or hardly visible without a microscope, but still it is impossible to produce layered objects with overall smooth surfaces. Post-processing maybe finds a remedy, but what could be a way more important problem, is that next to visible effects, there are also structural effects: Really filigree structures become easily brittle. Besides the layer thickness, the accuracy has also an influence on the surface quality (Figure 15).

Another characteristic of additive manufacturing is that the complexity of a part has a way smaller influence on the build time and costs than in conventional manufacturing methods, because there is neither a tool or machine change nor a position or orientation change necessary.

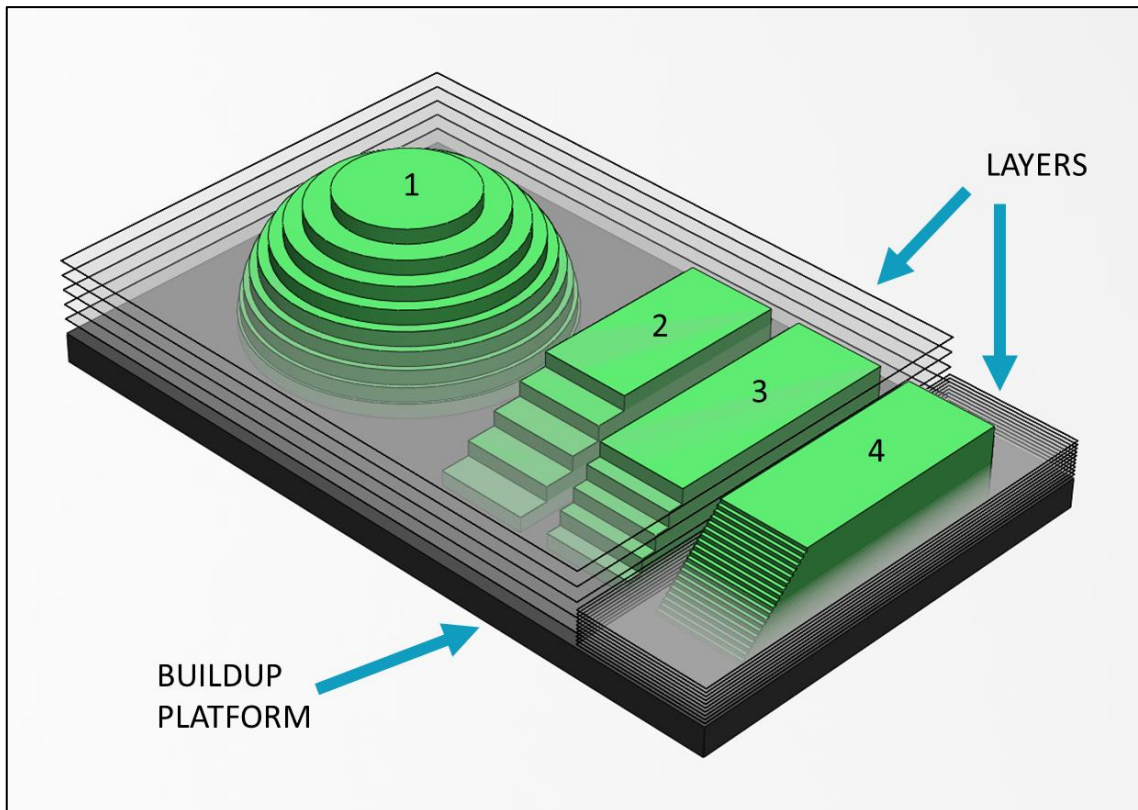


Figure 14: 1 Spherical part – layer-steps-effect through curvature

2 and 3 Different angles at same the layer thickness lead to different step sizes of inclined surface

3 and 4 Different layer thicknesses at the same angle lead to different inclined surface qualities

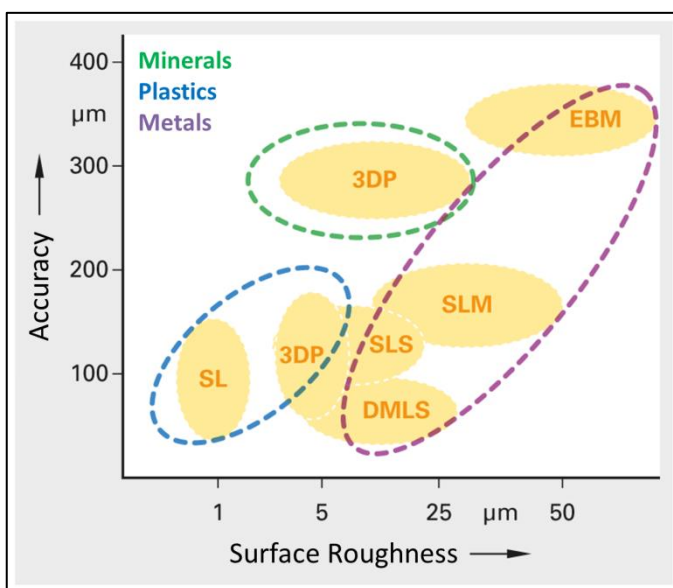


Figure 15: Influence of accuracy on surface roughness [AdF13]

2.2.2 Additive Manufacturing of Designed Cellular Materials

For the production of micro-structures (cellular materials) it needs some more advanced additive manufacturing techniques. Researchers at Massachusetts Institute of Technology use a system called *Projection Micro-Stereolithography* [mit]. [ill] Digital images on a dynamic mask are projected via UV-Light and a projection lens on a polymer resin. A polymerization occurs and a layer with the certain shape of the digital image is produced. After this, the system shifts the substrate and the next layer can be generated upon the first. Layer thicknesses in the order of 400nm are reachable.



Figure 16: Left: octet-truss unit cell | Right: micro building [mit]

Another technique, the *3D Dip-in Laserlithography* was invented at Karlsruhe Institute of Technology. An objective lens is dipped into a special photoresist [BSK12]. The solidification of the material is carried out by a laser beam. Diameters of struts smaller than 100 nanometers are feasible.

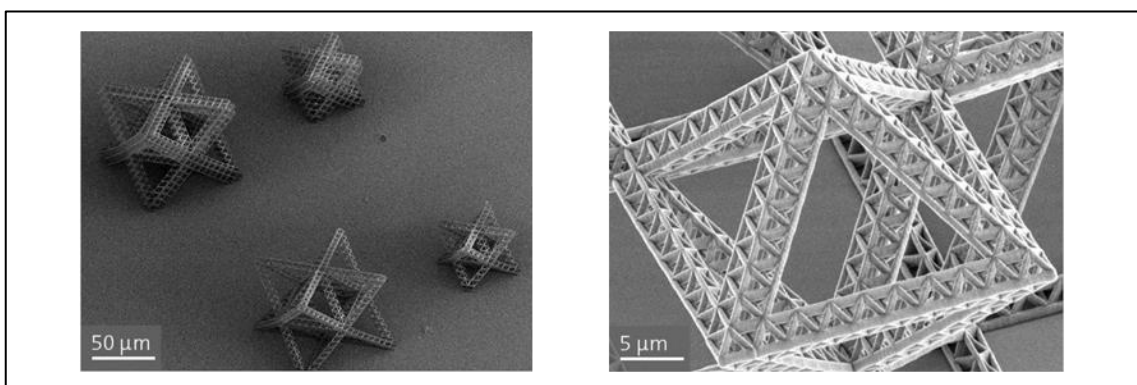


Figure 17: Octet-truss unit cell consisting itself out of a cellular triangular structure [nsc]

2.2.3 Material Properties depending on Part Orientation

This research is limited to polymeric materials and the associated additive manufacturing processes.

Prior to the additive buildup, the part(s) is (are) oriented with appropriate software. Today, the focus mostly is on an efficient buildup, which means that the part is oriented such that a minimum of support material is needed and the part is built up in the shortest time possible. Concurrently there is disregarded, that additive manufactured parts are not isotropic due to the layered buildup and may have totally different material behaviors than conventionally produced parts.

Thus, different persons have tried to figure out, how the mechanical properties of additive manufactured parts change due to the orientation in the buildup volume. Therefore, tensile specimens were produced oriented *flat*, *edgewise* and *straight up* (Figure 18) in relation to the buildup platform with different additive manufacturing methods and tested afterwards. The layers were always parallel to the platform.

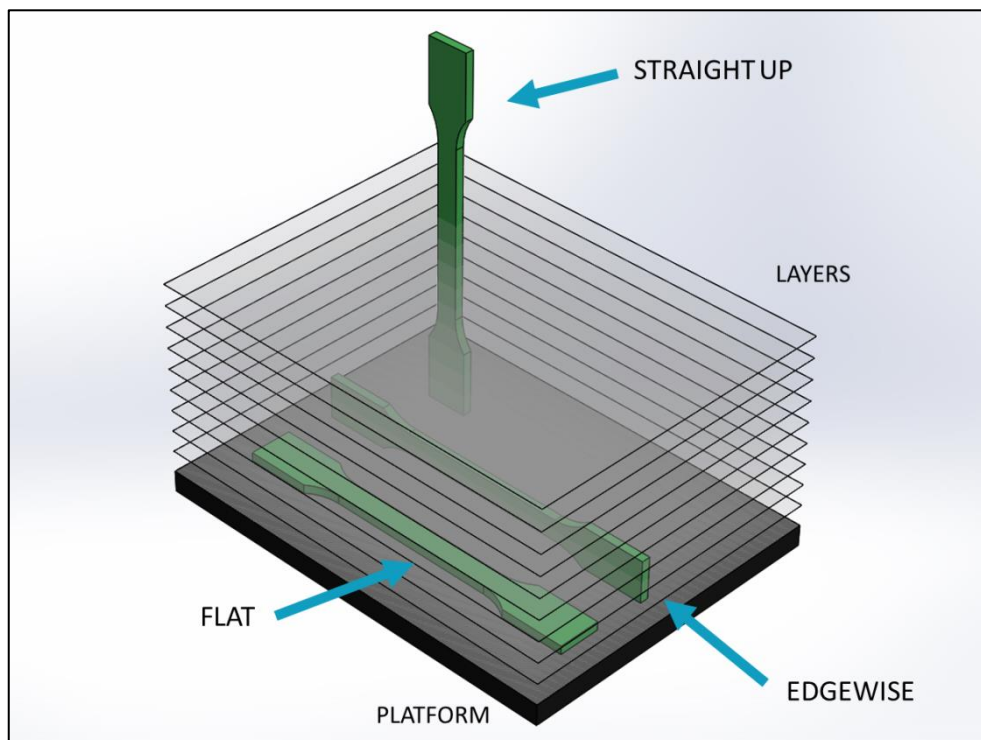


Figure 18: Buildup orientations (layers are only schematic)

Selected tensile strength (σ_{\max}) values of the references (Table 1) state that there is no general rule for the different manufacturing methods. Joshi et al. used two tensile specimens for each orientation [JBR10]. For trustable statistical significance in tensile testing, there are at least five specimens (for each type) needed [ISO527-1]. Disregarding these results, better mechanical properties in *edgewise* and *flat* buildup than in *straight up* become apparent. However, not only the tensile strength should be taken into account, but also the strain. Many additive manufactured parts might have the same tensile strength than an equivalent conventionally manufactured part, but often they have a lower maximal strain at break (ϵ_B) and fail under brittle conditions.

Kühnlein et al. give reasons for the different behavior through different orientations: Notch effects through the layered structure and lacking connections between the layers [KD11]. The notch effects were proofed by testing the specimens with orientation *straight up* with and without milled side faces. With the milled smooth surface a significant increase of the yield stress and the elongation at break were achieved.

In addition, specimens manufactured with an orientation of 45 degrees to the buildup platform were tested. The mechanical property values lay between the ones of the specimens with orientations *flat* and *straight up*.

Apart from the orientation of the part, the mechanical properties can vary a lot due to the process parameters of the respective manufacturing method [BS11, GS97].

For example:

- Fused Deposition Modeling: layer infill pattern and density, layer thickness
- Selective Laser Sintering: laser-power, scan-size and spacing
- Poly-Jet Modeling: resolution

COMPARISON OF LITERATURE VALUES				
MATERIAL AND DATASHEET		FLAT	EDGEWISE	STRAIGHT UP
ULTEM*9085 (PEI)	#1 Fused Deposition Modeling (FDM) ASTM D638 [BS11]			
IM: $\sigma_y = 85 \text{ MPa}$ $\epsilon_B = 72 \%$ ASTM D638 Ductile [mdc]	σ_B	65 MPa	81 MPa	42 MPa
AM: $\sigma_B = 71.6 \text{ MPa}$ $\epsilon_B = 6\%$ ASTM 638 Edgewise Brittle [sys]	ϵ_B	5.2 %	7.7 %	2.5 %
	Behavior	Brittle	Brittle	Brittle
Polycarbonate	#2 Fused Deposition Modeling (FDM) ASTM D638 [JBR10]			
IM: $\sigma_y = 66 \text{ MPa}$ $\epsilon_B = >80 \%$ ISO 527, Ductile [krn]	σ_y	-	50 MPa	50 MPa
AM: $\sigma_{\max} = 68 \text{ MPa}$ $\epsilon_B = 5 \%$ ASTM D638 Edgewise Brittle [sys]	ϵ_B	-	-	-
	Behavior	-	Brittle	Brittle
Resin ZP130 Binder ZB58	#3 3D-Printing (3DP) ASTM D638 [Fra07]			
No values available.	σ_B	12.5 MPa	17.9 MPa	5.5 MPa
	ϵ_B	-	-	-
	Behavior	-	-	-
PA 66	#4 Selective Laser Sintering (SLS) ASTM D638 [GS97]			
IM: $\sigma_y = 85 \text{ MPa}$ $\epsilon_B = 40 \%$ ISO 527 Ductile [krn]	σ_B	15 MPa	14.5 MPa	6 MPa
AM: no values available	ϵ_B	-	-	-
	Behavior	-	-	-
PA 12	# 5 Selective Mask Sintering (SMS) ISO 527 [KD11]			
IM: $\sigma_y = 46 \text{ MPa}$ $\epsilon_B = 280 \%$ ISO 527 Ductile [krn]	σ_B	50.9 MPa	<i>45° inclined</i> 32.1 MPa	12.2 MPa
AM: $\sigma_B = 50 \text{ MPa}$ $\epsilon_B = 15 \%$ St.=? Or.=? Beh.=? [Kel99]	ϵ_B	8.46 %	2.21 %	0.81 %
	Behavior	Brittle	Brittle	Brittle

Table 1: Comparison of literature values

Annotation Table 1

- The literature values of the material properties are differed into “AM” (additive manufactured) and “IM” (injection molded). These are the methods used to produce the tensile test specimens for the data sheets.
- ASTM 638 and ISO 527 are the used tensile testing standards for plastic materials.
- Moreover, the following has to be considered regarding the additive manufacturing of the test specimens:

#1 - FDM: The specimens for the data sheet (Ultem*9085 [sys]) were produced *edgewise*, with a layer thickness of 0.254 millimeters. Other specifications, like infill pattern or spacing are not stated, but they have a big influence on the material properties. The used machine was the Fortus 400mc by Stratasys.

The specimens tested in the paper #1 [BS11] were manufactured with an infill pattern of zero and 90 degree (with respect to the longitudinal axis) alternating from layer to layer; with one filament as perimeter, a 0.66 to 0.76 millimeters filament thickness, a 0.0254 millimeters negative air-gap (which means overlapping) between the filaments of the pattern, and 0.0635 millimeters negative air-gap between infill pattern and perimeter.

#2 - FDM: The specimens for the data sheet (PC [sys]) were produced *edgewise*, with a layer thickness of 0.254 millimeters. Other specifications, like infill pattern or spacing are not stated, but they have a big influence on the material properties. The used machine was the Fortus 400mc by Stratasys.

There is no information about the manufacturing parameters of the specimens tested in paper #2 [JBR10]. The used machine was the Fortus 360mc by Stratasys.

#3 – 3DP: No information about manufacturing parameters; no data sheets are available for the material used (Resin ZP130, Binder ZB58).

The specimens in paper #3 [Fra07] were produced with a layer thickness of 0.101 millimeters. After removing from the printer, they were placed in an oven at 82 degrees Celsius for one hour to remove the moisture inside the parts. The machine used is the Spectrum Z510 by 3DSystems (formerly ZCorporation).

#4 – SLS: No information about manufacturing parameters; no data sheets are available for the material used (PA 66).

The specimens in paper #4 [GS97] were manufactured with a layer thickness of 0.1 millimeters, a fill laser power of 3.5 watts, a scan spacing of 0.15 millimeters and a scan size of 73.

#5 – SMS: No detailed information about the manufacturing method. The machine used was the Eosint P by EOS [Kel99]. No data sheets are available (PA 12).

There is no information about the manufacturing parameters of the specimens tested in paper #5 [KD11].

2.2.4 Layer-less Additive Manufacturing

As already indicated previously, there are existing first trials of real three-dimensional, so layer-less additive manufacturing through holographic exposure or spatially intersecting laser beams [AdF13]. Another way would be to manufacture a casting mold. But not all kind of shapes are realizable and the step structure of form surfaces could lead to irregular flow of material during casting. Moreover, it could lead to notches on the casted part, which can especially influence filigree structures a lot. And, there are still to processes: The manufacturing of the mold and the casting.

Another process uses a UV-curing tool which operates inside a container of liquid resin in various build directions and selectively solidifies the resin into solid material [CZL11]. But this method is as well not fully developed yet.

Furthermore, architectural students from Barcelona have invented a method called *Mataerial* [aer]. A nozzle and two heat guns are mounted to a six-axis industrial robot. The heat guns solidify the extruded material directly along an arbitrary slope in room. However, as soon as two strings meet each other, the extrusion has to be paused.

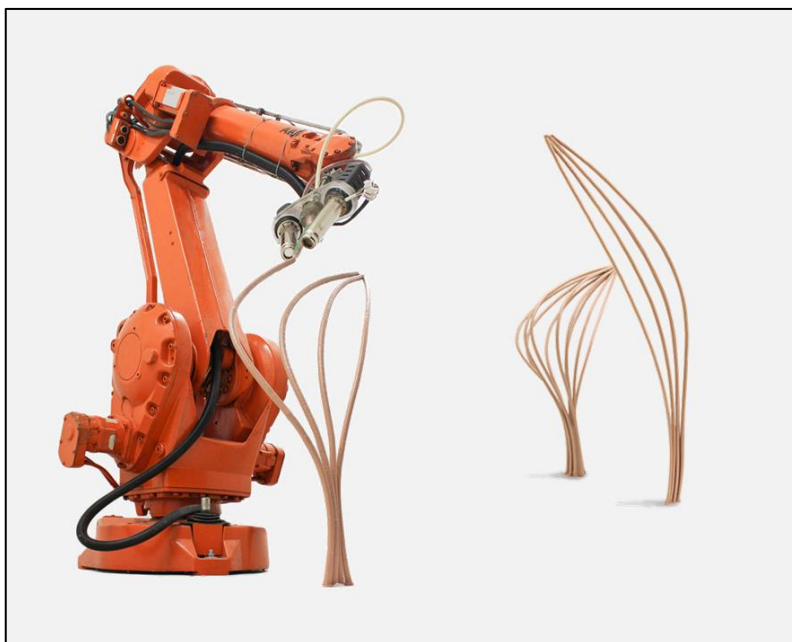


Figure 19: *MATAERIAL* – layer-less additive manufacturing [aer]

Thinkable would be also a system where one or multiple nozzles spray material, which is solidified directly by a laser beam. In layered technique, such a system already exists. It is called *Laser Engineered Net Shaping* (LENS) [Ins].

Another creative, playful method are *3D-drawing pens*. A plastic filament is connected to a pen, which itself is a small hot-melt gun [3do]. Hence, small and middle sized objects can be drawn in space. As the pen is operated by hand, it is not a very accurate method, but connected to a robot like above it could probably lead to some resonable results.

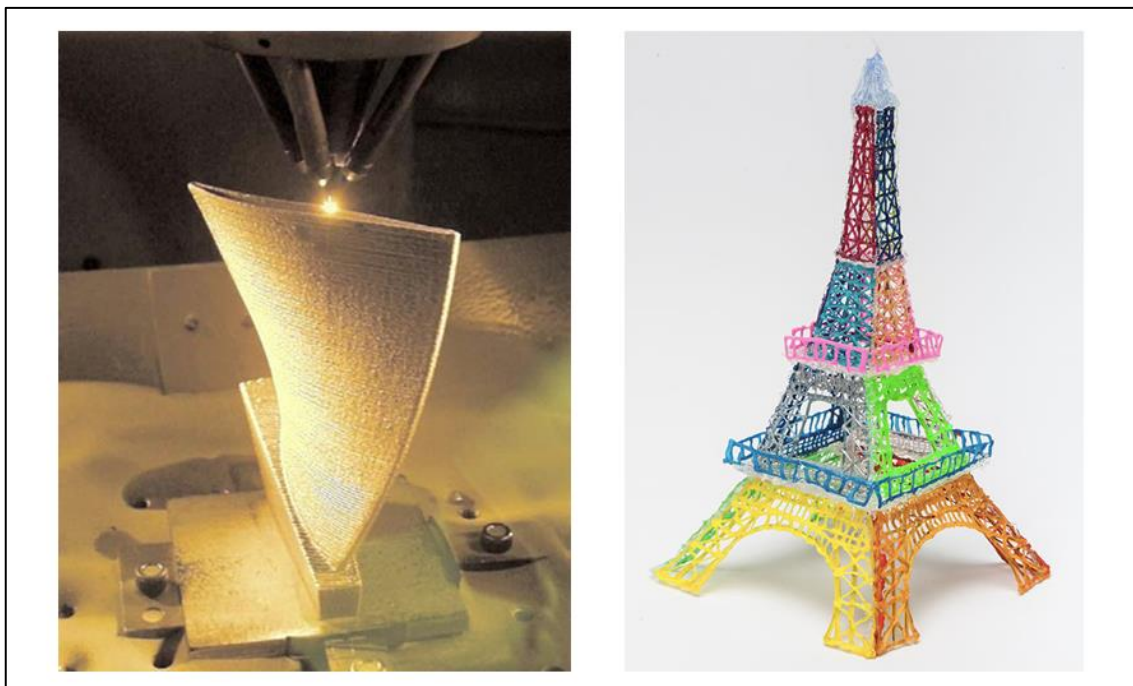


Figure 20: Left: *LENS* [Ins] | Right: Eiffel Tower made with 3D-Pen *3Doodler* [3do]

Advantages of a three-dimensional buildup over the two and a half dimensional-techniques would be the abolition of the layered structure, therefore probably better mechanical properties and surface qualities; the abolition of support material, which means saving material and having no residuals. But on the other hand, layer-less additive manufacturing leads possibly to an increasing buildup time and most likely to new complications for example like interface connections of struts in lattice structures.

Chapter 3 : PROBLEM DEFINITION AND OBJECTIVES

Problem Definition and Objectives

As stated in the literature review, it seems like mechanical properties of additive manufactured parts depend on the buildup direction. Consequently, especially for designed cellular structures, the layered buildup could lead to fatal consequences. Cell walls in different directions will have different abilities to withstand interfering forces. Hence, parts with cellular structures could be way underdesigned in one direction.

This leads to the question if there are advantages for material properties in a buildup of cell walls along their primary axis.

First, a proof of the stated facts about the mechanical properties of plastic materials in the different source papers should be made, and an analysis to find possible rules being valid for the different Additive Manufacturing methods.

Furthermore, a method has to be developed to explore the existence of advantages through manufacturing along the primary axis of the cell walls within a cellular structure instead of the conventional layered buildup.

As well, the additive manufacturing methods have to be analyzed in order to find the specific advantages and limitations. Thus, conclusions about further development of the methods from two and a half dimensions-techniques into real three-dimensional applications have to be made.

Chapter 4: RESEARCH APPROACH

Research Approach

The literature review shows, that the mechanical properties of additive manufactured parts are depended on the buildup orientation and the manufacturing process parameters.

Tensile specimens built up *flat* and *edgewise* show good properties, whereas the properties decline with an increase of the angle between the buildup platform and the generated specimen (Figure 21).

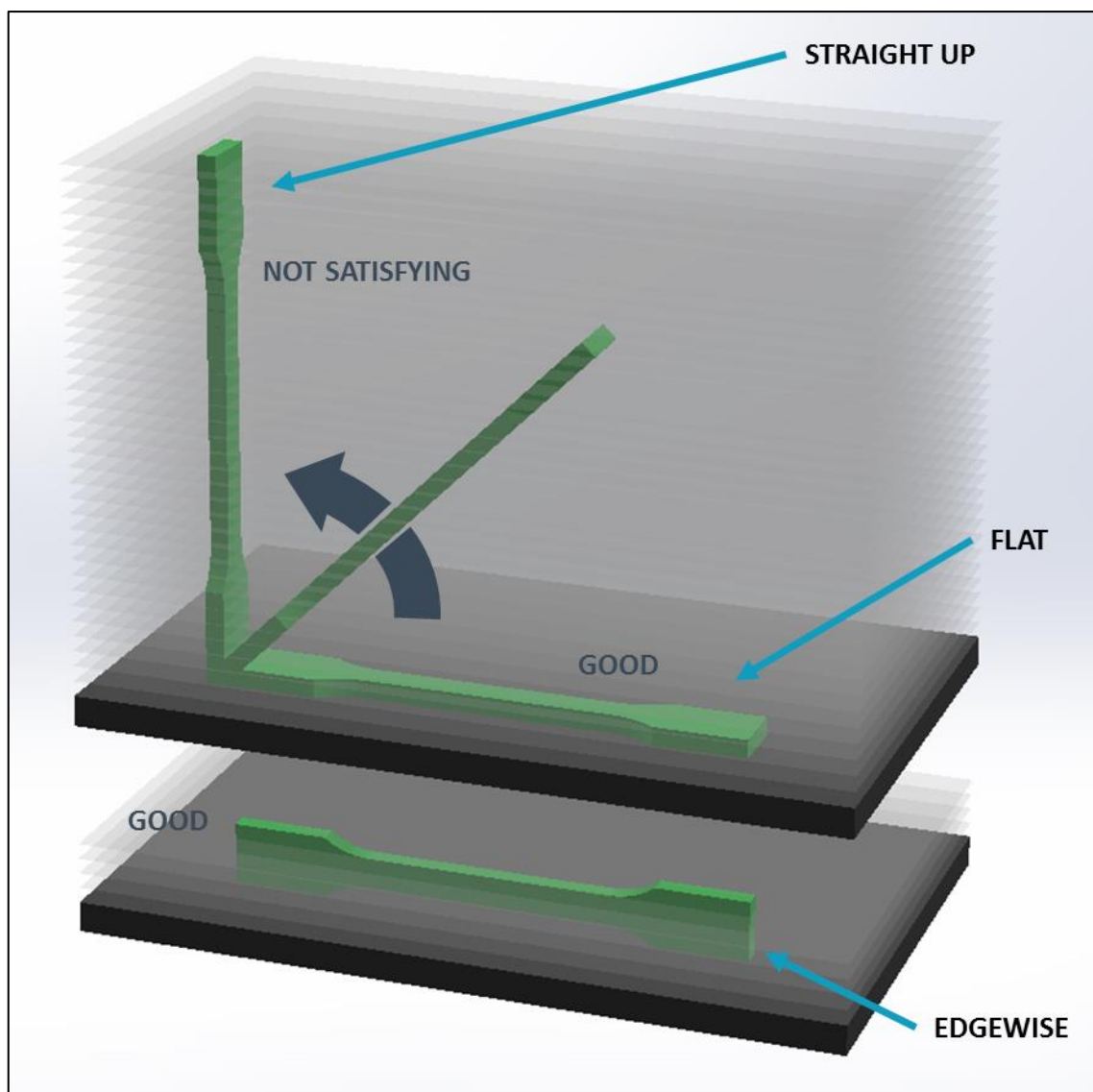


Figure 21: Material properties depending on part orientation

Assuming a truss-structure (Figure 22), built up layered by an additive manufacturing process, it occurs that there are different buildup orientations of struts within the structure. Taking the statement mentioned for granted, it means that the different struts have different mechanical properties. Given this fact, a loading in various spatial directions would lead to different results in mechanical behavior (Figure 23).

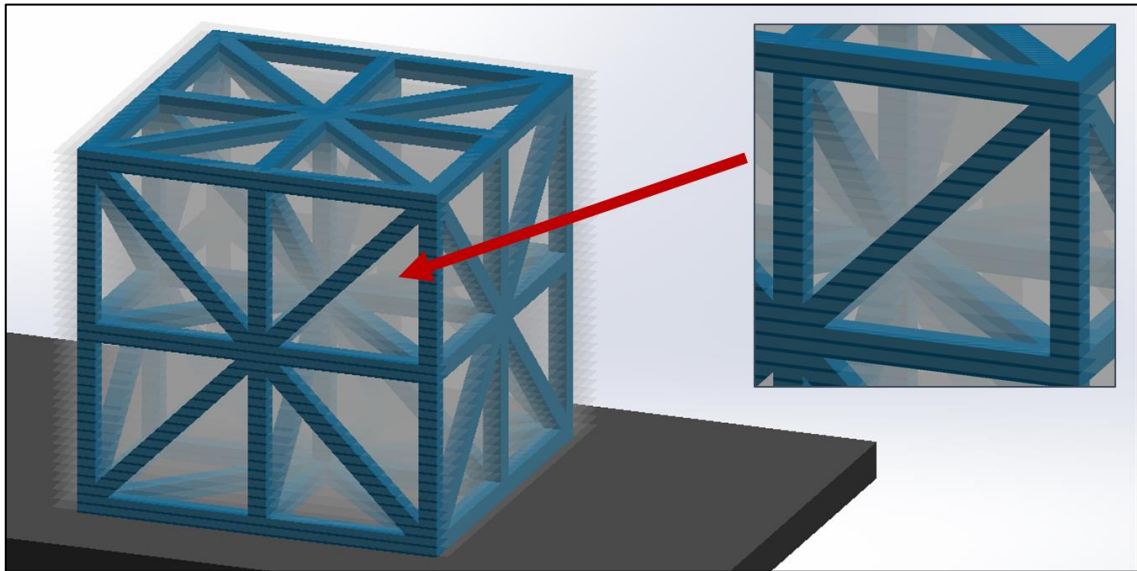


Figure 22: Different buildup orientations within one cellular structure

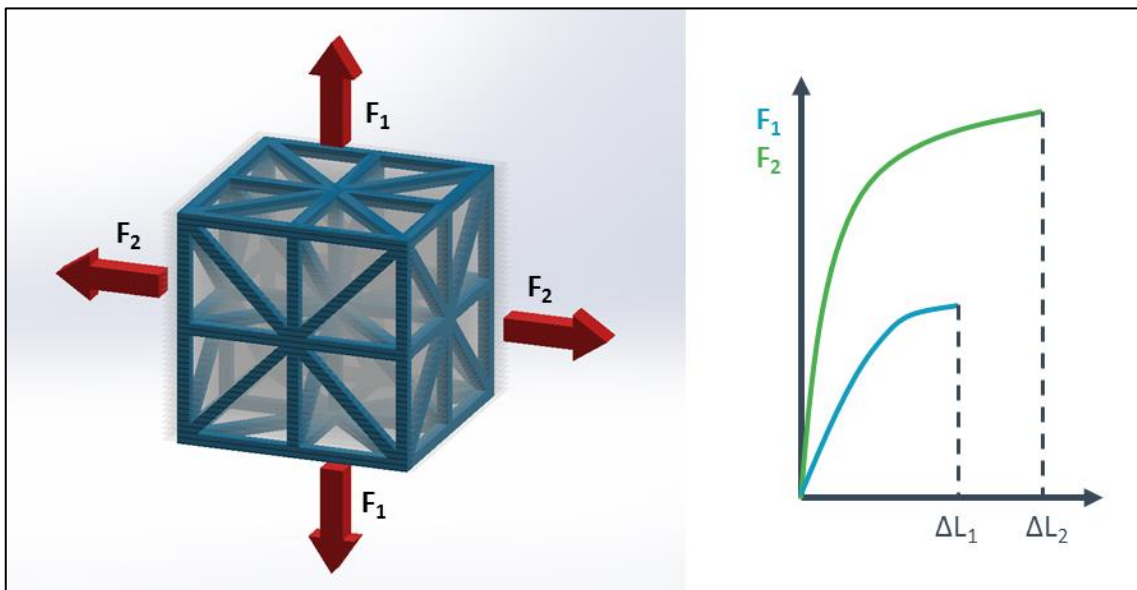


Figure 23: Loading of layered truss-structure (hypothetical)

To avoid different properties throughout the cellular structure, the struts should be produced along their primary axis.

Considering a honeycomb structure (a two-dimensional structure) a generation of material along the primary axis of the cell walls could mean one string of material throughout the height of the cells. This would be the optimal case, with an isotropic⁵ state of the material. It would represent a full three-dimensional buildup (Figure 24 – A).

But it could also mean still a layered buildup, where the cell walls in each layer are generated along their primary axis. This would be an orthotropic⁶ state and represent the local orientation *flat*, considering in-plane loading (x_1 - x_2 plane; Figure 24 – B). The main, global buildup orientation is *flat* as well, where due to the literature the solid materials have reasonable mechanical properties values.

In contrary, the same structure with cell walls having different strut orientations is needed. This succeeds through a global buildup direction *edgewise*, which stands for reasonable values in solid material too. Locally, the cell walls have orientations of *straight up* and *inclined under 30 degrees*, considering in-plane loading as well (Figure 24 – C).

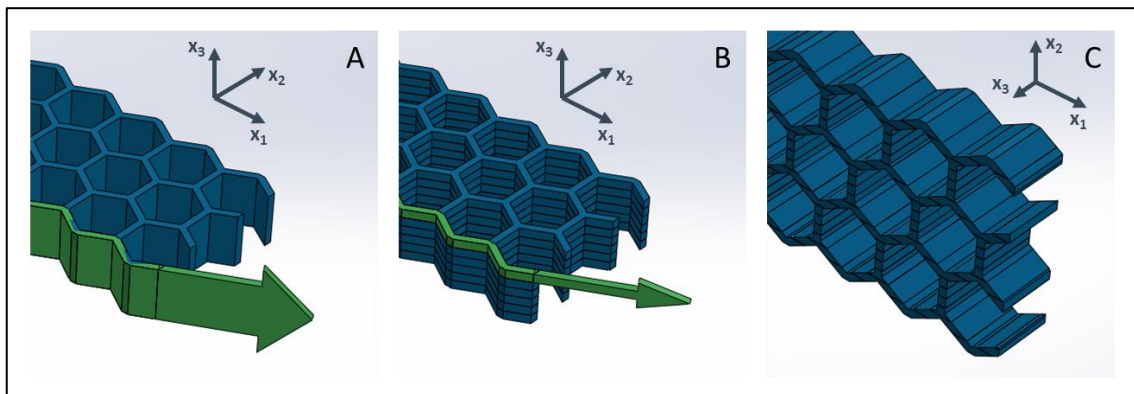


Figure 24: A Layer-less buildup, full cell generation along primary axis | B Layered buildup, cell generation along primary axis per layer | C Layered buildup, different buildup orientations of struts

⁵ Isotropic = Same material properties in every direction at a point in a body [Mor13]

⁶ Orthotropic = The material properties are different in three mutually perpendicular directions at a point in a body / three mutually perpendicular planes of material property symmetry / the properties depend on the orientation at a point in a body [Mor13]

To proof the properties, tensile testing could be used as a methodology. Therefore, tensile specimens with a cellular structure are needed. The tensile test has the advantage that solid specimens can be produced as well, and a comparison and proof of the facts stated in the literature review is possible.

As the thickness of a tensile specimen, which stands for the axial width of a cell, is greater than the maximal layer thickness, the specimen has to be manufactured conventionally (ref. Table 1). More detailed information is provided in the following chapters.

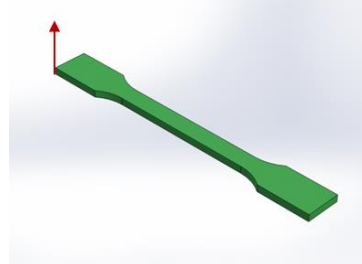
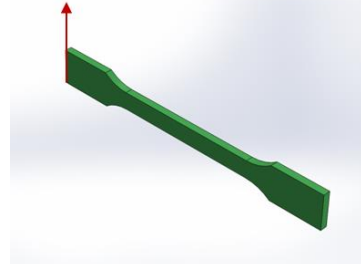
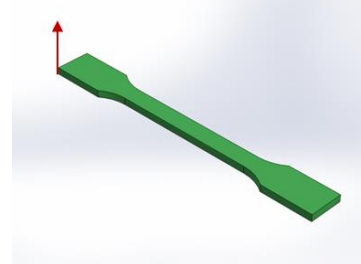
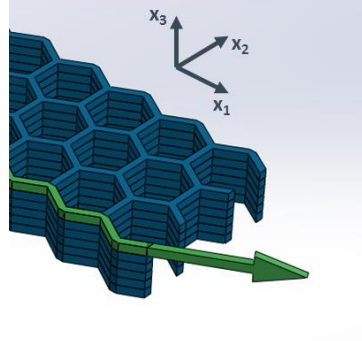
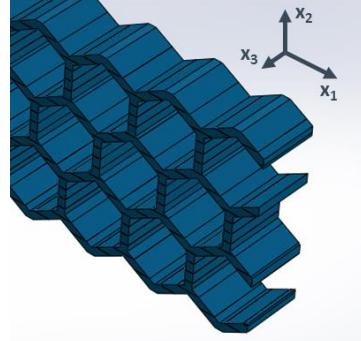
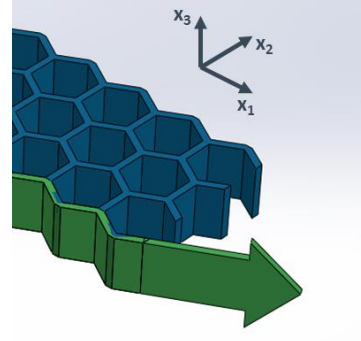
Layered Buildup along Primary Axis of Cell Walls	Layered Buildup, Different Buildup Orientations within Structure	Layer-less Buildup along Primary Axis of Cell Walls
Additive Manufacturing	Additive Manufacturing	Conventional Manufacturing
Global Buildup Orientation: Flat	Global Buildup Orientation: Edgewise	Global Orientation: Flat
		
Local Cell Wall Buildup Orientation: Flat	Local Cell Wall Buildup Orientation: Straight Up and 30°	No Layers; No Cell Wall Buildup Orientation
		

Table 2: Honeycomb structure – buildup specifications

Chapter 5: ACCOMPLISHMENT

Accomplishment

This chapter is about developing and running a method to fulfill the objectives stated in the research approach.

5.1 Design and Development of Tensile Specimens

As contemplated before, tensile tests will be carried out to do research about the mechanical behavior of the three stated types of the buildup of a honeycomb structure. Therefore, tensile specimens with a cellular structure are needed. Their development is a circle of validation consisting of design, simulation, material selection and production until finding a most likely solution. Moreover, they are predominantly designed for the additive manufacturing method Fused Deposition Modeling. This should be respected regarding the following subchapters.

Plastic is set as buildup material.

The standard ISO 527 regulates tensile testing for plastics. The commonly used specimen is the multi-purpose flat bar tensile specimen type 1A (Figure 25).

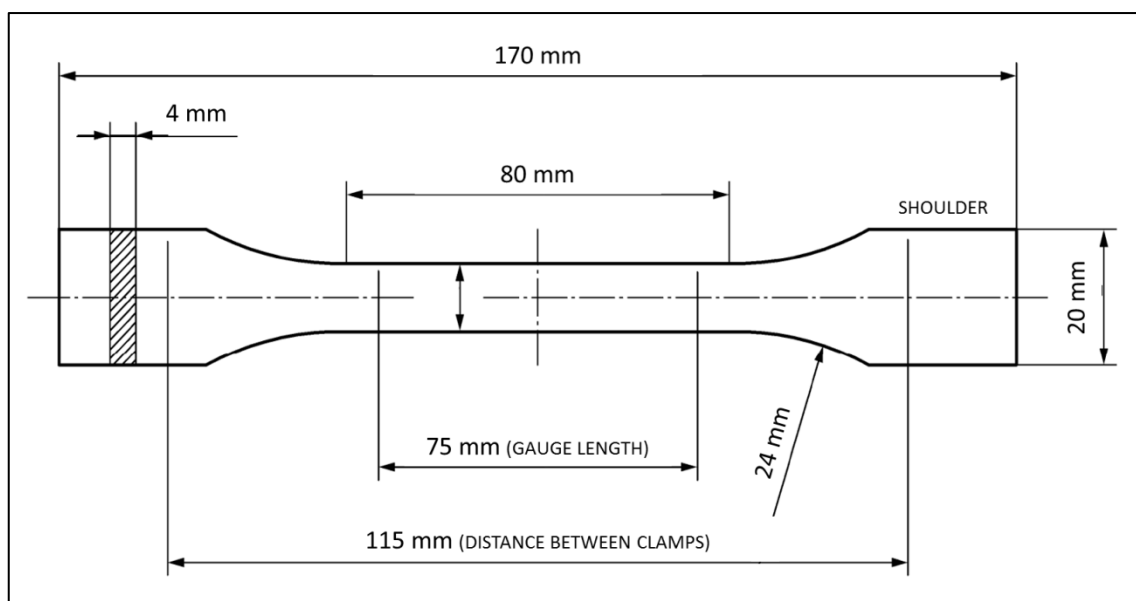


Figure 25: Multi-purpose tensile specimen for testing plastics [ISO527-2]

5.1.1 Honeycomb Specimen

For the honeycomb specimen, the specimen due to ISO 527 is modified. A **hexagon honeycomb structure** with a cell wall thickness of 0.8 millimeters is set as cellular structure, due to manufacturing constraints which are discussed in more detail later. The hexagons are regular, which means the six sides are of the same length (3.33 millimeters) and the six interior angles are of the same dimension (120 degrees).

As well because of manufacturing constraints, the honeycombs cannot be too small. Otherwise they would be more circles than hexagons. Hence, the dimensions of the multi-purpose tensile specimen presented above are not usable. The smaller parallel area has to be expanded from ten to 20 millimeters. The clamping shoulder width is set on 30 millimeters, which does not exceed the width of the clamps of the tensile testing machine. The total length and the distance between the clamps stay on 115 millimeters. Accordingly, the radii stay on 24 millimeters.

Clamping a specimen to the tensile testing machine causes sometimes a bit of bending due to subsidence of the clamps. Preliminary tests showed that increasing the thickness from four to six millimeters is reasonable and initial fracture of the filigree honeycomb structure can be avoided.

Various connection passages between the solid shoulders and the honeycomb structure of the specimen, as well as various shapes of boundaries are analyzed by simulation with *ANSYS Workbench*. Tips with half the length of the cell walls and the connection passage showed in Figure 27 lead to the smallest local stress peaks and smallest distortion of the hexagons during loading. The gauge length is scaled down from 75 to 50 millimeters as the hexagonal honeycombs stretch parallel to the load direction in this area. All shapes, declarations and dimensions are stated in Figure 26 and Figure 27.

The orientation of the hexagons is also influenced by manufacturing constraints, as turning the hexagon through 90 degrees would've led to difficulties (Chapter 5.3). Besides, the stretching behavior would have been different.

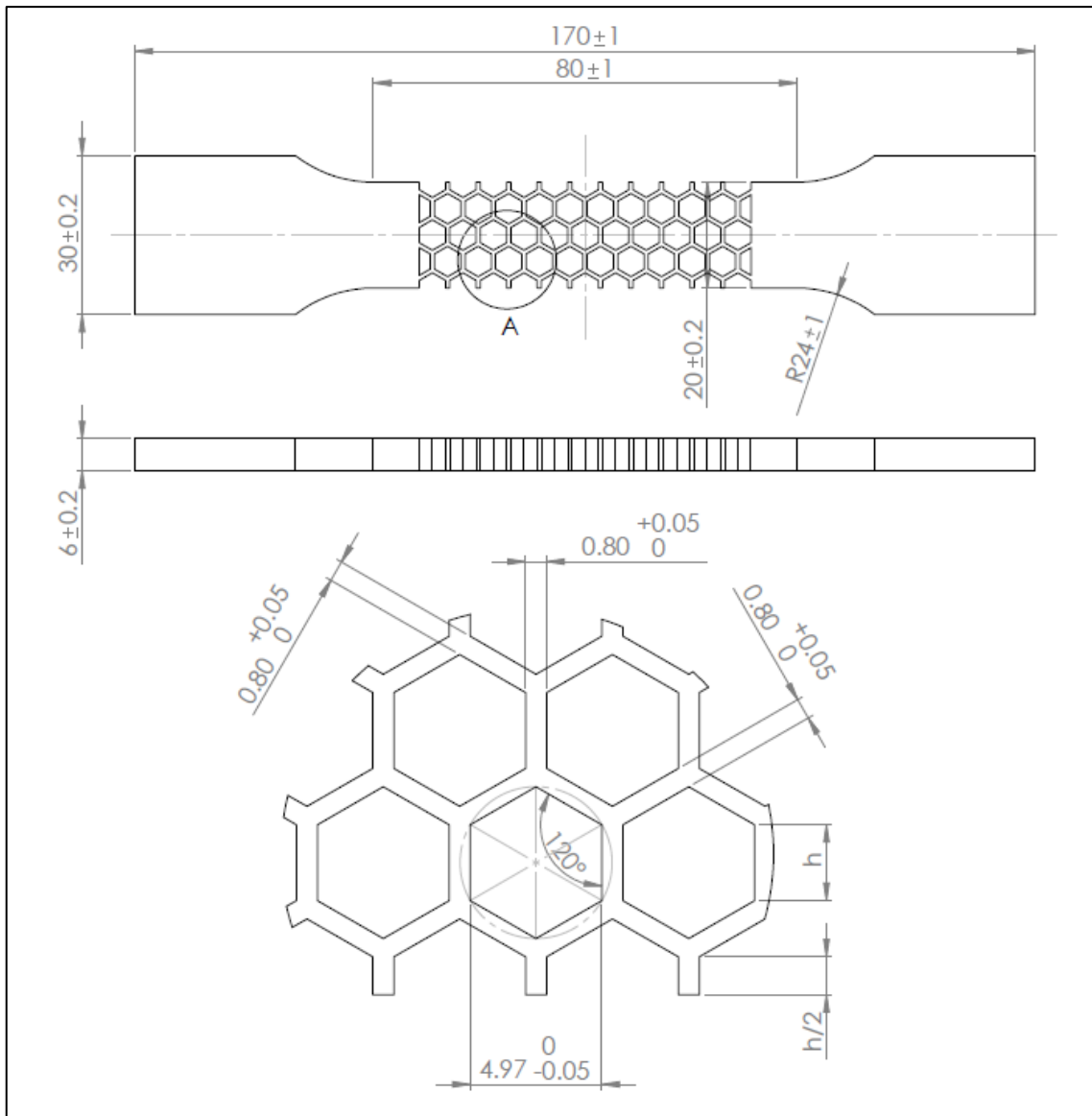


Figure 26: Drawing of honeycomb tensile specimen

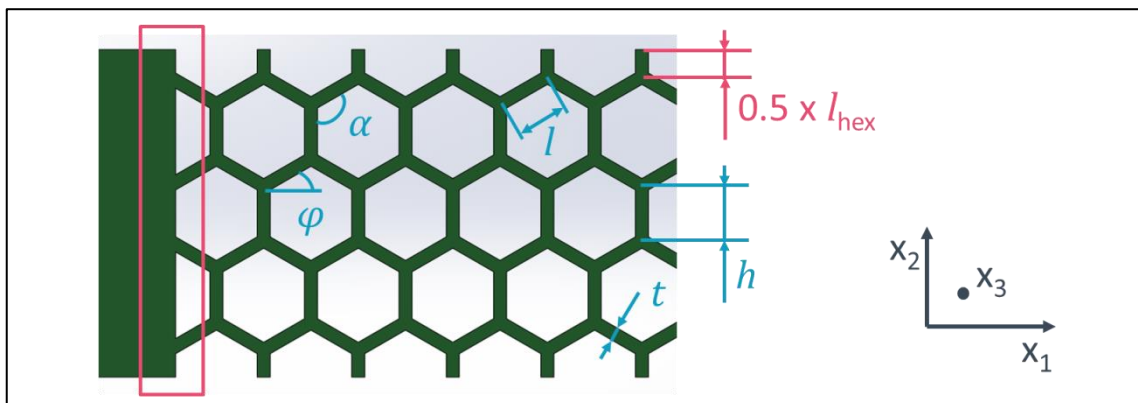


Figure 27: Connection passage and tips (light red) | dimensions hexagon cell (light blue)

5.1.2 Solid Specimen

Solid tensile specimens are needed to proof the statements of the literature review paper and to compare with the values out of the data sheets of the materials used later.

To have a uniform design, only the honeycombs are erased and the outer shape stays like in the honeycomb tensile specimens.

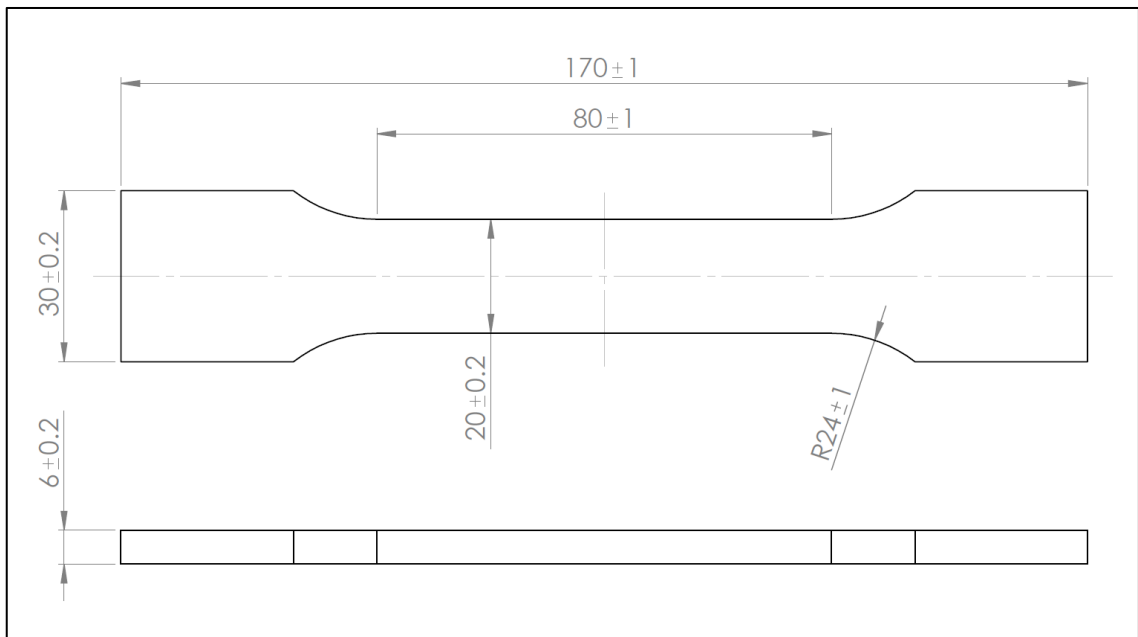


Figure 28: Solid tensile specimen – drawing

5.2 Mechanical Behavior of Honeycombs

Gibson and Ashby [GA97] describe the behavior of honeycombs under in-plane (x_1 - x_2 plane (Figure 27)) uniaxial tension as an initial bending of the cell walls, but no elastic buckling. In case of a plastically yielding cell wall material, the honeycombs itself will show plasticity. If the cell walls are brittle, the honeycombs will fracture brittle as well (Figure 29).

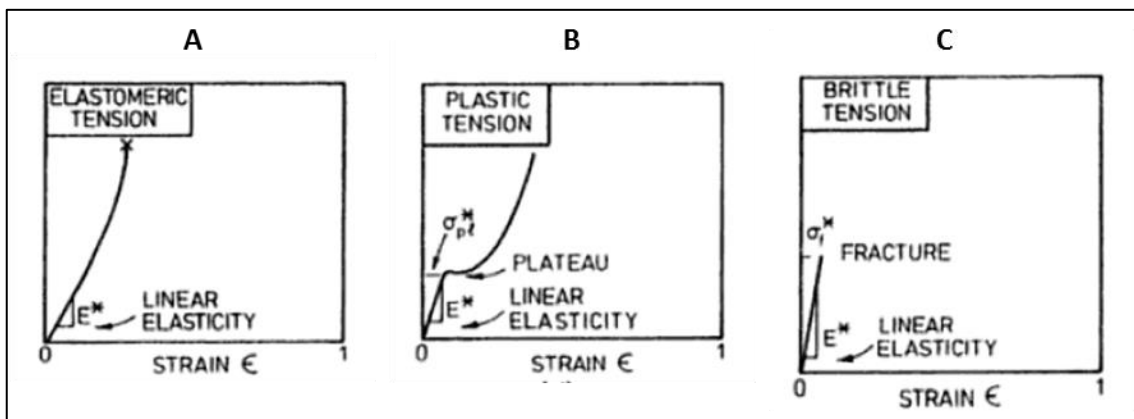


Figure 29: A elastomeric honeycombs, B elastic-plastic honeycombs and C elastic-brittle honeycombs under tension

Further they describe regular hexagons with constant wall thickness (like in this research) ($h = l$ and $\alpha = 120^\circ$ (Figure 27)) as isotropic. They assume “that deformations are sufficiently small that changes in geometry can be neglected” [GA97] for $t/l > 1/4$ (here: $t/l = 0.8 \text{ mm} / 3.33 \text{ mm} = 0.24$) and strains smaller than 20 percent. But, the additive manufactured cell walls are layered and not solid, which means that mechanical properties depend on directions. Hence, the basic assumptions of strength of solid materials supporting the mathematical models of Gibson and Ashby are probably not valid for this research.

5.3 Manufacturing of Specimens

To achieve the requirements stated in the approach the additive manufactured specimens will be oriented *flat* and *edgewise* on the machine platform (Figure 30). This is valid for both, the solid and honeycomb version. In addition, comparable materials processible with additive and conventional manufacturing methods are needed. The only possibility found (with respect to the available machines) is using **polycarbonate** as production material, **Fused Deposition Modeling** as additive manufacturing method and **milling** as conventional manufacturing method.

To get some comparison between different additive manufacturing methods, **Poly-Jet Modeling** and **Selective Laser Sintering** are chosen. However, the machines do not provide polycarbonate as a buildup material. As the materials mostly are tailored to the particular manufacturing method, it is nearly impossible to find one uniform solution. Nevertheless, the tensile tests certainly will give useful answers about general rules of orientation dependency and new insights.

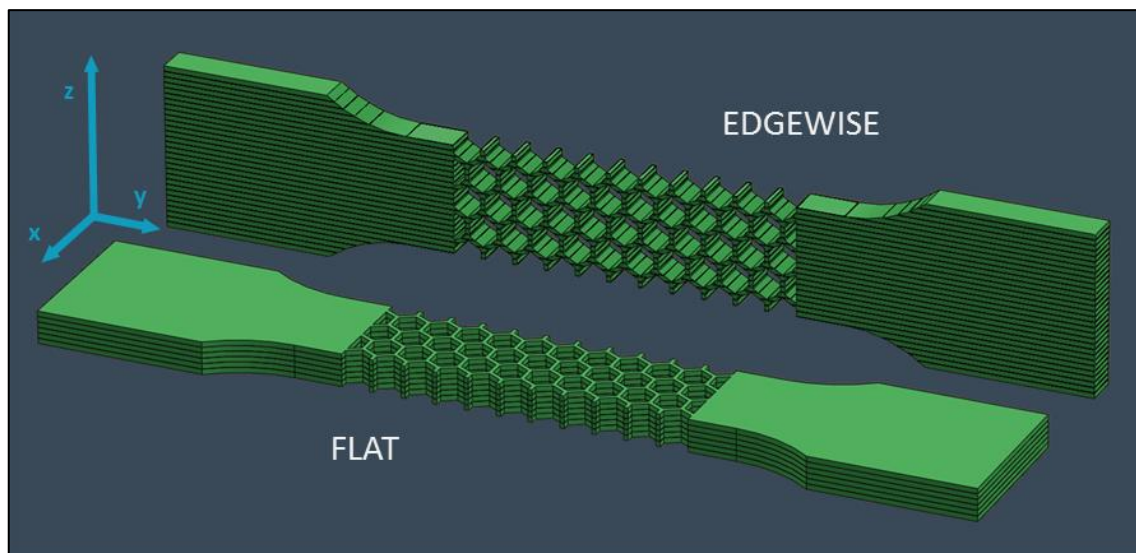


Figure 30: Honeycomb specimens – flat and edgewise buildup orientation

5.3.1 Fused Deposition Modeling (FDM)

In Fused Deposition Modeling a plastic wire is unrolled from a spool and is inserted into an extruder (Figure 31). There, the wire is melted through a heat element and extruded through a nozzle onto the buildup platform. The nozzle or print head follows a print path in x- and y-direction and generates one layer by extruding a weak plastic filament. As soon as the first layer is generated, the platform is lowered (z-direction) by a defined distance and enables the print head to print another layer upon the first. Like this, little by little an entire part is generated.

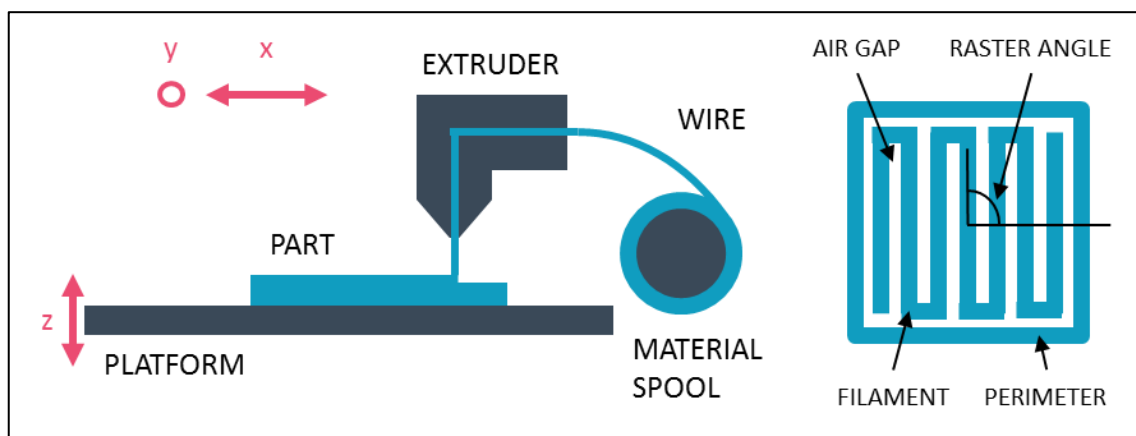


Figure 31: Functional principle Fused Deposition Modeling (FDM)

To produce the tensile specimen, initially a personal printer (Hofi X1 by Boayan Automation) is used. The printer can only print one type of plastic at a time. This means that support and buildup material are the same and therefore hard to remove from one another. Thus, using support material should be avoided. According to this, the honeycomb structure is designed with the tips of the hexagons oriented vertically. This is because horizontal lines cannot be printed without support material, as the plastic is weak and would drop down.

Before the specimens are printed, the CAD-model is uploaded to a part orienting, part slicing and path generating software. The filament diameter is set by the nozzle diameter of 0.4 millimeters. To achieve satisfying quality, the layer thickness should not be greater than this value too.

Also, the cell wall thickness is limited to the filament width. Only 0.4 millimeters or multiple are feasible. Besides this fact, the honeycombs are also depended on the path: A wall thickness of only one filament width would lead to gaps or insufficient bonding, because there would be dead ends where the extrusion has to be stopped. Continuance at another point forces the printer to make mistakes.

Printing each hexagon with one perimeter of one filament will result in a wall thickness of 0.8 millimeters (Figure 32). Moreover, the hexagons need to have a certain size, otherwise they are only circles. If the print head drives a corner, the extruded filament curves as it is still weak. This is why the specimens were designed like previously presented (Chapter 5.1.1).

For the infill a 0-90 degrees raster, without a gap between the filaments is chosen. One perimeter surrounds the infill, to keep the influence, especially for the solid specimens, as small as possible (Figure 32).

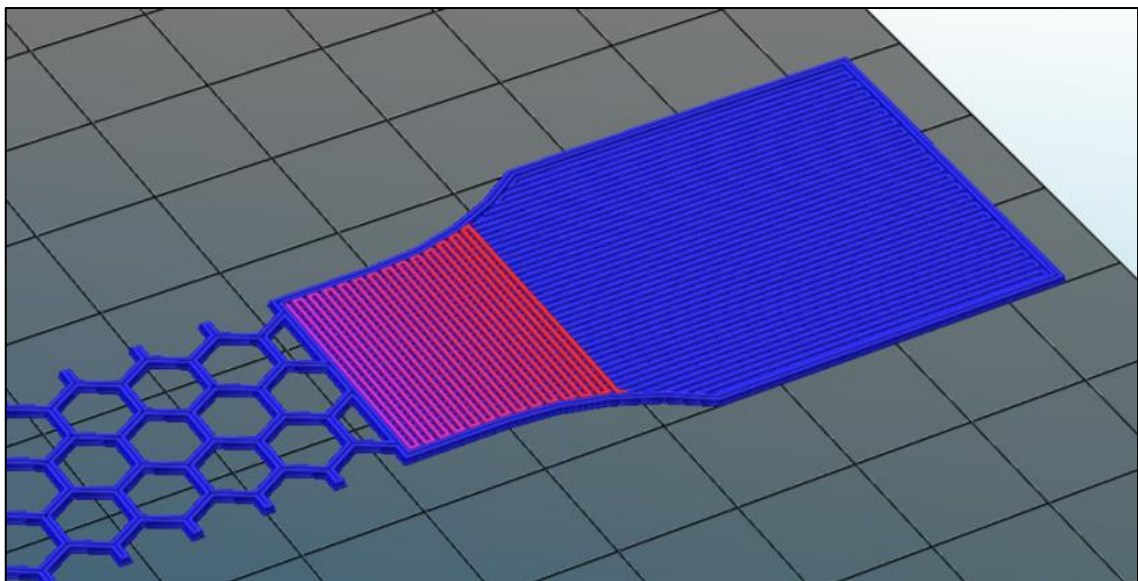


Figure 32: Path generation with pre-processing software

Limitations in software: Individual adjustments for each layer or specific areas are not possible, which leads to errors, like incorrect infill density, gaps, path interruptions, wrong number of perimeters.

Next to diverse problems with the pre-processing software (for example slicing and path generation mistakes), the printing process with the personal printer has some additional limitations:

- The maximum temperature of nozzle is around 265 degrees Celsius. After a few minutes at this temperature or an initially set temperature beyond this value, the machine will shut down;
- The extruded material is not always sticking to the surface of platform. Through tests with different toppings on the surface, better results were achieved. But a change of the material brand or color causes new problems;
- A heat chamber does not exist. Thus, there is no stable environmental temperature and the printed filament can cool down too fast with the result of flaws or total failure (depending on the material and the required temperature);
- The printing sequence leads to errors (Figure 33). Tilting or coupled motion of parts caused by the nozzle appears. Upwards curling of sharp edges happens through the heat of or even contact with the nozzle.

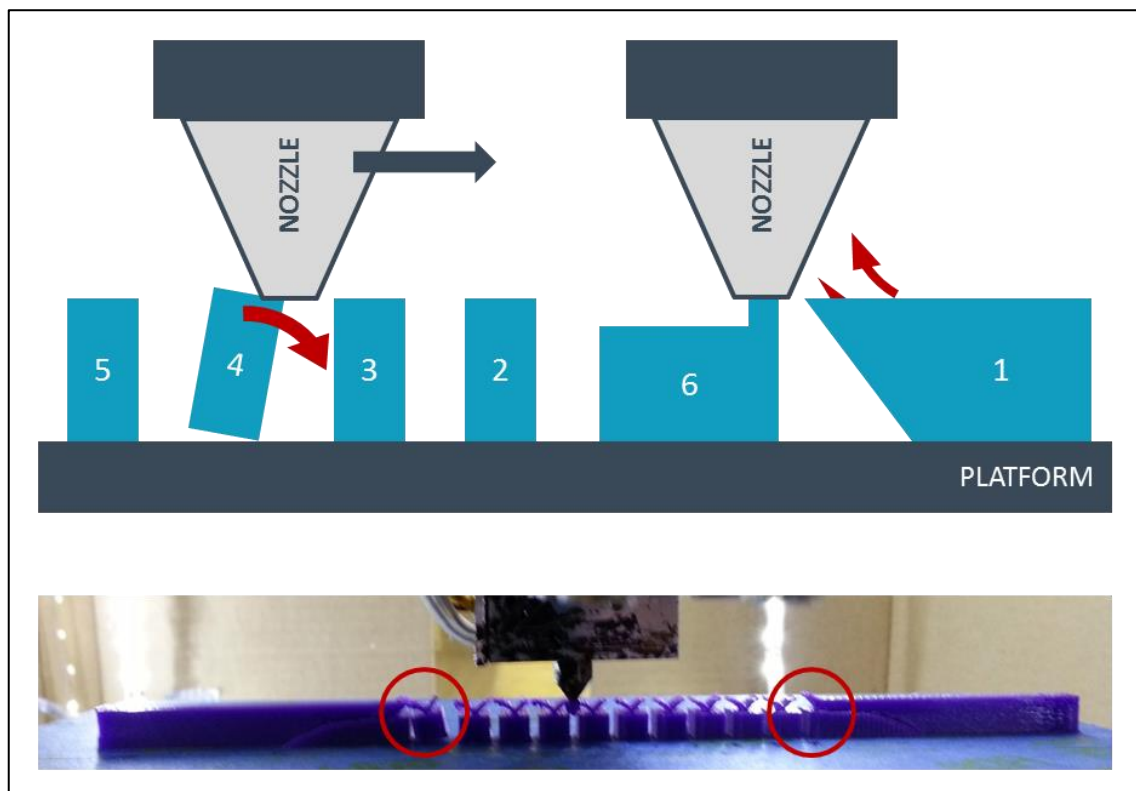


Figure 33: Errors caused by printing sequence

Because of the reasons mentioned, polycarbonate is hardly printable. It needs an extrusion temperature of minimum 270 degrees Celsius. Moreover, it does not stick to the platform and it cooles down to fast.

Due to these limitations, a more professional machine and pre-processing software (Figure 34) is needed. The manufacturing of the polycarbonate (PC) tensile specimens is done with the Fortus 360mc by Stratasys. The printer provides a sealed chamber and support material which is different to the buildup material. The pre-processing software of the Fortus 360mc is way more professional than the one of the personal printer. It allows modifying each layer individually.

PROCESS PARAMETERS – FUSED DEPOSITION MODELING	
Type	Stratasys Fortus 360mc
Material	Stratasys Polycarbonate (PC)
Support Material	Stratasys PC Support Break-away
Heat Bed Temperature	145 °C
Chamber Temperature	145 °C
Layer Thickness	0.254 mm (0.01 in)
Infill Density	100 %
Filament Width	0.4064 mm (0.016 in)

AMOUNT OF USED MATERIAL AND PRINTING TIME OF ONE SPECIMEN			
Specimen Type	PC	Support	Time
Honeycomb Flat	20532.99 mm ³ (1.253 in ³)	1474.83 mm ³ (0.09 in ³)	1:25 h
Honeycomb Edgewise	25236.08 mm ³ (1.54 in ³)	3441.28 mm ³ (0.21 in ³)	1:46 h
Solid Flat	27366.40 mm ² (1.67 in ³)	1147.09 mm ³ (0.07 in ³)	0:37 h
Solid Edgewise	26055.43 mm ³ (1.59 in ³)	3769.02 mm ³ (0.23 in ³)	2:13 h

Table 3: Process parameters – FDM

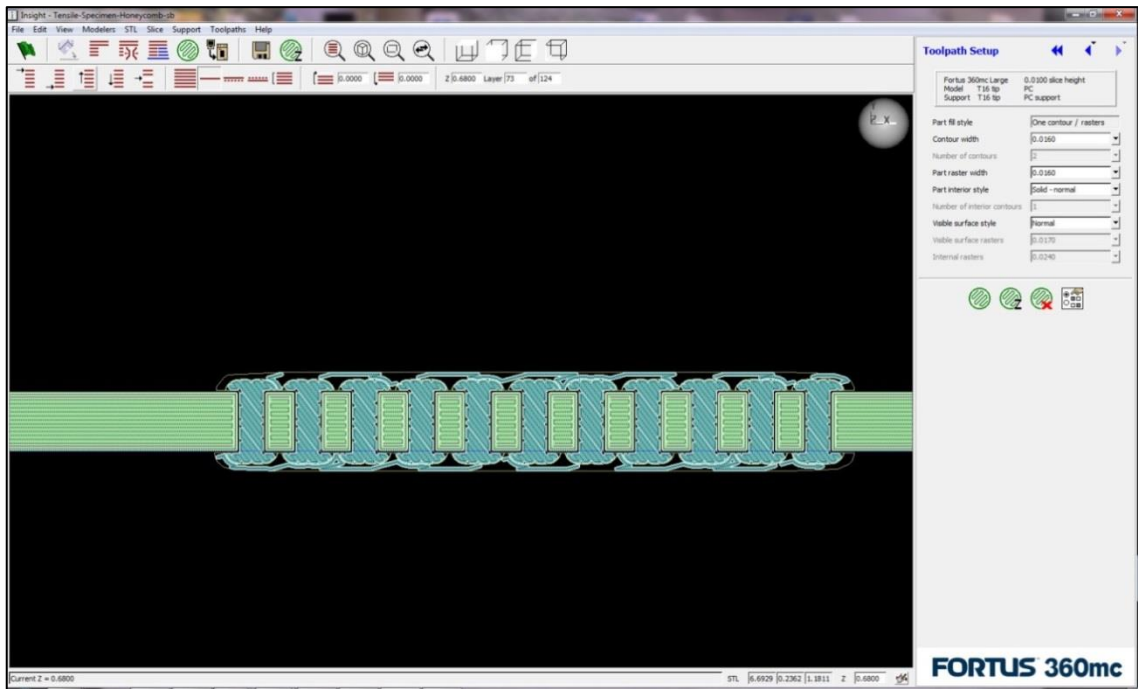


Figure 34: Pre-processing software by Stratasys for Fortus 360mc

The support material of the edgewise oriented honeycomb specimens is hardly erasable, although it was different to the buildup material. The corners of the flat oriented hexagons are still curved, with a radius around 0.8 millimeters. The dimensions and their tolerances are met.

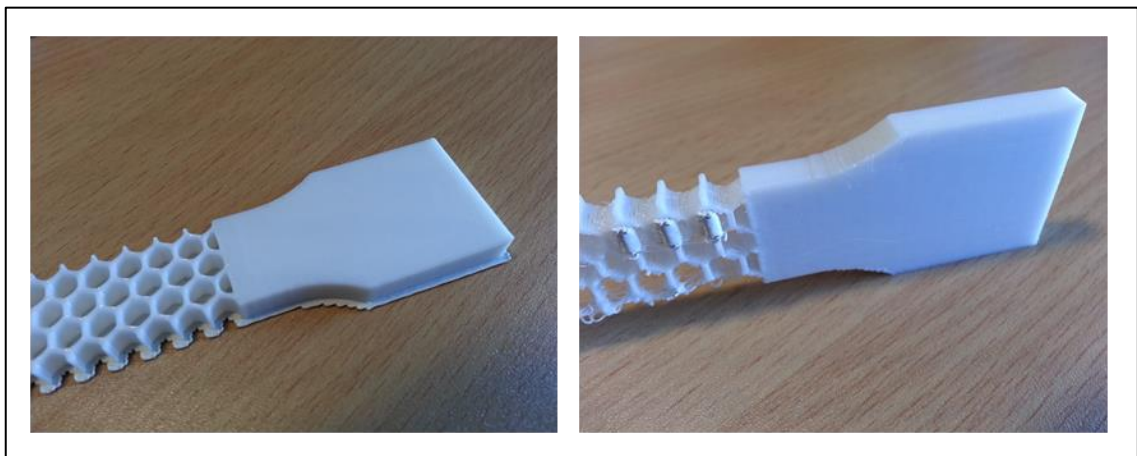


Figure 35: Polycarbonate FDM honeycomb-specimens – buildup orientation flat (left) and edgewise (right; problems with buildup and support material)

5.3.2 Milling

In manufacturing the FDM honeycomb specimens, radii arose at the corners of the hexagons. This is not a limitation, but quite ideal. Because in milling a cylindrical tool is used, which leaves radii at the edges of the hexagons (Figure 36). A radius of 0.8 millimeters fits most likely to the curvature and therefore a milling tool with a diameter of 1.6 millimeters comes into operation.

The specimens are milled out of a six millimeters thick polycarbonate sheet. A high precision four-axis CNC rapid prototyping machine [rol] is used (Roland MDX-540).

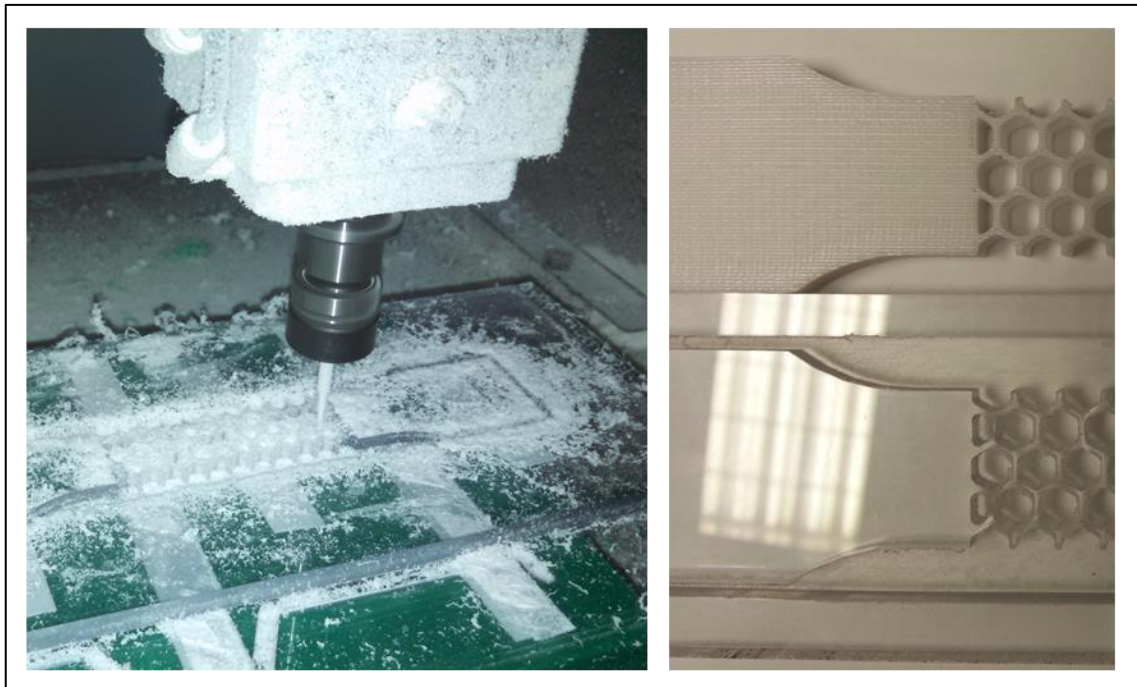


Figure 36: Milling process | comparison of FDM specimen (top) with milled specimen (bottom)

5.3.3 Poly-Jet Modeling (PJM)

[AdF13] Poly-Jet Modeling is an additive manufacturing method with a selective application of UV-curable photopolymer resin drops and an areal solidification through exposure (Figure 37). First, the photopolymer is jetted onto the buildup platform by the printing head. Nearly in the same moment, the photopolymer drops are leveled by a roller and solidified by a UV-light. Afterwards the platform is lowered. Like this, a part is generated layer by layer. For each layer the machine needs two drives. Because in order to avoid a flowing together of the drops, the machine jets a raster during the first drive and fills it up during the second one. It is the so called interlacing procedure.

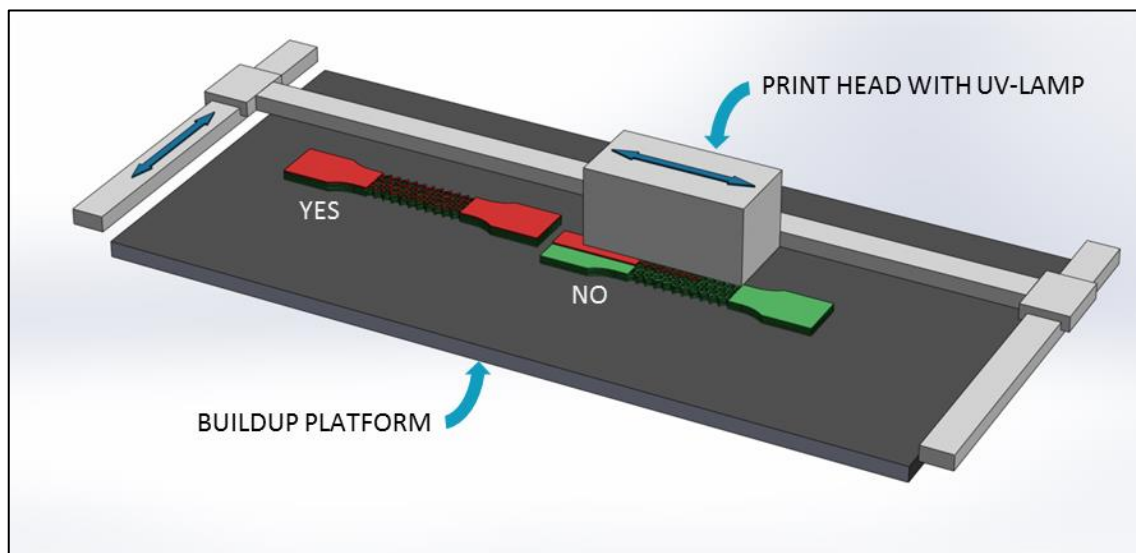


Figure 37: Functional principle Poly-Jet Modeling (PJM)

The specimens are manufactured with the Stratsys Objet350 Connex. RGD720 is used as buildup material. It is declared as a transparent material, but leads to a more yellow milky color in the end. The applied support material is different to the buildup material and is jetted and solidified at the same time. The attention is on printing the specimen in one stripe to avoid interstitions in the hexagon structure (Figure 37). Poly-jet Modeling suits well for manufacturing cellular structures as it provides high accuracy and sharp edges.

PROCESS PARAMETERS – POLY-JET MODELING	
Type	Stratasys Objet350 Connex
Material	Stratasys FullCure 720 RGD 720
Support Material	Stratasys FullCure 705 Support Resin
Heat Bed Temperature	35 °C
Chamber Temperature	35 °C
Layer Thickness	0.032 mm
Mode	High Speed

AMOUNT OF USED MATERIAL AND PRINTING TIME OF ONE SPECIMEN			
Specimen Type	PC	Support	Time
Honeycomb Flat	32 g	8 g	0:20 h
Honeycomb Edgewise	36 g	20 g	1:18 h
Solid Flat	41 g	8 g	0:20 h
Solid Edgewise	41 g	8 g	0:20 h

Table 4: Process parameters – PJM

After the printing process the support material is erased with a water jet, the recommended procedure. However, the specimens absorb some water, which leads to strong deformation through inner stresses (Figure 38). With a relaxation in an oven at 40 degrees Celcius the initial form of the specimens is recovered.

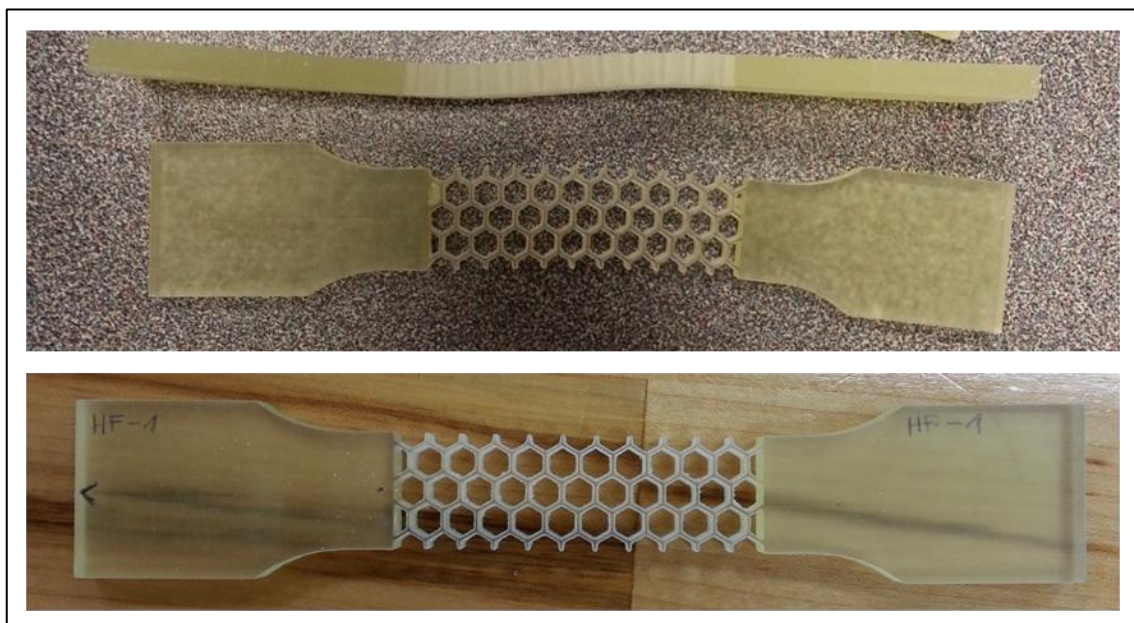


Figure 38: Top: deformed specimens due to moisture | bottom: PJM – honeycomb tensile specimen

5.3.4 Selective Laser Sintering (SLS)

[AdF13] Selective Laser Sintering is an additive manufacturing method with areal application of powder material and selective solidification through an infrared laser beam. The powder is distributed by a roller over the buildup platform. Subsequently, the laser beam melts the powder grains and they connect with each other. If one layer is generated like this, the platform is lowered and the process starts from the beginning. Therby, the remaining powder stays around the layers and supports the arising part. Even several parts can be stacked like this in one buildup space.

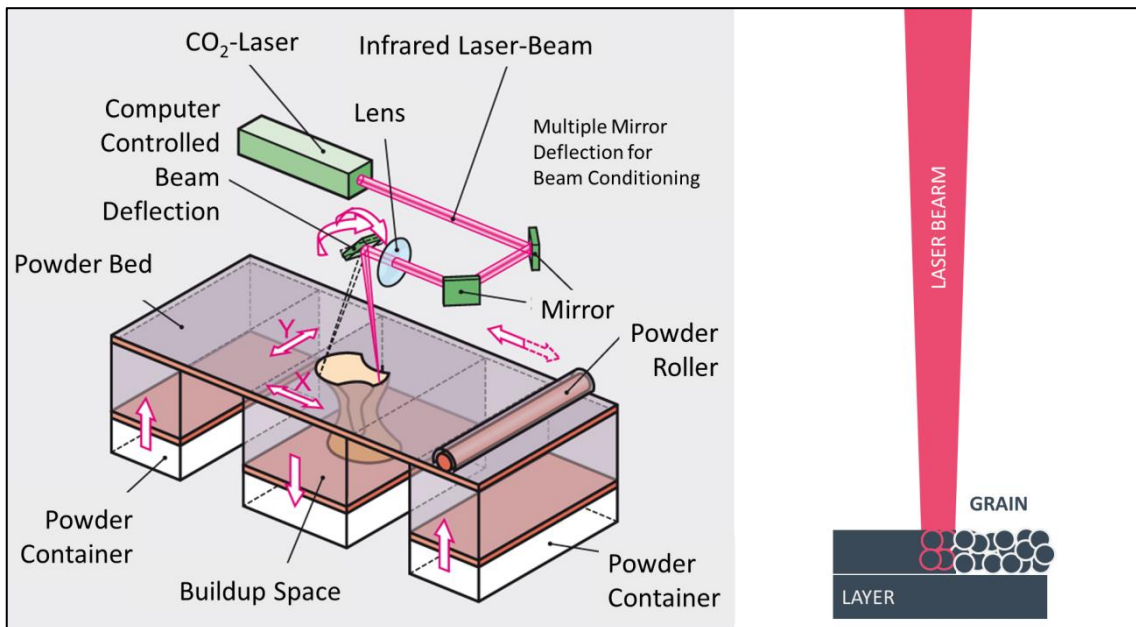


Figure 39: Functional principle Selective Laser Sintering (SLS) [AdF13]

PROCESS PARAMETERS – SELECTIVE LASER SINTERING	
Type	3D Systems SPro60 HDHS
Material	DuraForm® Polyamide (PA)
Support Material	Same – Powder Bed
Process Temperature	174 °C
Laser Power	44 W
Scan Spacing	0.1778 mm (0.007")
Layer Thickness	0.0762 mm (0.003")

Table 5: Process Parameters – SLS

The specimens are manufactured with the SPro60 by 3D Systems. The used material is a polyamide powder. The solidification as well is executed along the primary axis of the cell walls, as stated in following picture.

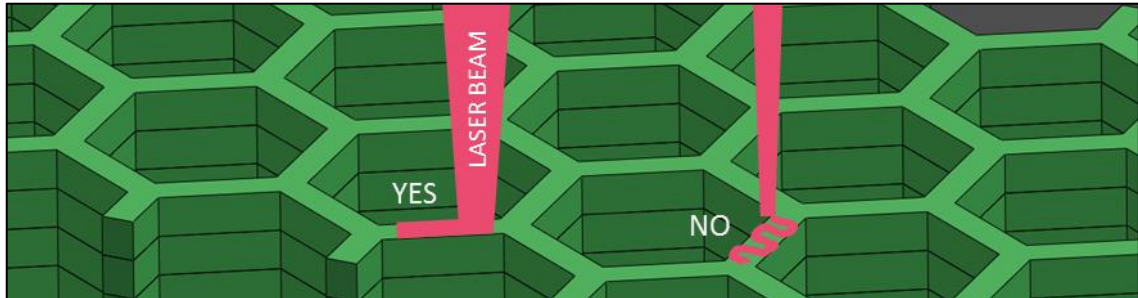


Figure 40: Solidification along the primary axis of the cell wall

Unfortunately, most of the received specimens have an unsatisfactory quality. Dimensions are not correctly and some of the shoulders are totally deformed. The shape of the honeycomb structure is quite good, but small areas already crumble away (Figure 41). A general problem of Selective Laser Sintering of cellular structures seems to be: The closer the cell wall thickness to the size of the grains, the worse the quality of the cellular structure will be.

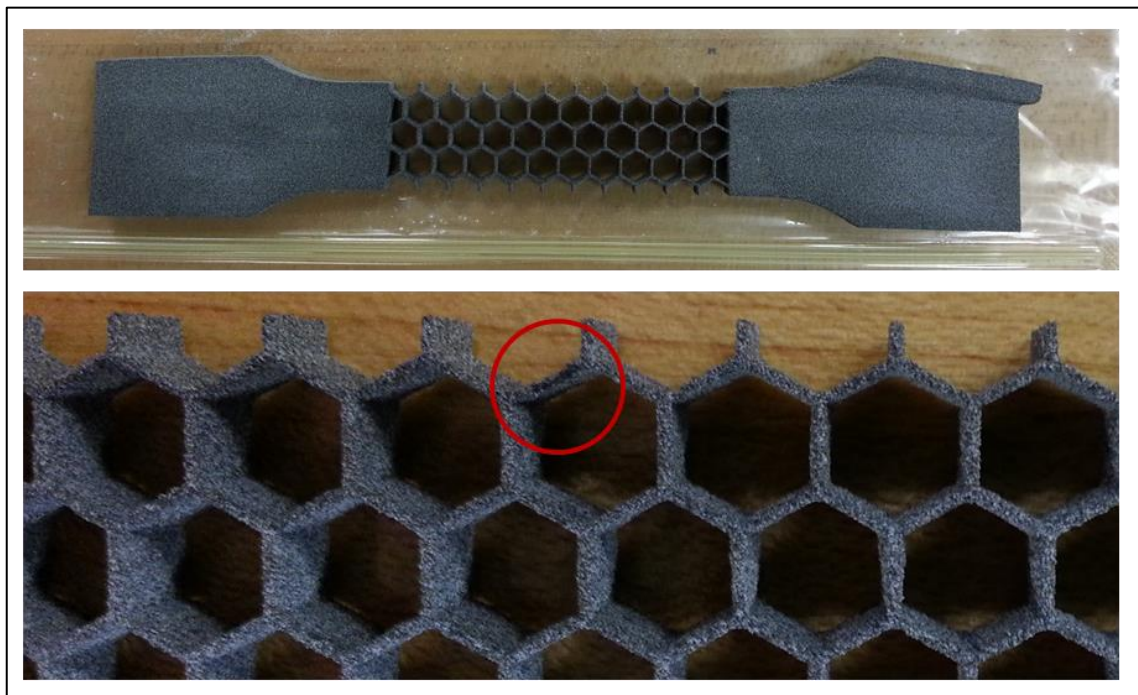


Figure 41: Top: incorrect dimensions and deformed shoulder | Bottom: brittle cells walls

5.4 Tensile Testing

The tensile test is a proven method to receive information about the mechanical behavior of materials, which is in the case of plastics depended on “the speed of deformation, the time and frequency of loading, the geometry of the specimens, the process parameters during manufacturing and the environmental conditions, especially the temperature” [Sae13]. As there is no standard defined for additive manufactured tensile specimens, the short-haul tensile test due to ISO 527-1 and 2 is carried out.

The tensile specimens are loaded with a constant speed in millimeters per minute. The force F acting along the primary axis of the specimen and the displacement ΔL of the gauge length L_0 are recorded and shown in a force-displacement diagram.

With the following formulas, the stress σ and strain ε can be calculated:

$$\sigma = \frac{F}{A_0} \quad [\text{Sae13}] \quad (4.1)$$

$$\varepsilon = \frac{\Delta L}{L_0} \quad [\text{Sae13}] \quad (4.2)$$

As plastic materials do not show a linear-elastic regime, the Young’s modulus is determined by the gradient between the 0.05 percent and 0.25 percent of strain.

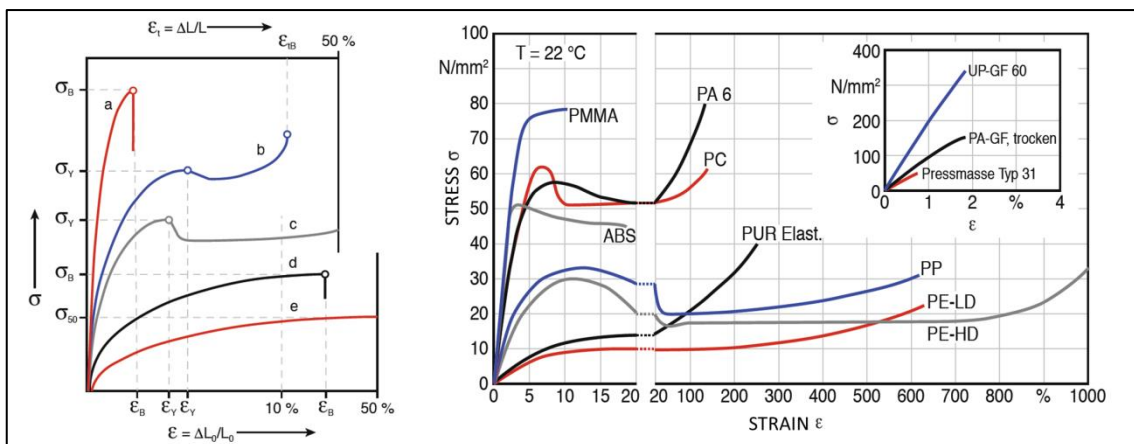


Figure 42: Left: Typical stress-strain curves for plastic materials – **a** brittle, **b** ductile, **c** drawable, **d** and **e** softened plastic | right: stress-strain curves of different plastic materials [Sae13]

5.4.1 Accomplishment of Tensile Tests

Tensile testing is executed according to ISO 527-1 and 2 with the following machine and parameters.

TENSILE TESTING: TOOLS AND PARAMETERS	
Tensile Testing Machine	Instron 8874
Load Cell	25 kN
Software	Bluehill
Extensometer	Epsilon 3542 (accuracy: $\pm 1 \mu\text{m}$)
Temperature T_0 (Humidity)	21 °C (50%)
Gauge Length L_0	50.8 mm (2 in)
Distance between the Clamps L	115 mm
Test Speed v	5 mm/min
Sampling of Displacement and Load	Every 0.1 seconds
Quantity Specimen	5 of each Type

Table 6: Tensile testing tools and parameters

Due to ISO527-1 the specimens have to be placed in the clamping device with their longitudinal axis being collinear to the tensile loading axis of the test machine. Specimens which break slip or break in the area of clamping have to be replaced by a new one [ISO527-1].

Five specimens of each type are tested with a constant test speed of five millimeters per minute until fracture. The types are:

- FDM-PC-Solid-Flat and Edgewise
- FDM-PC-Honeycomb-Flat and Edgewise
- Milling-PC-Solid
- Milling-PC-Honeycomb
- PJM-RGD720-Solid-Flat and Edgewise
- PJM-RGD720-Honeycomb-Flat and Edgewise
- SLS-PA-Solid-Flat and Edgewise
- SLS-PA-Honeycomb-Flat and Edgewise

For measuring the displacement of the gauge length an extensometer with an accuracy of ± 1 micrometer is used, because the machine measures the displacement over the full length of the specimen. The maximum displacement of the extensometer is around 25 millimeters, starting at a gauge length of 50.8 millimeters.

Trial test showed that the arrangement of the extensometer on the wide side of the specimen (Figure 43) has a smaller influence on the failure behavior. By mounting the extensometer to the specimen with rubber bands, small notches are engraved due to the pressure. However, less pressure would mean that the extensometer starts to slip during the test run. The depth of the notch depends on the material. Due to the notches, some of the samples break earlier (cf. highlighted comment in the test results – Chapter 5.4.2).

The test results are collected by the software *Bluehill* and evaluated in *Microsoft Excel* later.

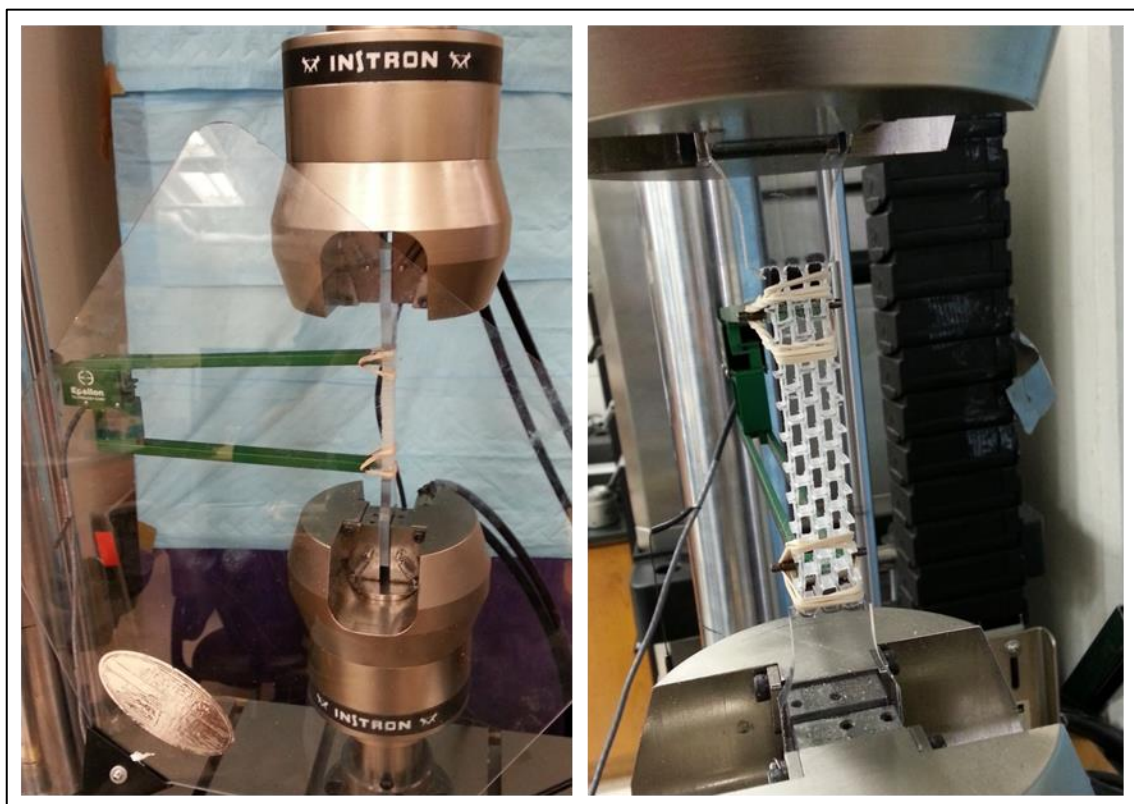


Figure 43: Tensile test | left and right: arrangement of extensometer | right: stretching of milled polycarbonate hexagons

5.4.2 Fracture Behavior

As previously mention, the specimens are loaded until fracture. The solid specimens break directly completely, as well as the honeycomb specimens of FDM and SLS, whereas the honeycomb specimens of PJM and Milling break in several steps. First one of the cell walls breaks and others follow. The diagrams in Chapter 5.4.2 show the values only until initial fracture.

The milled hexagon cells stretch ideal until they are rectangles. Then, yielding starts in the cell walls and the fracture follows shortly afterwards. All additive manufactured hexagons break before the maximum stretching. Most of them break under an angle of more or less 60 degrees respectively to the loading direction.

The solid specimens break brittle (FDM and SLS) or shows yielding and a reduction of the gauge area (PJM and Milling). The solid specimens of PJM break in most cases due to the notches caused by the extensometer.

The fractures and descriptions are stated in following figures.

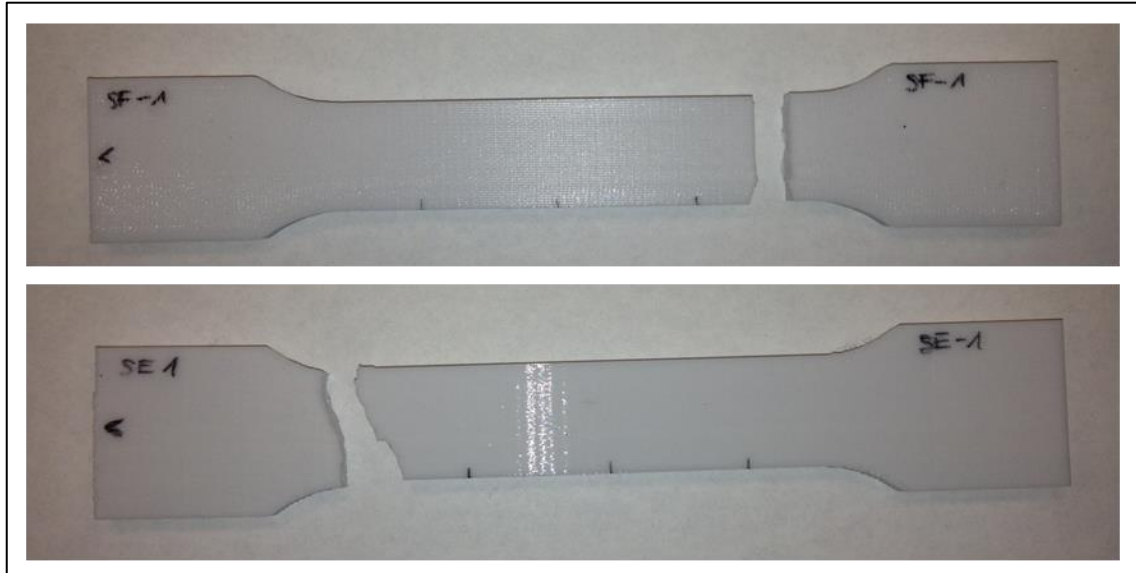


Figure 44: Top: FDM-PC-Solid-Flat: brittle fracture (cf. Figure 51)

Bottom: FDM-PC-Solid-Edgewise: brittle fracture (cf. Figure 52)

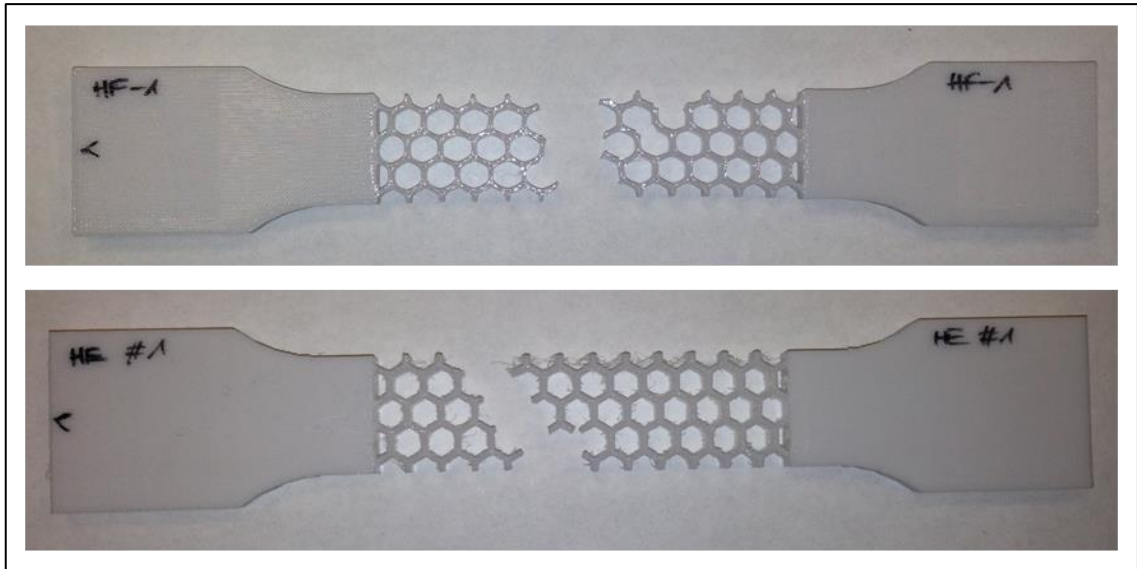


Figure 45: Top: FDM-PC-Honeycomb-Flat: little residual plastic deformation of hexagons; fracture under 60 degrees (**elastic-plastic behavior**) (cf. Figure 29 and Figure 51)
Bottom: FDM-PC-Honeycomb-Edgewise: brittle fracture under 60 degrees (**elastic-brittle behavior**) (cf. Figure 29 and Figure 54)

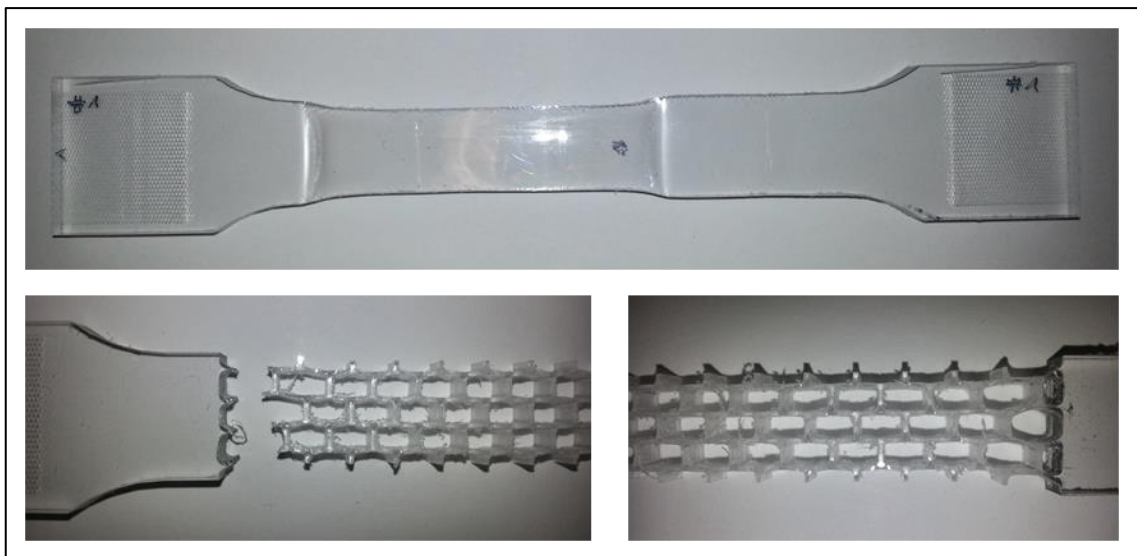


Figure 46: Top: Milling-PC-Solid: ductile (no fracture, because machine limit was reached)
Bottom: Milling-PC-Honeycomb: full stretched hexagon (**elastic-plastic behavior**) (cf. Figure 29 and Figure 57) plus plastic reduction in area of cell walls before fracture (plateau at the end of the curves in Figure 57; in excel there is even a small drop down of the curve visible).

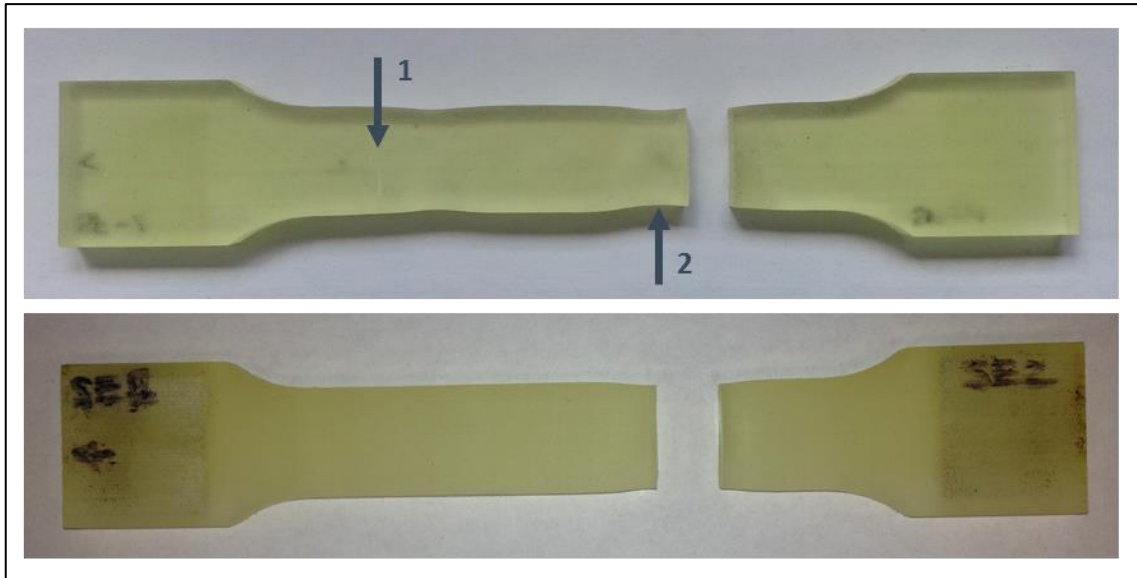


Figure 47: Top: PJM-RGD720-Solid-Flat: first yielding, then fracture due to notch caused by the extensometer (1), not at lowest point of the reduction in area (2) (cf. Figure 58)
Bottom: PJM-RGD720-Solid-Edgewise: first yielding, then fracture due to notch caused by the extensometer (cf. Figure 59)

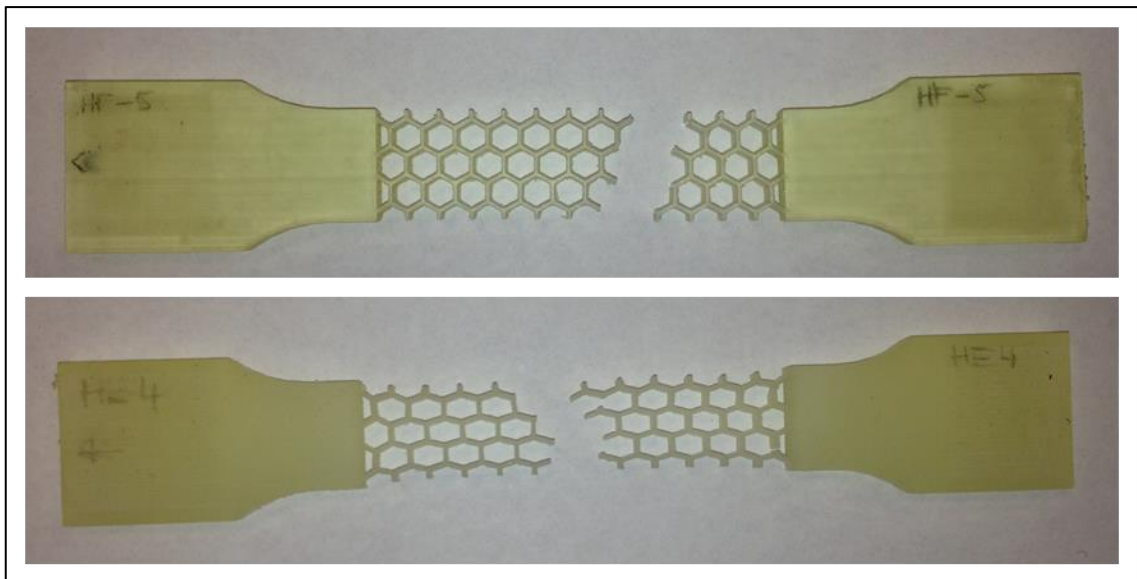


Figure 48: Top: PJM-RGD720-Honeycomb-Flat: little or no residual plastic deformation of hexagons; fracture under 60 degrees (**elastic-plastic behavior** and **elastic-brittle behavior**) (cf. Figure 29 and Figure 60)
Bottom: PJM-RGD720-Honeycomb-Edgewise: great residual plastic deformation of hexagons; fracture under 60 degrees (**elastic-plastic behavior**) (Figure 29 and Figure 61)

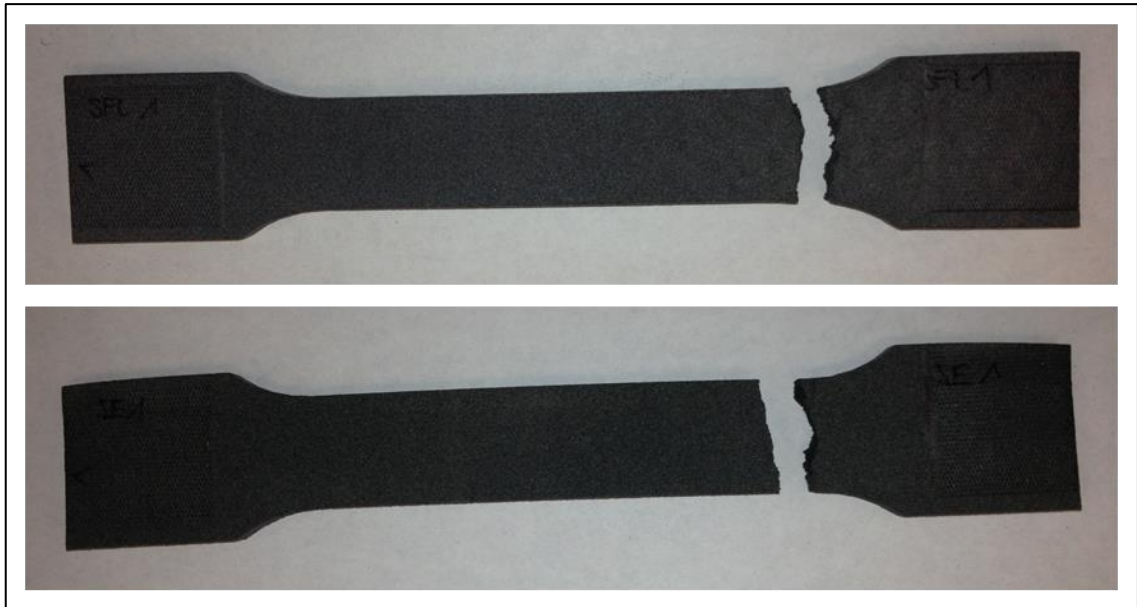


Figure 49: Top: SLS-PA-Solid-Flat: brittle fracture (cf. Figure 62)

Bottom: SLS-PA-Solid-Flat: brittle fracture (cf. Figure 63)

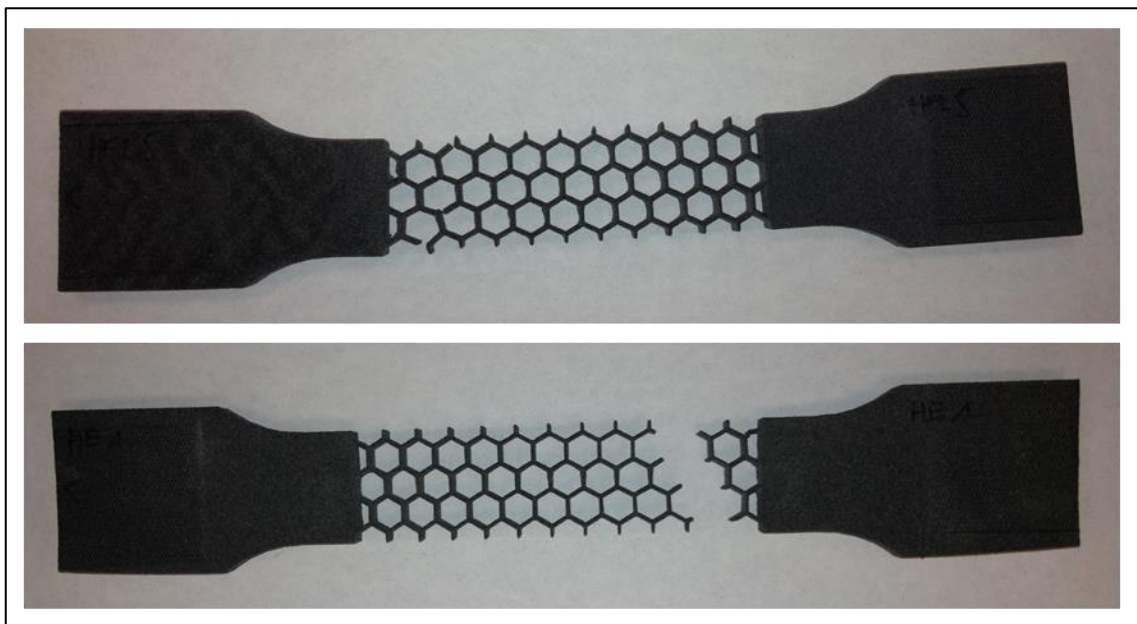


Figure 50: Top: SLS-PA-Honeycomb-Flat: stretching of hexagons during loading; no plastic deformation; brittle fracture under 60 degrees (only cracks visible) (**elastic-brittle behavior**) (cf. Figure 29 and Figure 64)

Bottom: SLS-PA-Honeycomb-Edgewise: stretching of hexagons; no plastic deformation; brittle fracture under 60 degrees (**elastomeric behavior**) (cf. Figure 29 and Figure 65)

5.4.3 Test Results and Comparison

I Fused Deposition Modeling

MATERIAL: POLYCARBONATE (STRATASYS)		
Measurement	Value	Method (Standard)
Stress at Yielding σ_y	-	ASTM D638
Tensile Strength σ_{max} = Stress at Break σ_B	68 MPa	ASTM D638
Strain at Yield ϵ_y	-	ASTM D638
Strain at Break ϵ_B	6 %	ASTM D638

Table 7: Material values – polycarbonate (Stratasys) [sys] (data sheet attached)

SPECIMEN TYPE: FDM-PC-SOLID-FLAT		
Measurement	Value	Method (Standard)
Mean Load, Maximum F_{max}	6186.81 N	ISO 527
Mean Load at Break F_B	6186.81 N	ISO 527
Mean Displacement at max. Load ΔL_y	1.89 mm	ISO 527
Mean Displacement at Break ΔL_B	1.89 mm	ISO 527
Mean Tensile Strength σ_{max}	51.56 MPa	ISO 527
Mean Stress at Break σ_B	51.56 MPa	ISO 527
Mean Strain at max. Load ϵ_{Fmax}	3.71 %	ISO 527
Mean Strain at Break ϵ_B	3.71 %	ISO 527

Table 8: Test results – FDM-PC-Solid-Flat

SPECIMEN TYPE: FDM-PC-SOLID-EDGEWISE		
Measurement	Value	Method (Standard)
Mean Load, Maximum F_{max}	6270.94 N	ISO 527
Mean Load at Break F_B	6270.94 N	ISO 527
Mean Displacement at max. Load ΔL_y	1.94 mm	ISO 527
Mean Displacement at Break ΔL_B	1.94 mm	ISO 527
Mean Tensile Strength σ_{max}	52.26 MPa	ISO 527
Mean Stress at Break σ_B	52.26 MPa	ISO 527
Mean Strain at max. Load ϵ_{Fmax}	3.83 %	ISO 527
Mean Strain at Break ϵ_B	3.83 %	ISO 527

Table 9: Test results – FDM-PC-Solid-Edgewise

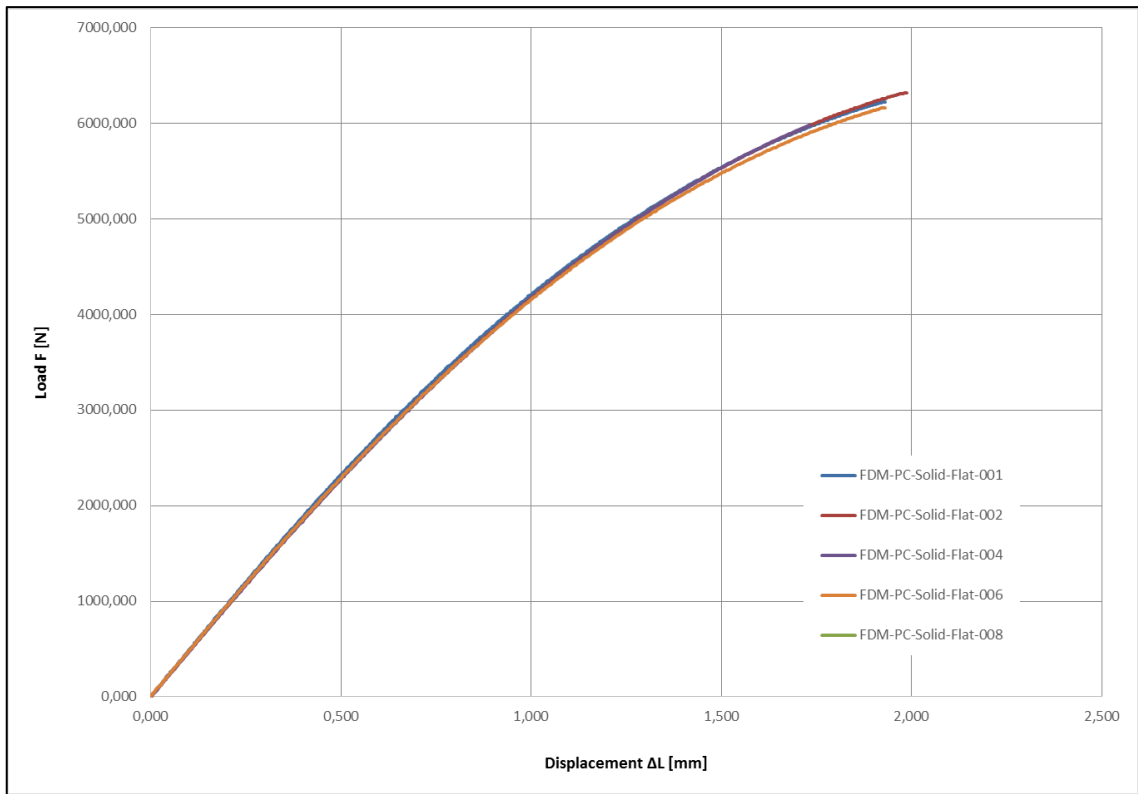


Figure 51: Load-displacement diagram – FDM-PC-Solid-Flat

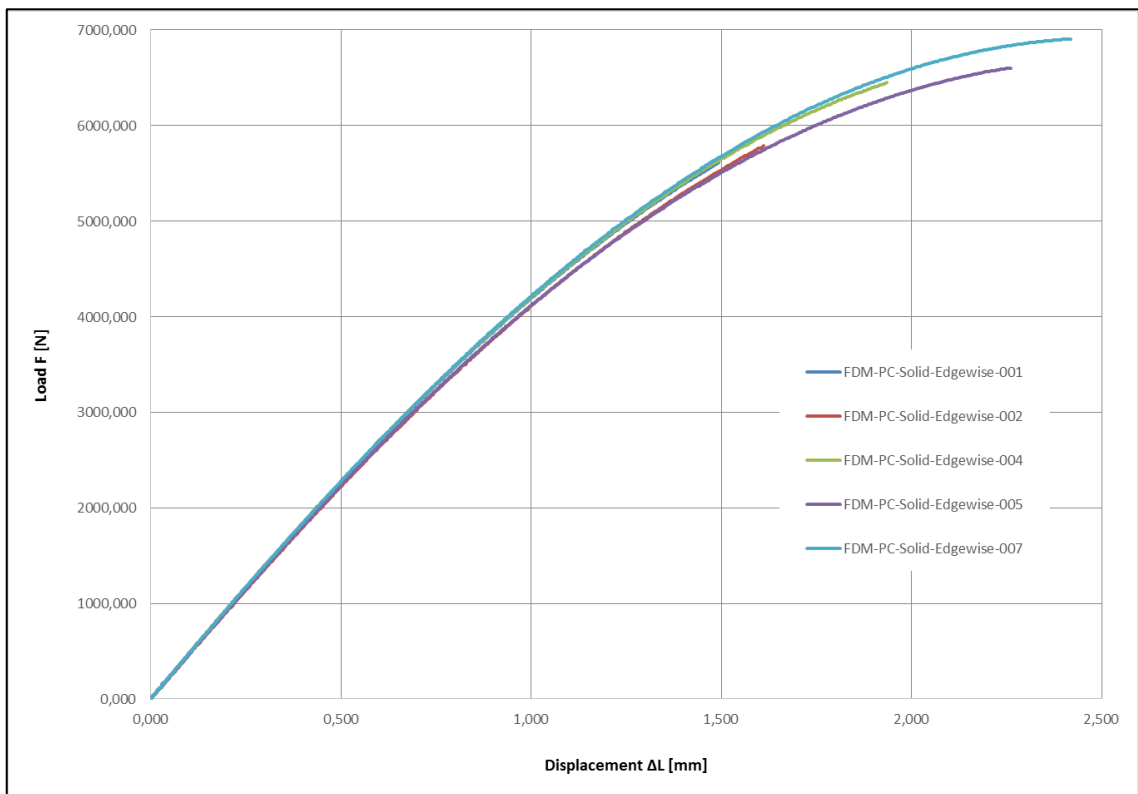


Figure 52: Load-displacement diagram – FDM-PC-Solid-Edgewise

SPECIMEN TYPE: FDM-PC-HONEYCOMB-FLAT		
Measurement	Value	Method (Standard)
Mean Load, Maximum F_{max}	664.63 N	ISO 527
Mean Load at Break F_B	664.63 N	ISO 527
Mean Displacement at max. Load ΔL_y	6.36 mm	ISO 527
Mean Displacement at Break ΔL_B	6.36 mm	ISO 527
Mean Tensile Strength σ_{max}	-	ISO 527
Mean Stress at Break σ_B	-	ISO 527
Mean Strain at max. Load ϵ_{Fmax}	12.52 %	ISO 527
Mean Strain at Break ϵ_B	12.52 %	ISO 527

Table 10: Test results – FDM-PC-Honeycomb-Flat

SPECIMEN TYPE: FDM-PC-HONEYCOMB-EDGEWISE		
Measurement	Value	Method (Standard)
Mean Load, Maximum F_{max}	137.58 N	ISO 527
Mean Load at Break F_B	137.58 N	ISO 527
Mean Displacement at max. Load ΔL_y	2.39 mm	ISO 527
Mean Displacement at Break ΔL_B	2.39 mm	ISO 527
Mean Tensile Strength σ_{max}	-	ISO 527
Mean Stress at Break σ_B	-	ISO 527
Mean Strain at max. Load ϵ_{Fmax}	4.71 %	ISO 527
Mean Strain at Break ϵ_B	4.71 %	ISO 527

Table 11: Test results – FDM-PC-Honeycomb-Edgewise

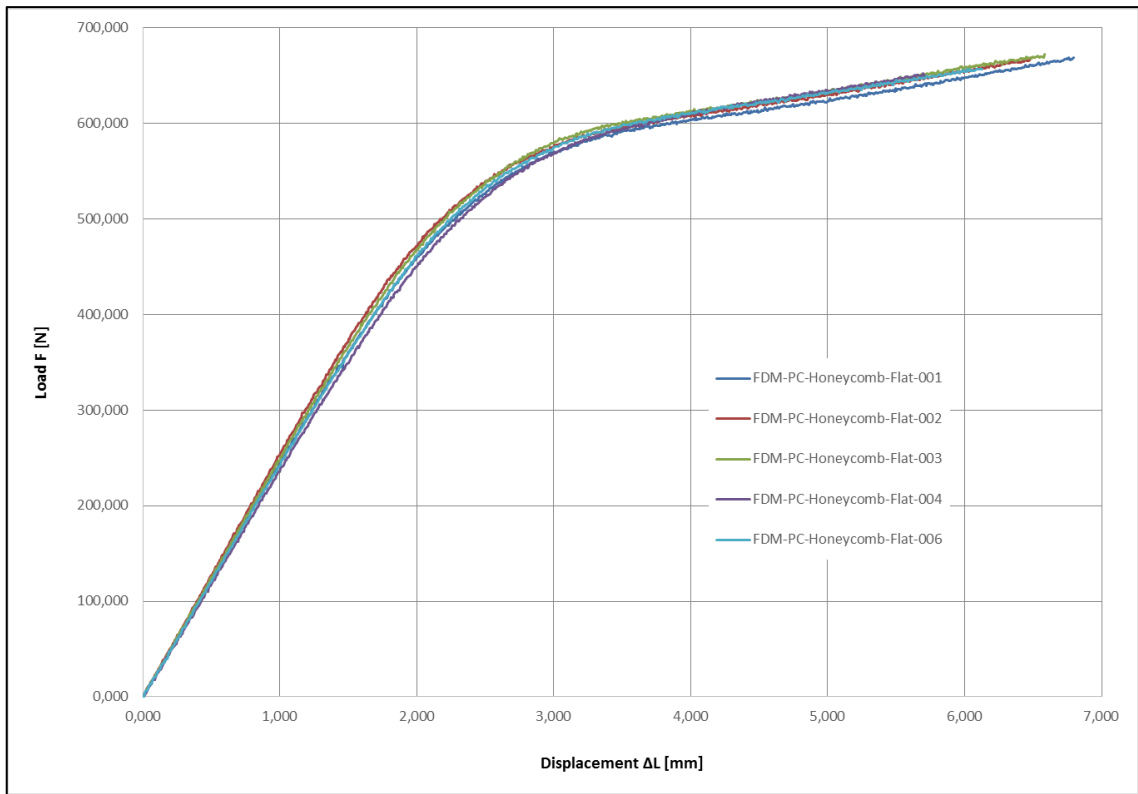


Figure 53: Load-displacement diagram – FDM-PC-Honeycomb-Flat (elastic-plastic)

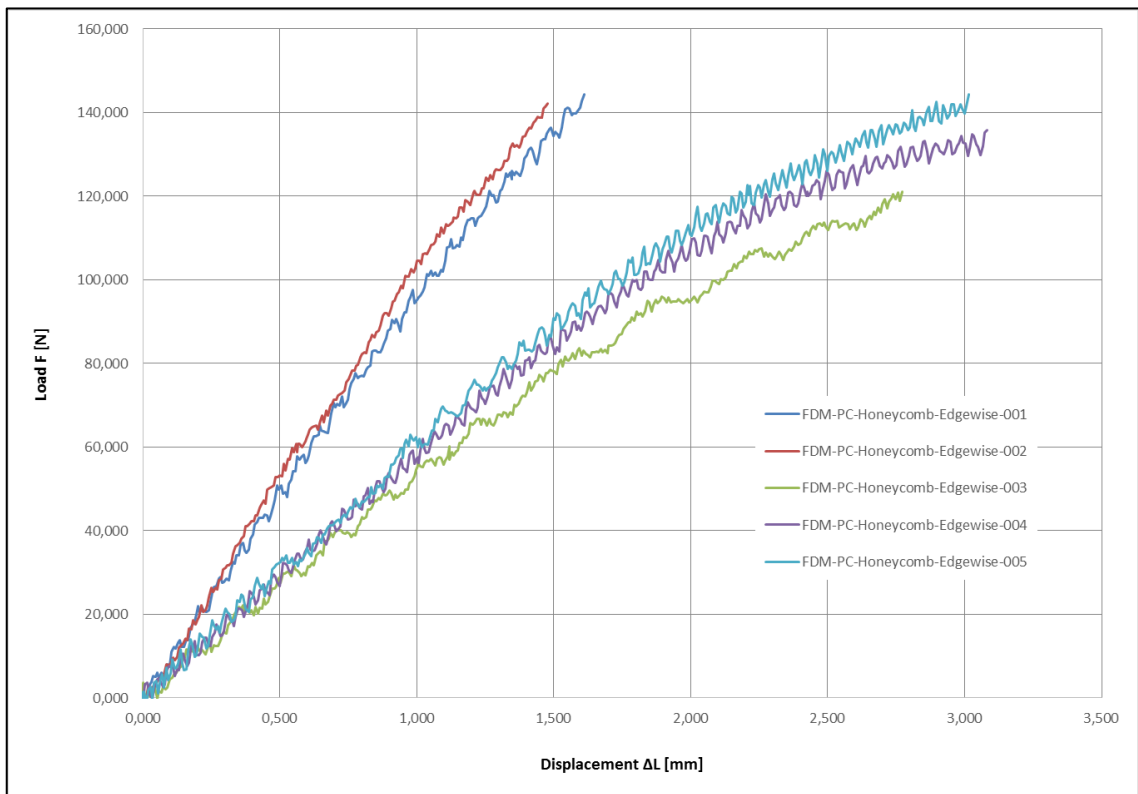


Figure 54: Load-displacement diagram – FDM-PC-Honeycomb-Edgewise (elastic-brittle)

II Milling

MATERIAL: POLYCARBONATE (MAKROLON® GP)		
Measurement	Value	Method (Standard)
Stress at Yielding σ_y	62 MPa	ASTM D638
Tensile Strength $\sigma_{max} = \text{Stress at Break } \sigma_B$	65.50 MPa	ASTM D638
Strain at Yield ϵ_y	-	ASTM D638
Strain at Break ϵ_B	110 %	ASTM D638

Table 12: Material values – polycarbonate (Makrolon® GP) [tap] (data sheet attached)

SPECIMEN TYPE: MILLING-PC-SOLID		
Measurement	Value	Method (Standard)
Mean Load, Maximum $F_{max} = F_y$	7688.12 N	ISO 527
Mean Load at Break F_B	extension limit reached	ISO 527
Mean Displacement at max. Load ΔL_y	3.13 mm	ISO 527
Mean Displacement at Break ΔL_B	extension limit reached	ISO 527
Mean Tensile Strength $\sigma_{max} = \sigma_y$	64.07 MPa	ISO 527
Mean Stress at Break σ_B	extension limit reached	ISO 527
Mean Strain at max. Load ϵ_{Fmax}	6.28 %	ISO 527
Mean Strain at Break ϵ_B	> 50 % extension limit reached	ISO 527

Table 13: Test results – Milling-PC-Solid (extension limit of extensometer was reached)

SPECIMEN TYPE: MILLING-PC-HONEYCOMB		
Measurement	Value	Method (Standard)
Mean Load, Maximum F_{max}	981.43 N	ISO 527
Mean Load at Break F_B	981.43 N	ISO 527
Mean Displacement at max. Load ΔL_y	14.60 mm	ISO 527
Mean Displacement at Break ΔL_B	14.60 mm	ISO 527
Mean Tensile Strength σ_{max}	51.12 MPa *	ISO 527
Mean Stress at Break σ_B	51.12 MPa	ISO 527
Mean Strain at max. Load ϵ_{Fmax}	28.74 %	ISO 527
Mean Strain at Break ϵ_B	28.74 %	ISO 527

Table 14: Test results – Milling-PC-Honeycomb

*** Calculation of Stresses for Milled Honeycomb-Specimens** (ref. Table 14)

As the strains are too large to calculate with the models of Gibson and Ashby (28.74 % > 20 %), another assumption is made:

The hexagons of the specimen stretch fully, which means that they are no longer hexagons, but rectangles. Hence, the load is acting in four cell walls (Figure 55) with an area of

$$A_{hex} = 4 \cdot t \cdot b = 4 \cdot 0.8 \text{ mm} \cdot 6 \text{ mm} = 19.2 \text{ mm}^2 \quad (5.1)$$

With an mean maximum load of $F = 981.43 \text{ N}$, this lead to a mean stress of

$$\sigma_{max} = \frac{F_{max}}{A_{hex}} = \frac{981.43 \text{ N}}{19.2 \text{ mm}^2} = 51.12 \frac{\text{N}}{\text{mm}^2} \text{ (or MPa)} \quad (5.2)$$

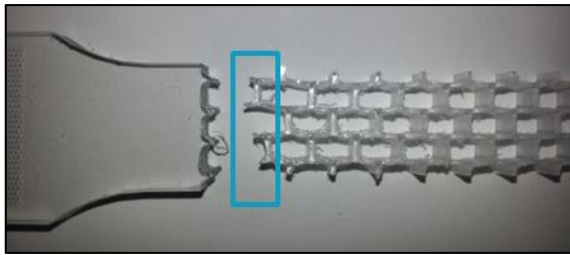


Figure 55: Fully stretched honeycombs

The curves in the following load-displacement diagram (Figure 56) of the “Milled-PC-Solid” specimens correspond to the literature (Figure 42).

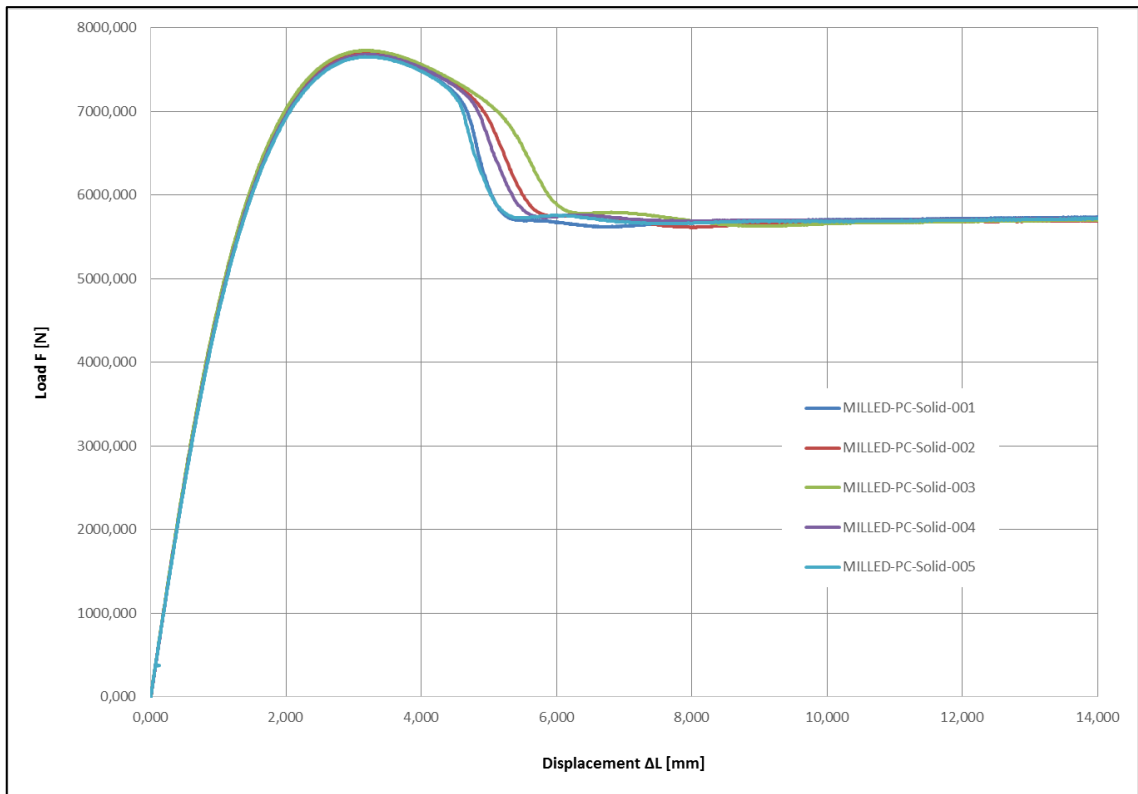


Figure 56: Load-displacement diagram – MILLING-PC-Honeycomb (extensometer limit reached)

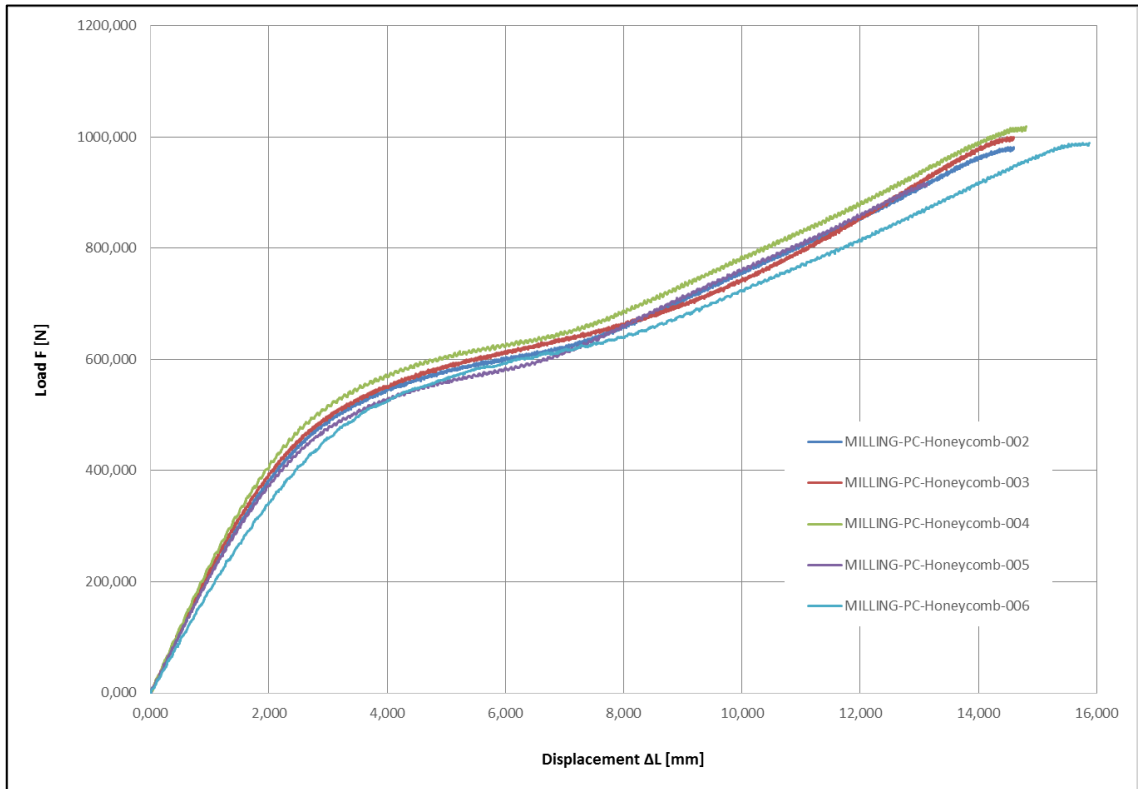


Figure 57: Load-displacement diagram – MILLING-PC-Honeycomb (elastic-plastic, plus reduction in area of cell walls)

III Poly-Jet Modeling

MATERIAL: RGD720 (STRATASYS)		
Measurement	Value	Method (Standard)
Stress at Yielding σ_y	50-65 MPa	ASTM D638
Tensile Strength $\sigma_{max} = \text{Stress at Yielding } \sigma_y$	50-65 MPa	ASTM D638
Strain at Yield ϵ_y	-	ASTM D638
Strain at Break ϵ_B	15-25 %	ASTM D638

Table 15: Material values – RGD720 (Stratsys) [sys] (data sheet attached)

SPECIMEN TYPE: PJM-RGD720-SOLID-FLAT		
Measurement	Value	Method (Standard)
Mean Load, Maximum F_{max}	6217.05 N	ISO 527
Mean Load at Break F_B	3811.18 N	ISO 527
Mean Displacement at max. Load ΔL_y	2.06 mm	ISO 527
Mean Displacement at Break ΔL_B	8.17 mm	ISO 527
Mean Tensile Strength $\sigma_{max} = \sigma_y$	51.81 MPa	ISO 527
Mean Stress at Break σ_B	31.76 MPa	ISO 527
Mean Strain at max. Load ϵ_{Fmax}	13.20 %	ISO 527
Mean Strain at Break ϵ_B	19.30 % Effect of Extensometer	ISO 527

Table 16: Test results – PJM-RGD720-Solid-Flat

SPECIMEN TYPE: PJM-RGD720-SOLID-EDGEWISE		
Measurement	Value	Method (Standard)
Mean Load, Maximum F_{max}	5508.27 N	ISO 527
Mean Load at Break F_B	2.09 mm	ISO 527
Mean Displacement at max. Load ΔL_y	3866.73 N	ISO 527
Mean Displacement at Break ΔL_B	4.46 mm	ISO 527
Mean Tensile Strength $\sigma_{max} = \sigma_y$	45.90 MPa	ISO 527
Mean Stress at Break σ_B	32.33 MPa	ISO 527
Mean Strain at max. Load ϵ_{Fmax}	3.43 %	ISO 527
Mean Strain at Break ϵ_B	7.32 % Effect of Extensometer	ISO 527

Table 17: Test results – PJM-RGD720-Solid-Edgewise

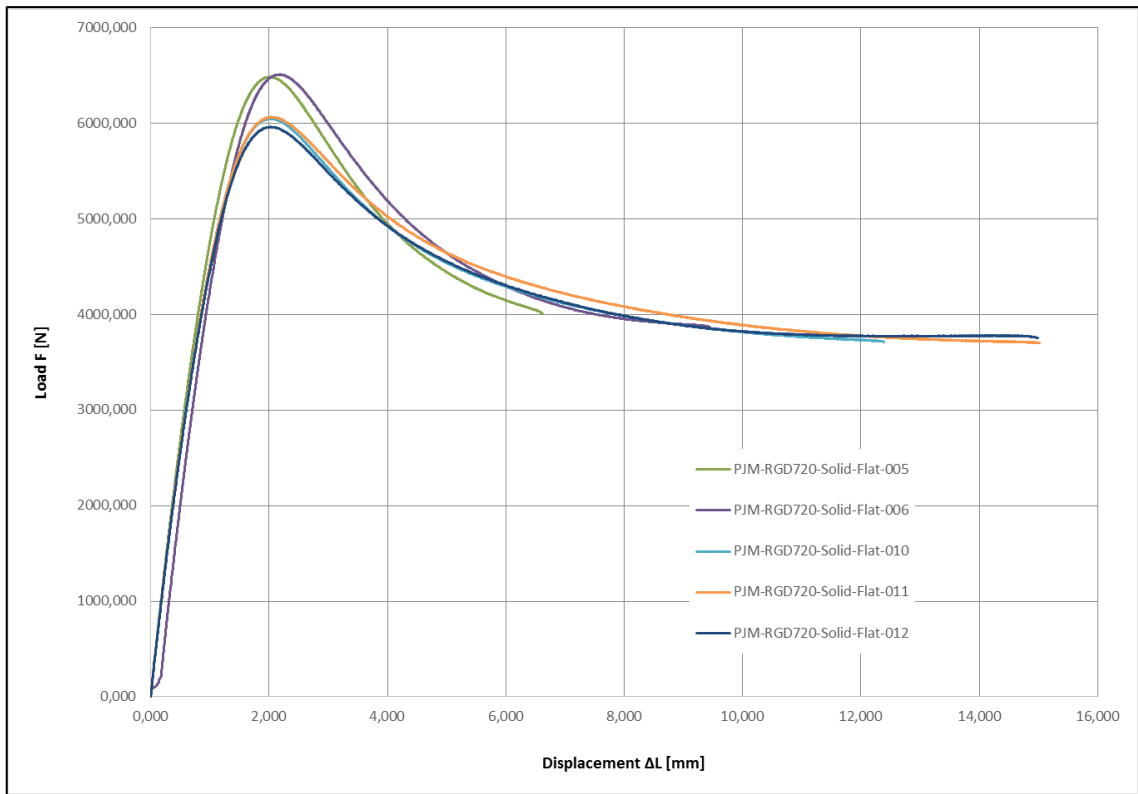


Figure 58: Load-displacement diagram – PJM-RGD720-Solid-Flat

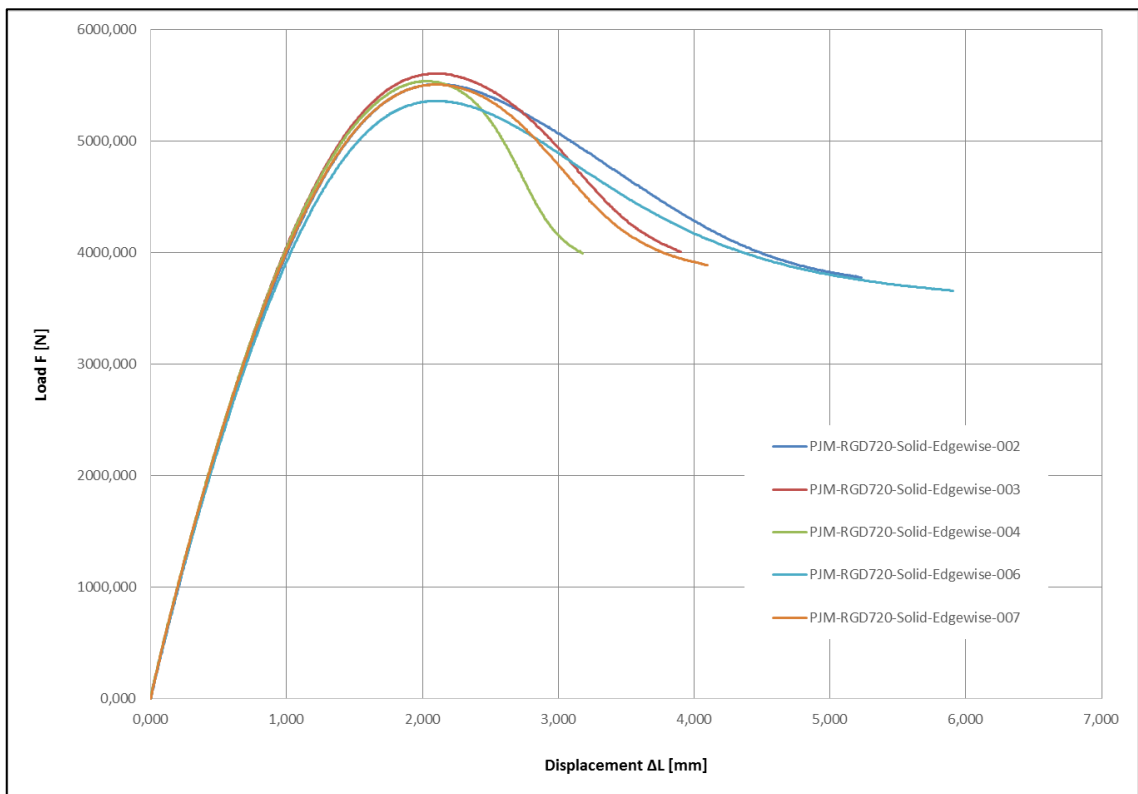


Figure 59: Load-displacement diagram – PJM-RGD720-Solid-Edgewise

SPECIMEN TYPE: PJM-RGD720-HONEYCOMB-FLAT		
Measurement	Value	Method (Standard)
Mean Load, Maximum F_{max}	165.27 N	ISO 527
Mean Load at Break F_B	165.27 N	ISO 527
Mean Displacement at max. Load ΔL_y	5.05 mm	ISO 527
Mean Displacement at Break ΔL_B	5.05 mm	ISO 527
Mean Tensile Strength $\sigma_{max} = \sigma_y$	-	ISO 527
Mean Stress at Break σ_B	-	ISO 527
Mean Strain at max. Load ϵ_{Fmax}	9.94 %	ISO 527
Mean Strain at Break ϵ_B	9.94 %	ISO 527

Table 18: Test results – PJM-RGD720-Honeycomb-Flat

SPECIMEN TYPE: PJM-RGD720-HONEYCOMB-EDGEWISE		
Measurement	Value	Method (Standard)
Mean Load, Maximum F_{max}	208.09 N	ISO 527
Mean Load at Break F_B	208.9 N	ISO 527
Mean Displacement at max. Load ΔL_y	11.30 mm	ISO 527
Mean Displacement at Break ΔL_B	11.30 mm	ISO 527
Mean Tensile Strength $\sigma_{max} = \sigma_y$	-	ISO 527
Mean Stress at Break σ_B	-	ISO 527
Mean Strain at max. Load ϵ_{Fmax}	17.63 %	ISO 527
Mean Strain at Break ϵ_B	17.63 %	ISO 527

Table 19: Test results – PJM-RGD720-Honeycomb-Edgewise

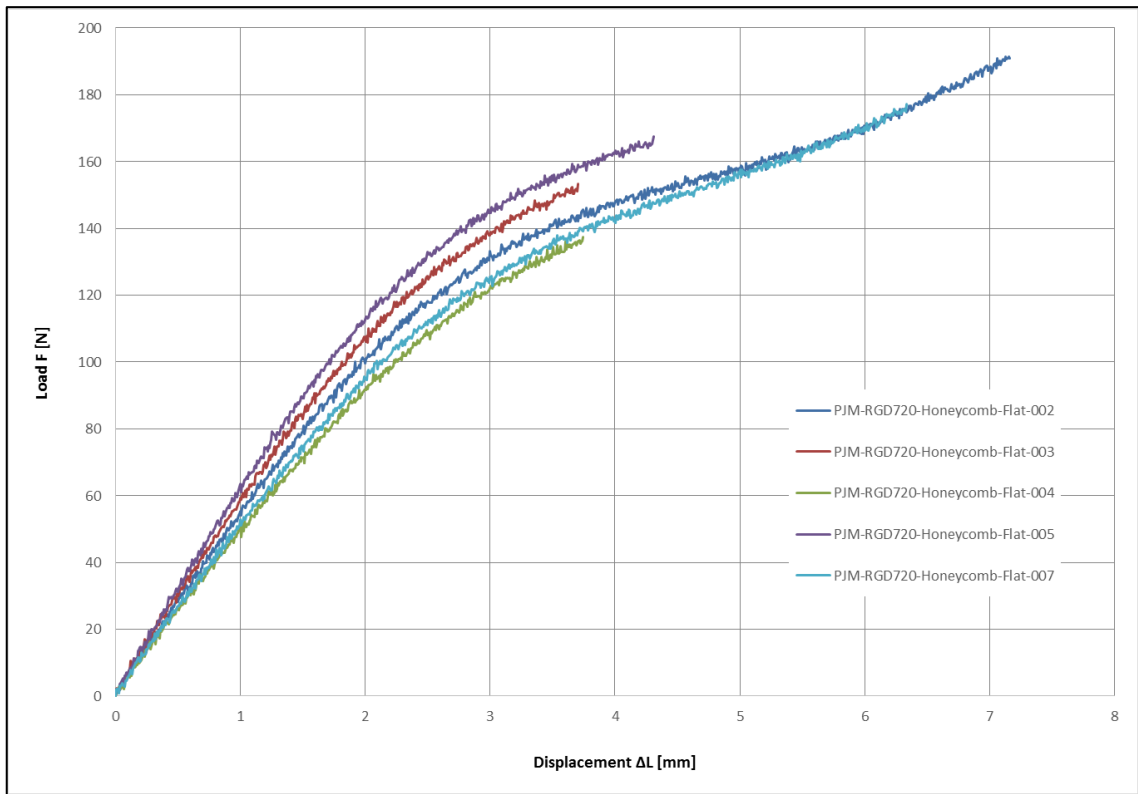


Figure 60: Load-displacement diagram – PJM-RGD720-Honeycomb-Flat (elastic-plastic and elastic-brittle)

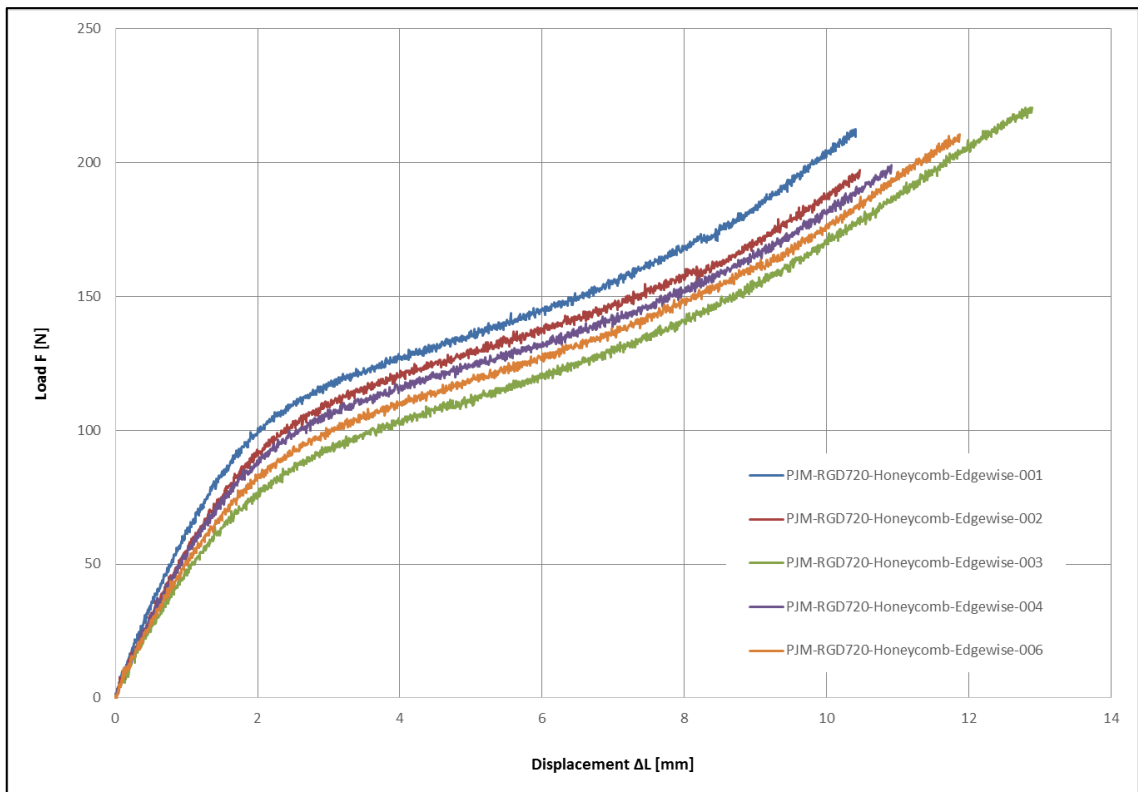


Figure 61: Load-displacement diagram – PJM-RGD720-Honeycomb-Edgewise (elastic-plastic)

IV Selective Laser Sintering

MATERIAL: DURAFORM® POLYAMIDE		
Measurement	Value	Method (Standard)
Stress at Yielding σ_y	-	ASTM D638
Tensile Strength σ_{max} (= σ_y ? / = σ_B ?)	43 MPa	ASTM D638
Strain at Yield ϵ_y	-	ASTM D638
Strain at Break ϵ_B	14 %	ASTM D638

Table 20: Material values – DuraForm® PA [3ds] (data sheet attached)

SPECIMEN TYPE: SLS-PA-SOLID-FLAT		
Measurement	Value	Method (Standard)
Mean Load, Maximum F_{max}	1293.46 N	ISO 527
Mean Load at Break F_B	1293.46 N	ISO 527
Mean Displacement at max. Load ΔL_y	1.59 mm	ISO 527
Mean Displacement at Break ΔL_B	1.59 mm	ISO 527
Mean Tensile Strength σ_{max}	10.78 MPa	ISO 527
Mean Stress at Break σ_B	10.78 MPa	ISO 527
Mean Strain at max. Load ϵ_{Fmax}	3.13 %	ISO 527
Mean Strain at Break ϵ_B	3.13 %	ISO 527

Table 21: Test results – SLS-PA-Solid-Flat

SPECIMEN TYPE: SLS-PA-SOLID-EDGEWISE		
Measurement	Value	Method (Standard)
Mean Load, Maximum F_{max}	2196.12 N	ISO 527
Mean Load at Break F_B	2196.12 N	ISO 527
Mean Displacement at max. Load ΔL_y	2.09 mm	ISO 527
Mean Displacement at Break ΔL_B	2.09 mm	ISO 527
Mean Tensile Strength σ_{max}	18.30 MPa	ISO 527
Mean Stress at Break σ_B	18.30 MPa	ISO 527
Mean Strain at max. Load ϵ_{Fmax}	4.12 %	ISO 527
Mean Strain at Break ϵ_B	4.12 %	ISO 527

Table 22: Test results – SLS-PA-Solid-Edgewise

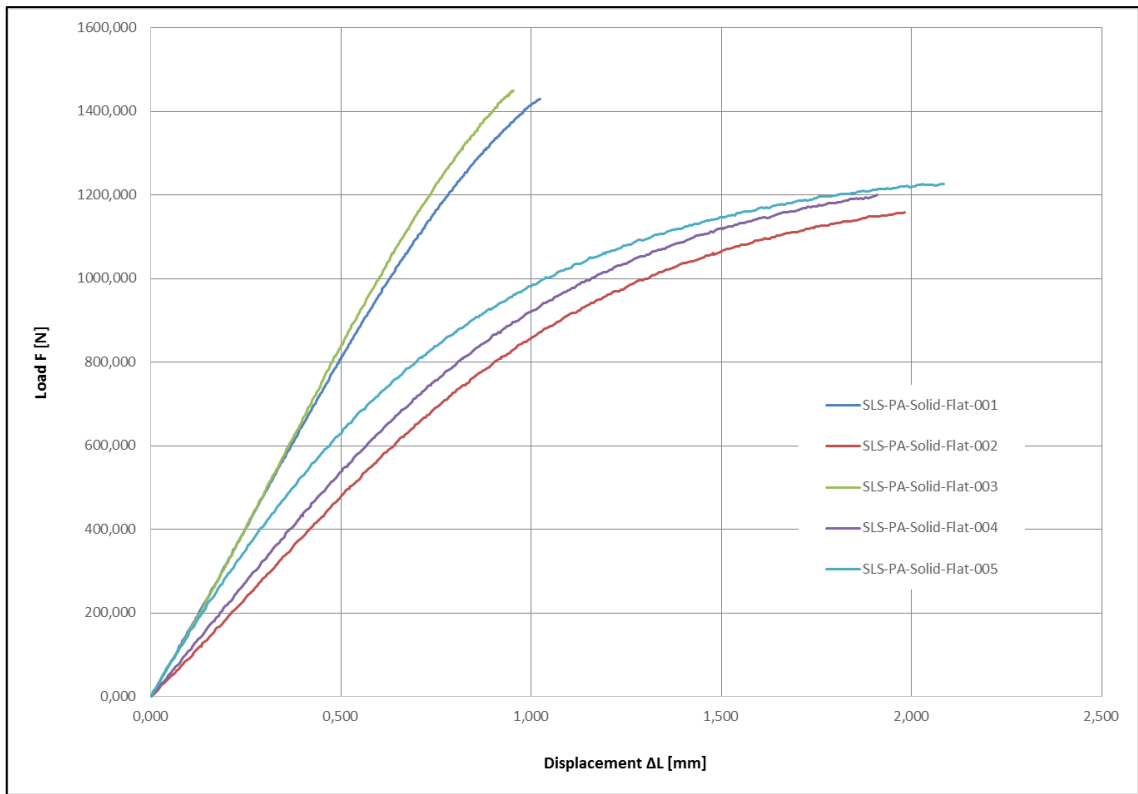


Figure 62: Load-displacement diagram – SLS-PA-Solid-Flat

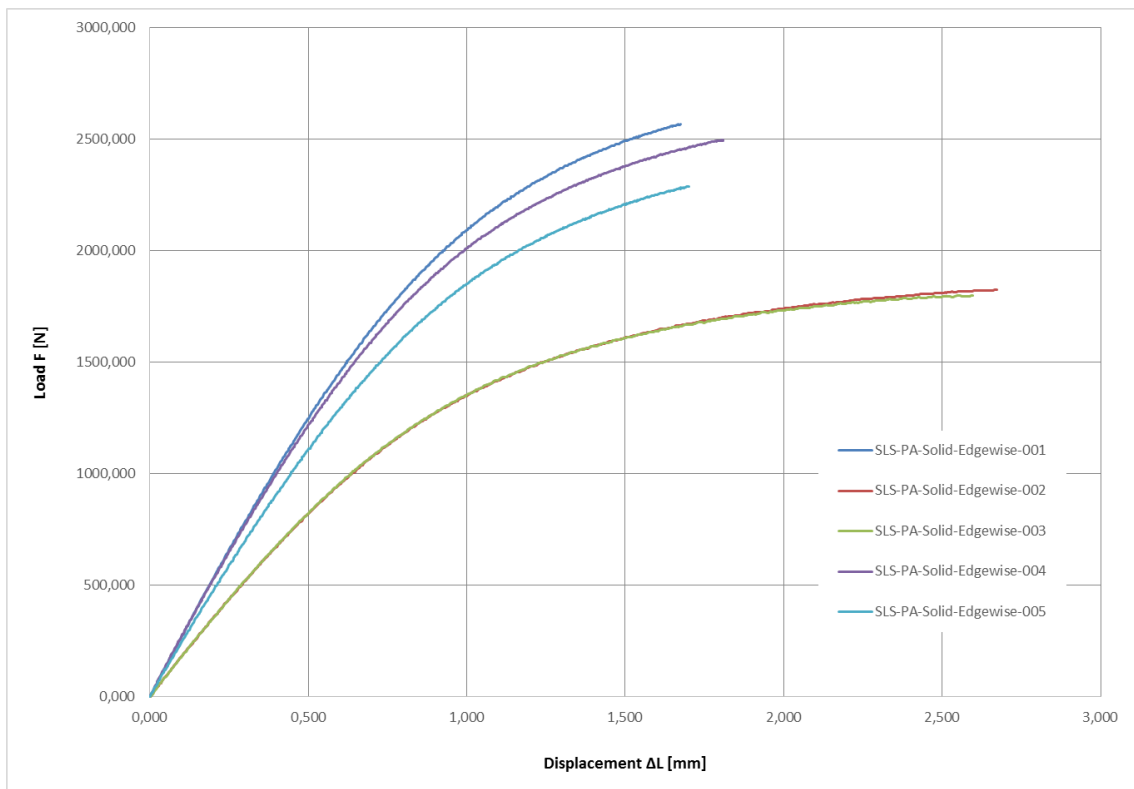


Figure 63: Load-displacement diagram – SLS-PA-Solid-Edgewise

SPECIMEN TYPE: SLS-PA-HONEYCOMB-FLAT // <i>only four specimens</i>		
Measurement	Value	Method (Standard)
Mean Load, Maximum F_{max}	32.29 N	ISO 527
Mean Load at Break F_B	32.39 N	ISO 527
Mean Displacement at max. Load ΔL_y	4.67 mm	ISO 527
Mean Displacement at Break ΔL_B	4.67 mm	ISO 527
Mean Tensile Strength σ_{max}	-	ISO 527
Mean Stress at Break σ_B	-	ISO 527
Mean Strain at max. Load ϵ_{Fmax}	9.19 %	ISO 527
Mean Strain at Break ϵ_B	9.19 %	ISO 527

Table 23: Test results – SLS-PA-Honeycomb-Flat

SPECIMEN TYPE: SLS-PA-HONEYCOMB-EDGEWISE		
Measurement	Value	Method (Standard)
Mean Load, Maximum F_{max}	27.76 N	ISO 527
Mean Load at Break F_B	27.76 N	ISO 527
Mean Displacement at max. Load ΔL_y	5.14 mm	ISO 527
Mean Displacement at Break ΔL_B	5.14 mm	ISO 527
Mean Tensile Strength σ_{max}	-	ISO 527
Mean Stress at Break σ_B	-	ISO 527
Mean Strain at max. Load ϵ_{Fmax}	10.12 %	ISO 527
Mean Strain at Break ϵ_B	10.12 %	ISO 527

Table 24: Test results – SLS-PA-Honeycomb-Edgewise

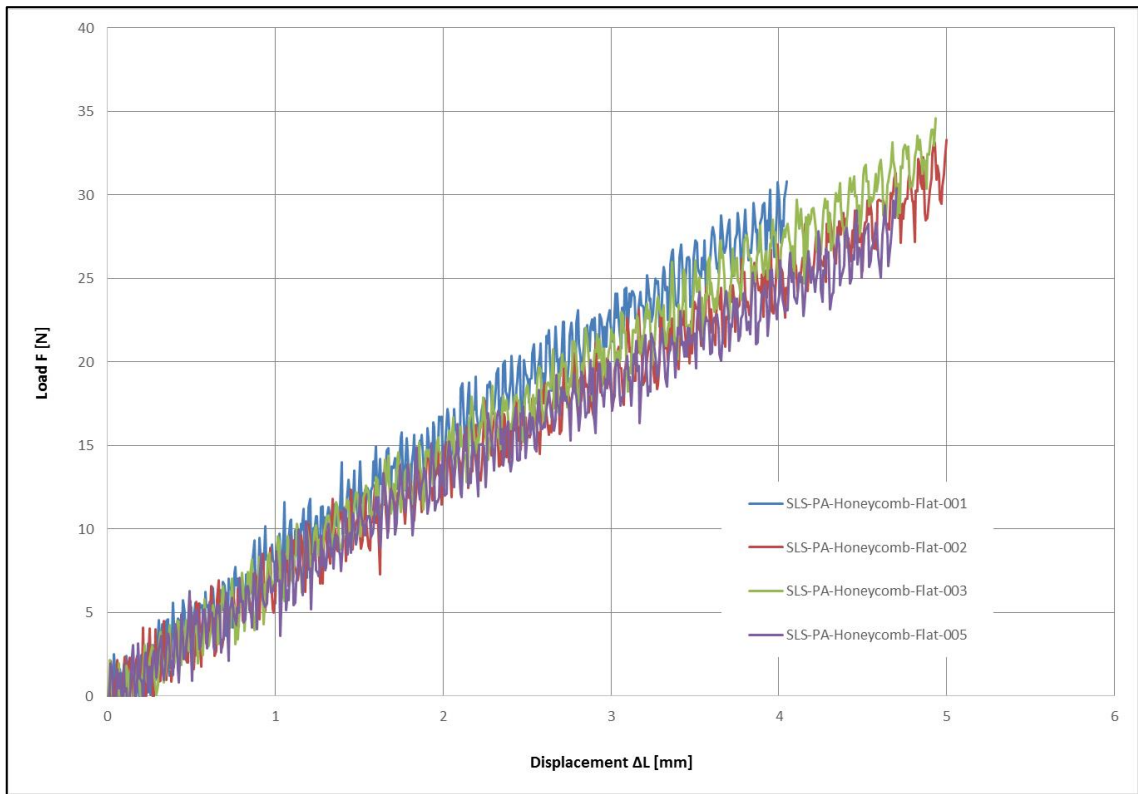


Figure 64: Load-displacement diagram – SLS-PA-Honeycomb-Flat (elastic-brittle)

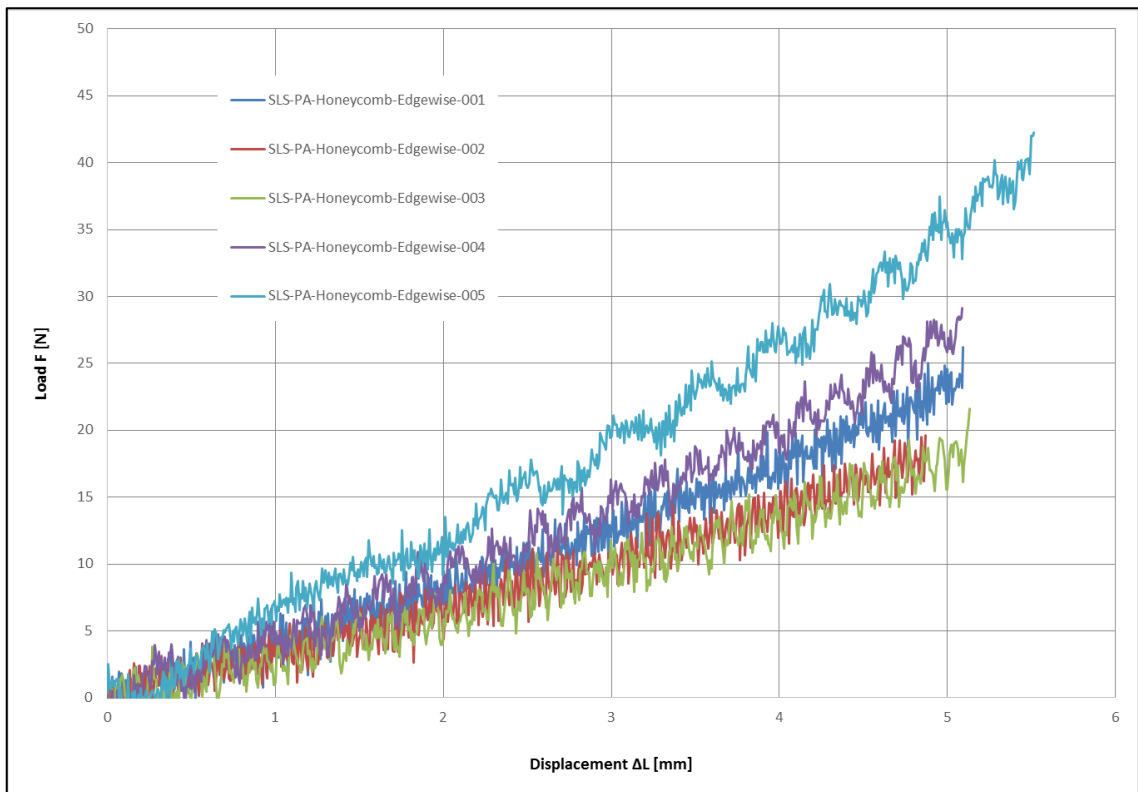


Figure 65: Load-displacement diagram – SLS-PA-Honeycomb-Edgewise (elastomeric)

V Comparison

COMPARISON OF TEST RESULTS					
Manufacturing Method and Material		Honey-comb Flat	Honey-comb Edgewise	Solid Flat	Solid Edgewise
I. Fused Deposition Modeling Polycarbonate (Stratasys) $\sigma_{\max} = 68 \text{ MPa} \mid \epsilon_B = 5 \%$	F_{\max}	664.63 N	137.58 N	6186.81 N	6270.94 N
	σ_{\max}	-	-	51.56 MPa	52.26 MPa
	ϵ_B	12.52 %	4.71 %	3.71 %	3.83 %
No information.		ductile	brittle	brittle	brittle
II. Milling Polycarbonate (Makrolon® GP) $\sigma_y = 62.05 \text{ MPa} \mid \epsilon_B = 110 \%$	F_{\max}	981.43 N		7688.12 N	
	σ_{\max}	51.12 MPa		64.07 MPa	
	ϵ_B	28.74 %		> 50 % (limit reached)	
ductile		ductile		ductile	
III. Poly-Jet Modeling RGD720 (Stratasys) $\sigma_{\max} = 50\text{-}65 \text{ MPa} \mid \epsilon_B = 15\text{-}25 \%$	F_{\max}	165.27 N	208.09 N	6217.05 N	5508.27 N
	σ_{\max}	-	-	51.81 MPa	45.90 MPa
	ϵ_B	9.94 %	17.63 %	19.30 %	7.32 %
No information		brittle / ductile	ductile	ductile	ductile
IV. Selective Laser Sintering DuraForm® PA $\sigma_{\max} = 43 \text{ MPa} \mid \epsilon_B = 14 \%$	F_{\max}	32.29 N	27.76 N	1293.46 N	2196.12 N
	σ_{\max}	-	-	10.78 MPa	18.30 MPa
	ϵ_B	9.19 %	10.12 %	3.13 %	4.12 %
No information		brittle	brittle	brittle	brittle

Table 25: Comparison of the tensile test results of the different manufacturing Methods (red highlighted: fracture due to extensometer) [properties of buildup materials → data sheets in appendix]

Annotation Table 25

- The elongations at break of the honeycomb-specimens are the total elongations consisting of the elongation of the hexagons and the elongation of the cell wall material. In most cases the honeycombs were not stretched fully.
- The elongations at break of the solid-specimens have to be regarded cautiously. They depend on process parameters (for example infill raster in FDM) and are partially affected due to notches caused by the extensometer (III Poly-Jet Modeling – highlighted in red). Hence, they are not comparable to the elongations at break from the material data sheets.
- Due to an absence of correct produced specimens, there have been tested only four specimens of “SLS-PA-Solid-Flat”. ISO 527-1 requests at least five specimens for a trustable statistical significance [ISO 527-1].
- The values of the SLS-specimens have to be regarded very cautiously as the manufacturing quality of the specimens was not satisfying.
- For the material values of the data sheets applies:

Polycarbonate (Stratasys)	
Additive Manufacturing Machine	Stratsys Fortus 400mc
Layer Thickness	0.254 mm (0.01 in)
Buildup Orientation	Edgewise
Tensile Testing Standard	ASTM D 638

Table 26: Polycarbonate (Stratasys) – information about manufacturing and testing (Data sheet in appendix) [sys]

Polycarbonate (Makrolon® GP)	
Tensile Testing Standard	ASTM D 638
No information about manufacturing (Injection Molded or Milled)	

Table 27: Polycarbonate (Makrolon® GP) – information about manufacturing and testing (Data sheet in appendix) [tap]

RGD720 (Stratasys)	
No information about manufacturing available	
Tensile Testing Standard	ASTM D 368

Table 28: RGD720 (Stratasys) – information about manufacturing and testing (Data sheet in appendix) [sys]

DuraForm®PA	
Additive Manufacturing Machine	3D Systems HiQ SLS
Laser Power	13 W
Scan Speed	5 m/s
Layer Thickness	0.1 mm
No information about orientation available	
Tensile Testing Standard	ASTM D 638

Table 29: DuraForm®PA – information about manufacturing and testing (Data sheet in appendix) [3ds]

Chapter 6 : CONCLUSION AND PERSPECTIVE

Conclusion and Perspective

Like in the literature review, this research as well shows that there are no general rules existing for all kind of additive manufactured parts in mechanical behavior depending on the buildup direction. The manufacturing methods are too different to one another and there are way too many process parameters existing which all have an influence on the outcome.

Regarding the **solid specimens**, reasonable results were achieved with the manufacturing methods Fused Deposition Modeling (FDM) and Poly-Jet Modeling (PJM).

The stress and strain values of the **FDM** specimens oriented *flat* and *edgewise* are really close together. The edgewise specimens provide marginally better values, but the diagrams show some variance, whereas all the load-displacement curves of the *flat* oriented specimens are quite the same.

The better values in edgewise orientation could result from more filaments laying parallel to the loading direction (*edgewise* 665 <> 624 *flat*). An abolition of the infill surrounding perimeters would lead a higher amount of filaments in loading direction in the buildup direction flat (*edgewise* 585 <> 600 *flat*).

In **PJM** the stress and strain values of the *flat* oriented specimens are in the range of the literature values and superior to the one of the *edgewise* oriented specimens. A reason for a behavior like this is hard to find, given the fact that the buildup is the same for both orientations.

The load-displacement curves of the *flat* oriented specimens show a variance in stress at yield and displacement at break, whereas the curves of the *edgewise* oriented specimens mainly show a variance in displacement at break. Both have a quite stable load at break.

On the contrary to FDM and PJM, the solid specimens manufactured with Selective Laser Sintering (**SLS**) show way smaller stress and strains than provided in the data sheet. However, the quality of the specimens was not satisfying. In addition the powder didn't seem to bond really well and the specimens were extremely

brittle, although or perhaps because the layer thickness was smaller than in the material data sheet. The closer the layer thickness to the size of the powder grains, the more brittle the manufactured parts are, could be one explanation.

Specimens manufactured *edgewise* resist nearly the double amount of stress than the *flat* ones, but both have close values in strain. Optical differences are indeterminable without using a microscope. A check with a scanning electron microscope would probably give some answers. The diagrams as well show a significant variance.

In general, the variance of curves in some load-displacement diagrams could be attributed to some irregularities in manufacturing. To increase the significance and get trustable results, more tensile specimens have to be tested.

The tensile testing standards for plastics like ISO 527 or ASTM D638 cannot necessarily be applied to specimens using additive manufacturing, but they are used in all data sheets of additive manufacturing materials. As the manufacturing methods are too different to each other, it has to be thought about a standard for mechanical properties of materials for each specific additive manufacturing methods (like for example Fused Deposition Modeling). Even not the manufacturers of additive manufacturing machines and materials provide all necessary information about the process parameters they used to create the test specimens for their material data sheets. A design for functionality can only be carried out, if the fundamental behavior of materials and the necessary process parameters to achieve this behavior are known.

Furthermore, it must also be mentioned that the breaking patterns of all solid brittle specimens show a failure at the end of the radii. Hence, it could be assumed, that the radii were underdesigned, which lead to a notch stress peak. To be sure, a redesign and tests have to be made.

As the honeycomb structure withstands a much smaller amount of loading (stress), the notch should not have an influence on the results, as the specimens will fail in the honeycomb area. The breaking patterns support this statement.

The main goal of this research was to explore the existence of advantages in generating the material along the primary axis of the cell walls instead of a layered buildup. For that, three different kind of tensile specimens out of polycarbonate with a hexagonal honeycomb structure were developed:

- The first one representing the full material generation along the primary axis of the cell walls, simulated by a milled honeycomb structure;
- the second one representing an layered material generation along the primary axis of the cell walls, using Fused Deposition Modeling;
- and the third one representing cell walls with a layered buildup perpendicular/under a certain angle to their primary axis, as well using Fused Deposition Modeling.

The test results show that

$F_{\max} = 981.43 \text{ N}$	>	$F_{\max} = 664.63 \text{ N}$	>	$F_{\max} = 137.58 \text{ N}$
100 %		67.72 %		14.02 %
$\epsilon_B = 28,74 \%$	>	$\epsilon_B = 12.52 \%$	>	$\epsilon_B = 4.71 \%$
100 %		43.56 %		16.38 %
Milling-PC-Honeycomb		FDM-PC-Honeycomb-Flat		FDM-PC-Honeycomb-Edgewise
Full material generation along primary axis of cell walls		Layered material generation along primary axis of cell walls		Layered material generation transversal / under a certain angle to primary axis of cell walls

and support the hypothesis of cell walls generated along their primary axis having superior mechanical properties.

The specimens “FDM-PC-Honeycomb-Flat” still withstand high loading in comparison to the “Milled-PC-Honeycomb” ones. In contrary, as suspected the “FDM-PC-Honeycomb-Edgewise” specimens carry only low loadings. A further exploration would be the effect of the reduction of the layer thickness on the results.

As seen in the Chapters 5.4.2 and 5.4.3, the milled hexagons stretch fully before a reduction in area of the cell walls inserts and the specimens break. The generation of cell walls along their primary axis with FDM still leads to a plastic deformation of the hexagons. The behavior could be characterized as elastic-plastic, without a second large increase of the load. This circumstance is probably caused by the layered structure. The hexagons with a layered structure merely display an elastic-brittle behavior, not as maybe assumed caused by delamination between the layers.

With **additional honeycomb specimens** manufactured by Poly-Jet Modeling and Selective Laser Sintering machines, a comparison between different additive manufacturing methods was aimed; however, with the constraint of different buildup materials.

The honeycomb specimens manufactured by SLS confirm the research theory in case of stress, as the laser solidified the powder grains along the primary axis of the cell walls. Regarding the strains at break, there is only a very small difference with an advantage on the specimens with the assumed inferior properties. The better mean value of the maximum force of the “SLS-PA-Honeycomb-Flat” specimens could also result from statistical manners. But, the outlier in the load-displacement diagram of the “SLS-PA-Honeycomb-Edgewise” specimens adjusts the mean value upwards and therefore gives a reason against this statement.

For the specimens manufactured by PJM the hypothesis is not valid regarding the tensile test results. The edgewise oriented specimens assumed to have inferior mechanical properties, displays significantly superior results in loading and displacement. A closer inspection of the printing sequence could provide reasons. As mentioned in Chapter 5.3.3, PJM is using an interlacing procedure, printing one layer in driving forth and back. Hence, the cell walls of the flat oriented hexagons are not printed along their primary axis. They are printed with lines being perpendicular or under an angle of 30 degrees to their primary axis. The single layers are probably not isotropic. More detailed material investigations have to be made. Furthermore, the fine layers could mean less influence due to the layer orientation.

The stated facts lead to **new research hypotheses**. One is the effect of the layer thickness on material properties. It should be explored if there are advantages in reducing the layer thickness. If so, it has to be explored if there is a point, where at a certain layer thickness the effects of layers on material properties are negligible. Especially for cellular materials this would be of great importance.

The other one is the effect of cell wall thicknesses on material properties. A variance of wall thicknesses at constant layer thickness and quantity could lead to a clarification. For that matter, the influence of flaws would play an important role. Voids and cracks can have fatal consequences for cellular structures and materials. The smallest scale feature must be considered in using additive manufacturing machines.

Research in the mentioned fields has to be differed into the types of manufacturing methods as well.

After these investigations and creating a standard for two and a half dimensional-techniques, it can be thought about a further development in real three-dimensional additive manufacturing methods. From the point of view after this research, theoretically, in case of Fused Deposition Modeling, real three-dimensional applications would help to increase problems with material properties depending on buildup directions. By having a generation of material in all spatial directions, all cell walls within a structure having different orientations could be generated along their primary axis. The layered structure would not exist anymore. But on the other hand, new challenges will arise, such as solutions for connection passages of cell walls or printing sequences to avoid collisions of the machine and its manufacturing object.

Indices

Books, Papers, Theses, Scripts

- [AdF13] Berger, U.; Hartmann, A.; Schmid, D. (2013): Additive Fertigungsverfahren – Rapid Prototyping – Rapid Tooling – Rapid Manufacturing.
Europa Lehrmittel, 1. Ausgabe
- [Ash06] Ashby M. F. (2006): The properties of foams and lattices.
Philosophical Transactions of the Royal Society A, 364, 15-30
- [BTS14] Bauer, J.; Hengsbach, S.; Tesari, I.; Schwaiger, R.; Kraft, O. (2014): High-strength cellular ceramic composites with 3D microarchitecture.
PNAS, 111 (7), 2453-2458
- [BS11] Bagsik, A.; Schöppner V. (2011): Mechanical properties of Fused Deposition Modeling parts manufactured with ULTEM*9085.
University of Paderborn
- [BSK12] Bückmann, T.; Stenger, N.; Kadic, M.; Kaschke, J.; Frölich, A.; Wegener, M. (2012): Tailored 3D mechanical metamaterials made by Dip-in Direct-Laser-Writing Optical Lithography.
Advanced Materials, 24, 2710-2714
- [CZL11] Chen, Y.; Zhou, C.; Lao, J. (2011): A layerless additive manufacturing process based on CNC accumulation.
Rapid Prototyping Journal, 17 (3), 218-227
- [DFA01] Deshpande V. S.; Fleck N. A.; Ashby M. F. (2001): Effective properties of the octet-truss lattice material.
Journal of the Mechanics and Physics of Solids, 49, 1747-1769
- [Eva91] Evans, K. E. (1991): Auxetic polymers: a new range of materials.
Endeavour, 15 (4), 170-174
- [EA00] Evans E.; Alderson A. (2000): Auxetic materials: Functional materials and structures from lateral thinking.
Advanced Materials, 12 (9), 617-628
- [Fra07] Frascati, J. (2007): Effects of position, orientation, and infiltrating material on three dimensional printing models.
Florida State University, College of Engineering and Computer Science, Department of Mechanical, Materials, and Aerospace Engineering

- [GA97] Gibson, L. J.; Ashby, M. F. (1997): Cellular solids – structure and properties.
Cambridge University Press, Second Edition
- [JBR10] Joshi, S.; Ju, J.; Berglind, L.; Rusly, R.; Summers, J. D.; DesJardins, J. D. (2010):
Experimental damage characterization of hexagonal honeycombs subjected to in-
plane shear loading.
Clemson University, Department of Mechanical Engineering and Department of Bioengineering
- [GS97] Gibson, I.; Shi, D. (1997): Material properties and fabrication parameters in selective
laser sintering process.
Rapid Prototyping Journal, 3 (4), 129-136
- [KD11] Kühnlein, f.; Drummer, D. (2011): Mechanische Eigenschaften und Bruchverhalten
maskengesinterter Kunststoffbauteile.
RT e journal, 8 (2011)
- [Kel99] Keller, P. (1999): Der Stoff, aus dem die Prototypen sind.
KU Kunststoffe, 89(11), 58-61
- [Mor13] Mortensen, F. (2013): Composite Materials – Scriptum Advanced FEM.
Aarhus University, Department of Engineering
- [NPR12] Nguyen, J.; Park, S.; Rosen, D. W.; Folgar, L.; Williams, J. (2012): Conformal lattice
structure design and fabrication.
Solid Freeform Fabrication Symposium, Texas, 2012
- [ORW11] Obrecht H.; Reinicke, U.; Walkowiak, M.; (2011): Auxetische Strukturen – neue Wege
zu gewichtseffizienten Konstruktionen.
lightweightdesign, 5 (2011)
- [Sae13] Baur, E.; Brinkmann, S.; Osswald T. A.; Rudolph N.; Schmachtenberg, E. (2013):
Saechtling – Kunststoff Taschenbuch.
Carl Hanser Verlag, 31. Auflage
- [ZLW14] Zheng, X.; Lee, H.; Weisgraber, T. H.; Shusteff, M.; DeOtte, J.; Duoss, E. B.; Kuntz, J. D.;
Biener, M. M.; Ge, Q.; Jackson, J. A.; Kucheyev, S. O.; Fang, N. X.; Spadaccini, C.M.
(2014): Ultralight, ultrastiff mechanical metamaterials.
Science, 344 (6190), 1373-1377

Internet Links

- [3do] <http://the3doodler.com/>
N.N. (March 6, 2015)
- [3ds] <http://www.3dsystems.com/>
N.N. (March 6, 2015)
- [aer] <http://www.mataerial.com>
N.N. (March 6, 2015)
- [ill] <http://nano-cemms.illinois.edu/media/uploads/content/111/files/microstereolithography.20101112082545.pdf>
Fang, N. (March 5, 2015)
- [kit] http://www.iam.kit.edu/wbm/73_925.php
Baer, J. (March 6, 2015)
- [krn] <http://www.kern.de/index.html?/kunststoff/service/werkstoffe/datenbank/werkstoffdatenbank.htm>
N.N. (March 6, 2015)
- [lms] <http://www.sandia.gov/mst/pdf/LENS.pdf>
N.N. (March 6, 2015)
- [mdc] <http://www.materialdatacenter.com/ms/de/Ultem/SABIC+Innovative+Plastics/Ultem+9085/49fdd153/1140>
N.N. (March 6, 2015)
- [mit] <http://newsoffice.mit.edu/2014/new-ultrastiff-ultralight-material-developed-0619>
Chandler, D. L. (March 5, 2015)
- [mut] <http://www.medizin-und-technik.de/home/-/article/33568401/40014715?returnToFullPageURL=back;>
Koll, S. (March 5, 2015)
- [nsc] <http://www.nanoscribe.de>
N.N. (March 6, 2015)
- [rep] <http://www.reprap.com>
N.N. (March 5, 2015)
- [rol] <http://www.rolanddga.com>
N.N. (March 6, 2015)

- [sys] <http://www.stratasys.com>
N.N. (March 6, 2015)
- [tap] <http://www.tapplastics.com/>
N.N. (March 6, 2015)
- [vir] <http://www.virginia.edu/ms/research/wadley/cellular-materials.html>
N.N. (March 05, 2014)

Standards

- [ISO527-1] ISO 527-01
N.N. (2012)
- [ISO527-2] ISO 527-02
N.N. (2012)

Notation

σ	stress
σ_y	stress at yielding
σ_B	stress at break
σ_{\max}	tensile strength (maximum stress)
F	load
F_y	load at yielding
F_{\max}	maximum load
F_B	load at break
A	area
ε	strain
ε_B	strain at break
$\varepsilon_{F_{\max}}$	strain at maximum load
ΔL	displacement
L_0	gauge length
t	cell wall thickness
l	hexagon cell wall length number one
h	hexagon cell wall length number two
b	hexagon/honeycomb width
α	interior angle of hexagon number one
φ	interior angle of hexagon number two
ρ	density
ν	Poisson's ratio

Abbreviation

AM	Additive Manufacturing
FDM	Fused Deposition Modeling
IM	Injection Molding
PA	Polyamide
PC	Polycarbonate
PJM	Poly-Jet Modeling
SLS	Selective Laser Sintering
cf.	compare
etc.	et cetera (and so on)
ref.	reference

Units

m	meter
mm	millimeter
μm	micrometer
nm	nanometer
in	inch
N	newton
kN	kilo newton
min	minute
h	hour
kg	kilogram
g	gram
$^{\circ}\text{C}$	degree Celsius
W	watt

Figure 1: Porous material cellular material characteristic cell length and types of structures	5
Figure 2: Types of three-dimensional cells: 1. Tetrahedron, 2. Triangular prism, 3. Rectangular prism, 4. Hexagonal prism, 5. Octahedron, 6. Rhombic dodecahedron, 7. Pentagonal dodecahedron,	6
Figure 3: Density over strength of solid and cellular materials [vir]	7
Figure 4: A Octet-truss unit cell, B and C Octet-truss lattice material, D Kelvin Foam unit cell, E and F Kelvin Foam [ZLW14]	8
Figure 5: Left: fully triangular micro-truss structure – the cube edge length is about 40 micrometers middle: deformed structure after uniaxial compression right: close-up view [kit]	8
Figure 6: Auxetic honeycomb structure	9
Figure 7: Non-auxetic and auxetic behavior [ORW11]	10
Figure 8: Process steps of additive manufacturing (according to figures of [AdF13])	12
Figure 9: Weight reduction through cellular structure – handle bar for a medical instrument [mut]	13
Figure 10: Types of AM-solidification of liquid buildup material (according to [AdF13])	14
Figure 11: Stereolithography (SL) [AdF13]	15
Figure 12: Types of AM-methods with initially solid buildup material (according to [AdF13])	16
Figure 13: Support material – direct and indirect version (according to [AdF13])	17
Figure 14: 1 Spherical part – layer-steps-effect through curvature	18
Figure 15: Influence of accuracy on surface roughness [AdF13]	18
Figure 16: Left: octet-truss unit cell Right: micro building [mit]	19
Figure 17: Octet-truss unit cell consisting itself out of a cellular triangular structure [nsc]	19
Figure 18: Buildup orientations (layers are only schematic)	20
Figure 19: <i>MATAERIAL</i> – layer-less additive manufacturing [aer]	25
Figure 20: Left: <i>LENS</i> [Ins] Right: Eifel Tower made with 3D-Pen <i>3Doodler</i> [3do]	26
Figure 21: Material properties depending on part orientation	30
Figure 22: Different buildup orientations within one cellular structure	31
Figure 23: Loading of layered truss-structure (hypothetical)	31
Figure 24: A Layer-less buildup, full cell generation along primary axis B Layered buildup, cell generation along primary axis per layer C Layered buildup, different buildup orientations of struts	32
Figure 25: Multi-purpose tensile specimen for testing plastics [ISO527-2]	35
Figure 26: Drawing of honeycomb tensile specimen	37
Figure 27: Connection passage and tips (light red) dimensions hexagon cell (light blue)	37
Figure 28: Solid tensile specimen – drawing	38
Figure 29: A elastomeric honeycombs, B elastic-plastic honeycombs and C elastic-brittle honeycombs under tension	39

Figure 30: Honeycomb specimens – flat and edgewise buildup orientation_____	40
Figure 31: Functional principle Fused Deposition Modeling (FDM) _____	41
Figure 32: Path generation with pre-processing software _____	42
Figure 33: Errors caused by printing sequence _____	43
Figure 34: Pre-processing software by Stratasys for Fortus 360mc _____	45
Figure 35: Polycarbonate FDM honeycomb-specimens – buildup orientation flat (left) and edgewise (right; problems with buildup and support material) _____	45
Figure 36: Milling process comparison of FDM specimen (top) with milled specimen (bottom) _	46
Figure 37: Functional principle Poly-Jet Modeling (PJM) _____	47
Figure 38: Top: deformed specimens due to moisture bottom: PJM – honeycomb tensile specimen _____	48
Figure 39: Functional principle Selective Laser Sintering (SLS) [AdF13] _____	49
Figure 40: Solidification along the primary axis of the cell wall _____	50
Figure 41: Top: incorrect dimensions and deformed shoulder Bottom: brittle cells walls_____	50
Figure 42: Left: Typical stress-strain curves for plastic materials – a brittle, b ductile, c drawable,	51
Figure 43: Tensile test left and right: arrangement of extensometer right: stretching of milled polycarbonate hexagons _____	53
Figure 44: Top: FDM-PC-Solid-Flat: brittle fracture (cf. Figure 51) _____	54
Figure 45: Top: FDM-PC-Honeycomb-Flat: little residual plastic deformation of hexagons; fracture under 60 degrees (elastic-plastic behavior) (cf. Figure 29 and Figure 51) _____	55
Figure 46: Top: Milling-PC-Solid: ductile (no fracture, because machine limit was reached) _____	55
Figure 47: Top: PJM-RGD720-Solid-Flat: first yielding, then fracture due to notch caused by the extensometer (1), not at lowest point of the reduction in area (2) (cf. Figure 58) _____	56
Figure 48: Top: PJM-RGD720-Honeycomb-Flat: little or no residual plastic deformation of hexagons; fracture under 60 degrees (elastic-plastic behavior and elastic-brittle behavior) (cf. Figure 29 and Figure 60) _____	56
Figure 49: Top: SLS-PA-Solid-Flat: brittle fracture (cf. Figure 62) _____	57
Figure 50: Top: SLS-PA-Honeycomb-Flat: stretching of hexagons during loading; no plastic deformation; brittle fracture under 60 degrees (only cracks visible) (elastic-brittle behavior) (cf. Figure 29 and Figure 64) _____	57
Figure 51: Load-displacement diagram – FDM-PC-Solid-Flat_____	59
Figure 52: Load-displacement diagram – FDM-PC-Solid-Edgewise _____	59
Figure 53: Load-displacement diagram – FDM-PC-Honeycomb-Flat (elastic-plastic) _____	61
Figure 54: Load-displacement diagram – FDM-PC-Honeycomb-Edgewise (elastic-brittle) _____	61
Figure 55: Fully stretched honeycombs _____	63
Figure 56: Load-displacement diagram – MILLING-PC-Honeycomb (extensometer limit reached) _____	64
Figure 57: Load-displacement diagram – MILLING-PC-Honeycomb (elastic-plastic, plus reduction in area of cell walls)_____	64
Figure 58: Load-displacement diagram – PJM-RGD720-Solid-Flat _____	66

Figure 59: Load-displacement diagram – PJM-RGD720-Solid-Edgewise _____	66
Figure 60: Load-displacement diagram – PJM-RGD720-Honeycomb-Flat (elastic-plastic and elastic-brittle)_____	68
Figure 61: Load-displacement diagram – PJM-RGD720-Honeycomb-Edgewise (elastic-plastic) __	68
Figure 62: Load-displacement diagram – SLS-PA-Solid-Flat_____	70
Figure 63: Load-displacement diagram – SLS-PA-Solid-Edgewise _____	70
Figure 64: Load-displacement diagram – SLS-PA-Honeycomb-Flat (elastic-brittle)_____	72
Figure 65: Load-displacement diagram – SLS-PA-Honeycomb-Edgewise (elastomeric) _____	72

Tables

Table 1: Comparison of literature values _____	22
Table 2: Honeycomb structure – buildup specifications _____	33
Table 3: Process parameters – FDM _____	44
Table 4: Process parameters – PJM _____	48
Table 5: Process Parameters – SLS _____	49
Table 6: Tensile testing tools and parameters _____	52
Table 7: Material values – polycarbonate (Stratasys) [sys] (data sheet attached) _____	58
Table 8: Test results – FDM-PC-Solid-Flat _____	58
Table 9: Test results – FDM-PC-Solid-Edgewise _____	58
Table 10: Test results – FDM-PC-Honeycomb-Flat _____	60
Table 11: Test results – FDM-PC-Honeycomb-Edgewise _____	60
Table 12: Material values – polycarbonate (Makrolon® GP) [tap] (data sheet attached) _____	62
Table 13: Test results – Milling-PC-Solid (extension limit of extensometer was reached) _____	62
Table 14: Test results – Milling-PC-Honeycomb _____	62
Table 15: Material values – RGD720 (Stratasys) [sys] (data sheet attached) _____	65
Table 16: Test results – PJM-RGD720-Solid-Flat _____	65
Table 17: Test results – PJM-RGD720-Solid-Edgewise _____	65
Table 18: Test results – PJM-RGD720-Honeycomb-Flat _____	67
Table 19: Test results – PJM-RGD720-Honeycomb-Edgewise _____	67
Table 20: Material values – DuraForm® PA [3ds] (data sheet attached) _____	69
Table 21: Test results – SLS-PA-Solid-Flat _____	69
Table 22: Test results – SLS-PA-Solid-Edgewise _____	69
Table 23: Test results – SLS-PA-Honeycomb-Flat _____	71
Table 24: Test results – SLS-PA-Honeycomb-Edgewise _____	71
Table 25: Comparison of the tensile test results of the different manufacturing Methods (red highlighted: fracture due to extensometer) [properties of buildup materials → data sheets in appendix] _____	73
Table 26: Polycarbonate (Stratasys) – information about manufacturing and testing (Data sheet in appendix) [sys] _____	74
Table 27: Polycarbonate (Makrolon® GP) – information about manufacturing and testing (Data sheet in appendix) [tap] _____	74
Table 28: RGD720 (Stratasys) – information about manufacturing and testing (Data sheet in appendix) [sys] _____	75
Table 29: DuraForm®PA – information about manufacturing and testing (Data sheet in appendix) [3ds] _____	75

Appendix

PC (polycarbonate)

Production-Grade Thermoplastic
for Fortus 3D Production Systems



A true industrial thermoplastic, PC (polycarbonate) is widely used in automotive, aerospace, medical and many other applications. PC offers accuracy, durability and stability, creating strong parts that withstand functional testing. A PC part manufactured on a Fortus® 3D Production System is 5-60 percent stronger than a part made on previous FDM® systems. It also has superior mechanical properties to ABS and a number of other thermoplastics. When combined with a Fortus system, PC gives you Real Parts™ for conceptual modeling, functional prototyping, manufacturing tools, and end-use-parts.

Mechanical Properties ¹	Test Method	English	Metric
Tensile Strength (Type 1, 0.125", 0.2"/min)	ASTM D638	9,800 psi	68 MPa
Tensile Modulus (Type 1, 0.125", 0.2"/min)	ASTM D638	330,000 psi	2,300 MPa
Tensile Elongation (Type 1, 0.125", 0.2"/min)	ASTM D638	5%	5%
Flexural Strength (Method 1, 0.05"/min)	ASTM D790	15,100 psi	104 MPa
Flexural Modulus (Method 1, 0.05"/min)	ASTM D790	324,000 psi	2,200 MPa
IZOD Impact, notched (Method A, 23°C)	ASTM D256	1 ft-lb/in	53 J/m
IZOD Impact, un-notched (Method A, 23°C)	ASTM D256	6 ft-lb/in	320 J/m

Thermal Properties ²	Test Method	English	Metric
Heat Deflection (HDT) @ 66 psi	ASTM D648	280°F	138°C
Heat Deflection (HDT) @ 264 psi	ASTM D648	261°F	127°C
Vicat Softening	ASTM D1525	282°F	139°C
Glass Transition (Tg)	DMA (SSYS)	322°F	161°C
Melt Point	-----	Not Applicable ³	Not Applicable ³

Electrical Properties ⁴	Test Method	Value Range
Volume Resistivity	ASTM D257	2.0x10e14 - 6.0x10e13 ohms
Dielectric Constant	ASTM D150-98	3.0 - 2.8
Dissipation Factor	ASTM D150-98	.0006 - .0005
Dielectric Strength	ASTM D149-09, Method A	360-80 V/mil

PC



Other ²	Test Method	Value
Specific Gravity	ASTM D792	1.2
Flame Classification	UL94	HB
Coefficient of Thermal Expansion	ASTM E831	3.8E-05 in/in/°F
Rockwell Hardness	ASTM D785	R115
UL File Number	-----	E345258

System Availability	Layer Thickness Capability	Support Structure	Available Colors
Fortus 360mc	0.013 inch (0.330 mm)	BASS, Soluble	□ White
Fortus 400mc	0.010 inch (0.254 mm)		
Fortus 900mc	0.007 inch (0.178 mm)		
	0.005 inch (0.127 mm) ⁵		

The information presented are typical values intended for reference and comparison purposes only. They should not be used for design specifications or quality control purposes. End-use material performance can be impacted (+/-) by, but not limited to, part design, end-use conditions, test conditions, etc. Actual values will vary with build conditions. Tested parts were built on Fortus 400mc @ 0.010" (0.254 mm) slice. Product specifications are subject to change without notice.

The performance characteristics of these materials may vary according to application, operating conditions, or end use. Each user is responsible for determining that the Stratasys material is safe, lawful, and technically suitable for the intended application, as well as for identifying the proper disposal (or recycling) method consistent with applicable environmental laws and regulations. Stratasys makes no warranties of any kind, express or implied, including, but not limited to, the warranties of merchantability, fitness for a particular use, or warranty against patent infringement.

¹Build orientation is on side long edge.

²Literature value unless otherwise noted.

³Due to amorphous nature, material does not display a melting point.

⁴All Electrical Property values were generated from the average of test plaques built with default part density (solid). Test plaques were 4.0 x 4.0 x 0.1 inches (102 x 102 x 2.5 mm) and were built both in the flat and vertical orientation. The range of values is mostly the result of the difference in properties of test plaques built in the flat vs. vertical orientation.

⁵PC can attain 0.005 inch (0.127mm) layer thickness when used with SR-100 soluble support. 0.005 inch layer thickness is not available on the Fortus 900mc.

Stratasys | www.stratasys.com | info@stratasys.com

7665 Commerce Way
Eden Prairie, MN 55344
+1 888 480-3548 (US Toll Free)
+1 952 937-3000 (Intl)
+1 952 937-0070 (Fax)

2 Holtzman St.,
Science Park, PO Box 2496
Rehovot 76124, Israel
+972 74 745-4000
+972 74 745-5000 (Fax)

Local Street Address
City, State, Zip
Phone #
Fax #

©2013 Stratasys Inc. All rights reserved. Stratasys, FDM, Fortus and Finishing Touch are registered trademarks of Stratasys Inc. FDM Technology, Fused Deposition Modeling, Fortus 200mc, Fortus 250mc, Fortus 360mc, Fortus 400mc, Fortus 900mc, Insight, Control Center, FDM Team, Smart Supports, SR-30, SR-100, ASplus, ABS-ES07, and TouchWorks are trademarks of Stratasys, Inc. ULTEM is a trademark of SABIC Innovative Plastics IP BV. All other trademarks are the property of their respective owners, and Stratasys assumes no responsibility with regard to the selection, performance, or use of these non-Stratasys products. Product specifications subject to change without notice. Printed in the USA. FortusPCMaterialSpecSheet-US-1013

At the core: Advanced FDM Technology™

Fortus systems are based on patented Stratasys FDM (Fused Deposition Modeling) technology. FDM is the industry's leading additive manufacturing technology, and the only one that uses production grade thermoplastics, enabling the most durable parts.

Fortus systems use a wide range of thermoplastics with advanced mechanical properties so your parts can endure high heat, caustic chemicals, sterilization, and high impact applications.

No special facilities needed

You can install a Fortus 3D Production System just about anywhere. No special venting is required because Fortus systems don't produce noxious fumes, chemicals, or waste.

No special skills needed

Fortus 3D Production Systems are easy to operate and maintain compared to other additive fabrication systems because there are no messy powders or resins to handle and contain. They're so simple, an operator can be trained to operate a Fortus system in less than 30 minutes.

Get your benchmark on the future of manufacturing

Fine details. Smooth surface finishes. Accuracy. Strength. The best way to see the advantages of a Fortus 3D Production System is to have your own part built on a Fortus system. Get your free part at: stratasys.com.



Makrolon® GP sheet

General purpose

Makrolon® GP sheet is a polished surface, UV stabilized, transparent polycarbonate product. It features outstanding impact strength, superior dimensional stability, high temperature resistance, and high clarity. This lightweight thermoformable sheet is also easy to fabricate and decorate. Makrolon GP sheet is offered with a five (5) year Limited Product Warranty against breakage. The terms of the warranty are available upon request.

Applications

Industrial glazing, machine guards, structural parts, thermoformed and fabricated components

Typical Properties

Property	Test Method	Units	Values
PHYSICAL			
Specific Gravity	ASTM D 792	–	1.2
Refractive Index	ASTM D 542	–	1.586
Light Transmission, Clear @ 0.118"	ASTM D 1003	%	86
Light Transmission, I30 Gray @ 0.118"	ASTM D 1003	%	50
Light Transmission, K09 Bronze @ 0.118"	ASTM D 1003	%	50
Light Transmission, I35 Dark Gray @ 0.118"	ASTM D 1003	%	18
Water Absorption, 24 hours	ASTM D 570	%	0.15
Poisson's Ratio	ASTM E 132	–	0.38
MECHANICAL			
Tensile Strength, Ultimate	ASTM D 638	psi	9,500
Tensile Strength, Yield	ASTM D 638	psi	9,000
Tensile Modulus	ASTM D 638	psi	340,000
Elongation	ASTM D 638	%	110
Flexural Strength	ASTM D 790	psi	13,500
Flexural Modulus	ASTM D 790	psi	345,000
Compressive Strength	ASTM D 695	psi	12,500
Compressive Modulus	ASTM D 695	psi	345,000
Izod Impact Strength, Notched @ 0.125"	ASTM D 256	ft-lbs/in	18
Izod Impact Strength, Unnotched @ 0.125"	ASTM D 256	ft-lbs/in	60 (no failure)
Instrumented Impact @ 0.125"	ASTM D 3763	ft-lbs	>47
Shear Strength, Ultimate	ASTM D 732	psi	10,000
Shear Strength, Yield	ASTM D 732	psi	6,000
Shear Modulus	ASTM D 732	psi	114,000
Rockwell Hardness	ASTM D 785	–	M70 / R118
THERMAL			
Coefficient of Thermal Expansion	ASTM D 696	in/in/°F	3.75 x 10 ⁻⁶
Coefficient of Thermal Conductivity	ASTM C 177	BTU-in/hr-ft ² -°F	1.35
Heat Deflection Temperature @ 264 psi	ASTM D 648	°F	270
Heat Deflection Temperature @ 66 psi	ASTM D 648	°F	280
Brittleness Temperature	ASTM D 746	°F	-200
Shading Coefficient, clear @ 0.236"	NFRC 100-2010	–	0.97
Shading Coefficient, Gray or Bronze @ 0.236"	NFRC 100-2010	–	0.77
U factor @ 0.236" (summer, winter)	NFRC 100-2010	BTU/hr-ft ² -°F	0.85, 0.92
U factor @ 0.375" (summer, winter)	NFRC 100-2010	BTU/hr-ft ² -°F	0.78, 0.85
ELECTRICAL			
Dielectric Constant @ 10 Hz	ASTM D 150	–	2.96
Dielectric Constant @ 60 Hz	ASTM D 150	–	3.17
Volume Resistivity	ASTM D 257	Ohm-cm	8.2 x 10 ¹⁴
Dissipation Factor @ 60 Hz	ASTM D 150	–	0.0009
Arc Resistance			
Stainless Steel Strip electrode	ASTM D 495	Seconds	10
Tungsten Electrodes	ASTM D 495	Seconds	120
Dielectric Strength, in air @ 0.125"	ASTM D 149	V/mil	380
FLAMMABILITY			
Horizontal Burn, AEB	ASTM D 635	in	<1
Ignition Temperature, Self	ASTM D 1929	°F	1022
Ignition Temperature, Flash	ASTM D 1929	°F	824
Flame Class @ 0.060"	UL 94	–	HB
@ 0.394"	UL 94	–	V-0

*Typical properties are not intended for specification purposes.

**Some properties characterized using non-textured sheet.



Materials Simulating Engineering Plastics

Digital ABS, Green (RGD5160-DM, RGD5161-DM) made of RGD515 & RGD531
Digital ABS, Ivory (RGD5130-DM, RGD5131-DM) made of RGD515 & RGD531

	ASTM	Units	Metric	Units	Imperial
Tensile strength	D-638-03	MPa	55-60	psi	8000-8700
Elongation at break	D-638-05	%	25-40	%	25-40
Modulus of elasticity	D-638-04	MPa	2600-3000	psi	375,000-435,000
Flexural Strength	D-790-03	MPa	65-75	psi	9,500-11,000
Flexural Modulus	D-790-04	MPa	1700-2200	psi	245,000-320,000
HDT, °C @ 0.45MPa	D-648-06	°C	58-68	°F	136-154
HDT, °C @ 0.45MPa after thermal post-treatment procedure A	D-648-06	°C	82-90	°F	180-194
HDT, °C @ 0.45MPa after thermal post-treatment procedure B	D-648-06	°C	92-95	°F	198-203
HDT, °C @ 1.82MPa	D-648-07	°C	51-55	°F	124-131
Izod Notched Impact	D-256-06	J/m	65-80	ft lb/inch	1.22-1.50
Tg	DMA, E _a	°C	47-53	°F	117-127
Shore Hardness (D)	Scale D	Scale D	85-87	Scale D	85-87
Rockwell Hardness	Scale M	Scale M	67-69	Scale M	67-69
Polymerized density	ASTM D792	g/cm3	1.17-1.18		

High Temperature Material (RGD525)

	ASTM	Units	Metric	Units	Imperial
Tensile strength	D-638-03	MPa	70-80	psi	10,000-11,500
Elongation at break	D-638-05	%	10-15	%	10-15
Modulus of elasticity	D-638-04	MPa	3200-3500	psi	465,000-510,000
Flexural Strength	D-790-03	MPa	110-130	psi	16,000-19,000
Flexural Modulus	D-790-04	MPa	3100-3500	psi	450,000-510,000
HDT, °C @ 0.45MPa	D-648-06	°C	63-67	°F	145-163
HDT, °C @ 0.45MPa after thermal post-treatment procedure A	D-648-06	°C	75-80	°F	167-176
HDT, °C @ 1.82MPa	D-648-07	°C	55-57	°F	131-135
Izod Notched Impact	D-256-06	J/m	14-16	ft lb/inch	0.262-0.300
Water Absorption, %	D-570-98 24hr	%	1.2-1.4	%	1.2-1.4
Tg	DMA, E _a	°C	62-65	°F	144-149
Shore Hardness D	Scale D	Scale D	87-88	Scale D	87-88
Rockwell Hardness	Scale M	Scale M	78-83	Scale M	78-83
Polymerized density	ASTM D792	g/cm3	1.17-1.18		
Ash content	USP281	%	0.38-0.42	%	0.38-0.42

Materials Simulating Standard Plastics

Transparent Materials

RGD720

Veroclear RGD810

	ASTM	Units	Metric	Units	Imperial
Tensile strength	D-638-03	MPa	50-65	psi	7250-9450
Elongation at break	D-638-05	%	15-25	%	15-25
Modulus of elasticity	D-638-04	MPa	2000-3000	psi	290,000-435,000
Flexural Strength	D-790-03	MPa	80-110	psi	12000-16000
Flexural Modulus	D-790-04	MPa	2700-3300	psi	390,000-480,000
HDT, °C @ 0.45MPa	D-648-06	°C	45-50	°F	113-122
HDT, °C @ 1.82MPa	D-648-07	°C	45-50	°F	113-122
Izod Notched Impact	D-256-06	J/m	20-30	ft lb/inch	0.375-0.562
Water Absorption	D-570-98 24hr	%	1.5-2.2	%	1.5-2.2
Tg	DMA, E _a	°C	48-50	°F	118-122
Shore Hardness (D)	Scale D	Scale D	83-86	Scale D	83-86
Rockwell Hardness	Scale M	Scale M	73-76	Scale M	73-76
Polymerized density	ASTM D792	g/cm3	1.18-1.19		
Ash content	USP281	%	0.01-0.02	%	0.01-0.02

	ASTM	Units	Metric	Units	Imperial
Tensile strength	D-638-03	MPa	50-65	psi	7250-9450
Elongation at break	D-638-05	%	10-25	%	10-25
Modulus of elasticity	D-638-04	MPa	2000-3000	psi	290,000-435,000
Flexural Strength	D-790-03	MPa	75-110	psi	11000-16000
Flexural Modulus	D-790-04	MPa	2200-3200	psi	320,000-465,000
HDT, °C @ 0.45MPa	D-648-06	°C	45-50	°F	113-122
HDT, °C @ 1.82MPa	D-648-07	°C	45-50	°F	113-122
Izod Notched Impact	D-256-06	J/m	20-30	ft lb/inch	0.375-0.562
Water Absorption	D-570-98 24hr	%	1.1-1.5	%	1.1-1.5
Tg	DMA, E _a	°C	52-54	°F	126-129
Shore Hardness (D)	Scale D	Scale D	83-86	Scale D	83-86
Rockwell Hardness	Scale M	Scale M	73-76	Scale M	73-76
Polymerized density	ASTM D792	g/cm3	1.18-1.19		
Ash content	USP281	%	0.02-0.06	%	0.02-0.06

Find material properties for color materials on the Color Digital Materials Data Sheet.

DuraForm® PA plastic

For use with all selective laser sintering (SLS®) systems

TECHNICAL DATA

General Properties

MEASUREMENT	METHOD/CONDITION	METRIC	U.S.
Specific Gravity	ASTM D792	1.00 g/cm ³	1.00 g/cm ³
Moisture Absorption - 24 hours	ASTM D570	0.07 %	0.07 %

Mechanical Properties

MEASUREMENT	METHOD/CONDITION	METRIC	U.S.
Tensile Strength, Yield	ASTM D638	N/A*	N/A*
Tensile Strength, Ultimate	ASTM D638	43 MPa	6237 psi
Tensile Modulus	ASTM D638	1586 MPa	230 ksi
Elongation at Yield	ASTM D638	N/A*	N/A*
Elongation at Break	ASTM D638	14 %	14 %
Flexural Strength, Yield	ASTM D790	N/A*	N/A*
Flexural Strength, Ultimate	ASTM D790	48 MPa	6962 psi
Flexural Modulus	ASTM D790	1387 MPa	201 ksi
Hardness, Shore D	ASTM D2240	73	73
Impact Strength (notched Izod, 23°C)	ASTM D256	32 J/m	0.6 ft-lb/in
Impact Strength (unnotched Izod, 23°C)	ASTM D256	336 J/m	6.3 ft-lb/in
Gardner Impact	ASTM D5420	2.7 J	2.0 ft-lb

Thermal Properties

MEASUREMENT	METHOD/CONDITION	METRIC	U.S.
Heat Deflection Temperature (HDT)	ASTM D648		
	@ 0.45 MPa	180 °C	356 °F
	@ 1.82 MPa	95 °C	203 °F
Coefficient of Thermal Expansion	ASTM E831		
	@ 0 - 50 °C	62.3 µm/m-°C	34.6 µin/in-°F
	@ 85 - 145 °C	124.6 µm/m-°C	69.2 µin/in-°F
Specific Heat Capacity	ASTM E1269	1.64 J/g-°C	0.392 BTU/lb-°F
Thermal Conductivity	ASTM E1225	0.70 W/m-K	4.86 BTU-in/hr-ft ² -°F
Flammability	UL 94	HB	HB

Electrical Properties

MEASUREMENT	METHOD/CONDITION	METRIC	U.S.
Volume Resistivity	ASTM D257	5.9 x 10 ¹³ ohm-cm	5.9 x 10 ¹³ ohm-cm
Surface Resistivity	ASTM D257	7.0 X 10 ¹³ ohm	7.0 x 10 ¹³ ohm
Dissipation Factor, 1 KHz	ASTM D150	0.044	0.044
Dielectric Constant, 1 KHz	ASTM D150	2.73	2.73
Dielectric Strength	ASTM D149	17.3 kV/mm	439 kV/in

* N/A = Data not applicable for this test condition

Data was generated by building parts under typical default parameters. DuraForm PA plastic was processed on a base-level Sinterstation HQ SLS system at 13 watts laser power, 200 inches/sec (5 m/sec) scan speed, and a powder layer thickness of 0.004 inches (0.1 mm).



3D Systems Corporation
333 Three D Systems Circle
Rock Hill, SC 29730 U.S.A.

Tel: 803.326.4080
Toll-free: 800.889.2964
Fax: 803.324.8810

moreinfo@3dsystems.com
www.3dsystems.com
NASDAQ: TDSC

Warranty/Disclaimer: The performance characteristics of these products may vary according to product application, operating conditions, material combined with, or with end use. 3D Systems makes no warranties of any type, express or implied, including, but not limited to, the warranties of merchantability or fitness for a particular use.

© 2006 by 3D Systems, Inc. All rights reserved. Specifications subject to change without notice. The 3D logo, DuraForm, Sinterstation and SLS are registered trademarks and HQ is a trademark of 3D Systems, Inc.

TRANSFORM YOUR PRODUCTS

PN 70715 Issue Date - 07 Nov 06

Sebastian Barner | 2015